To the Graduate Council:

I am submitting herewith a dissertation written by John Kennedy McCall entitled "Design Methodology For Composite Structures Consisting Of Reinforced Hollow Brick Walls And Concrete Beams Connected At A Joint With Flashing And Subject To In-Plane Bending." I have examined the final copy of this dissertation for form and content and recommend that it be accepted in partial fulfillment of the requirements for the degree of Doctor of Philosophy, with a major in Civil Engineering.

Dr. Richard M. Bennett, Major Professor

We have read this dissertation
and recommend its acceptance:

Accepted for the Council:

Associate Vice Chancellor and
Dean of The Graduate School

Design Methodology

For

Composite Structures Consisting Of

Reinforced Hollow Brick Walls And Concrete Beams

Connected At A Joint With Flashing

And

Subject To In-Plane Bending

A Dissertation

Presented for the

Doctor of Philosophy

Degree

The University of Tennessee, Knoxville

John Kennedy McCall

May, 1996

Dedication

This thesis is dedicated to my loving family: Sandra, my wife, Jean, Rachel and James, my three children, and J. Kennedy and Isodene, my parents. Without my family's love, support, and occasional prodding this effort would not have been successful.

Abstract

Due to waterproofing requirements, a flashing joint is generally used at the base of a brick wall to facilitate transport of moisture from the back of a brick wall to the outside of the building. The flashing results in a loss of bond and reduced friction between the reinforced brick wall and the supporting structure. This loss of strength is of little consequence to veneer; however, it may impact wall behavior for reinforced hollow brick. This research, which uses hollow Suprking bricks as manufactured by the General Shale Co., develops data to assess the in-plane shear behavior of the flashing joint.

The research scope includes: (a) testing wall components, shear joints with flashing, and small scale walls; (b) developing numerical models and comparing test results and analysis based on numerical models; (c) developing design details and methods; and (d) demonstrating the use of the methods developed with several design examples. Strength design methods were found applicable to design of composite structures consisting of reinforced brick walls and concrete beams connected at a joint with flashing and subject to in-plane bending. Several specific construction details were found necessary to assure performance including (a) the use of #4 or smaller reinforcing steel bars, (b) grouting of cells in the first two courses of brick adjacent to cells with reinforcing, (c) use of bond beam brick elements on each side of reinforcing steel, and (d) minimum spacing of reinforcing steel of twenty inches.

TABLE OF CONTENTS

CHAPTER	TITLE	PAGE
1	**INTRODUCTION**	**1**
1.1	Purpose	1
1.2	Summary	2
1.3	Conclusion	6
2	**BACKGROUND**	**7**
2.1	Introduction	7
2.2	Flashing Joint Forces Associated With In-plane Bending Due To Vertical Displacements	11
2.3	Suprking Brick Wall System	11
2.4	Brick Prism Strength	13
2.5	Flashing Joints, Shear Friction and Shear Dowels	14
2.6	Masonry Wall In-plane Bending	25
3	**MECHANICAL BEHAVIOR OF WALL COMPONENTS**	**30**
3.1	Introduction	30
3.2	Summary	31
3.3	Component Testing Equipment and Data Evaluation	31
3.4	Compressive Strength of Bricks	36

3.5	Splitting Strength Of Bricks	39
3.6	Compressive Strength Of Type N Mortar Used In Specimens	40
3.7	Compressive Strength Of Premixed 10K Grout	43
3.8	Compressive Strength Of Grout Made By Thinning Mortar (Called Mortar Grout)	45
3.9	Compressive Strength Of Ungrouted Brick Prisms	47
3.10	Compressive Strength Of Brick Prisms Grouted With 10K Grout	55
3.11	Compressive Strength Of Brick Prisms Grouted With Mortar Grout	58
3.12	Compressive Strength Of Concrete Used In Wall Specimens	60
3.13	Splitting Tension Tests Of Concrete Used In Wall Specimens	61
3.14	Mill Test Reports For Reinforcing Steel Used In Wall Specimens	62
4	**MECHANICAL BEHAVIOR OF REINFORCED SHEAR JOINTS WITH PVC FLASHING**	**63**
4.1	Introduction	63
4.2	Summary	64

4.3	Shear Test Specimen Configuration And Test Method	67
4.4	Shear Test Of Joint With Vinyl Flashing, #4 Reinforcing Bar, 10K Grout In Reinforced Cells	69
4.5	Shear Test Of Joint With Vinyl Flashing, #4 Reinforcing Bar, Mortar Grout In Reinforced Cells	72
4.6	Shear Test Of Joint With Vinyl Flashing, #4 Reinforcing Bar, 10K Grout In All Cells	73
4.7	Shear Test Of Joint With Vinyl Flashing, #6 Reinforcing Bar, 10K Grout In Reinforced Cells Or In All Cells	76
5	**BEHAVIOR OF SMALL SCALE TEST WALLS**	**79**
5.1	Introduction	79
5.2	Summary	79
5.3	Wall Test Specimen Configuration	80
5.4	Wall Specimen Testing And Data Collection	83
5.5	In-plane Bending Test Of Wall Specimens With Vertical #4 Steel Reinforcing Bars Crossing PVC Flashing Joint	84
5.6	Modeling Of Small Scale Test Wall Behavior	88
5.7	Evaluation Of Results	106

6		**METHODOLOGY FOR DESIGN OF WALL STRUCTURES**	**108**
	6.1	General	108
	6.2	Materials	109
	6.3	Construction Requirements	110
	6.4	General Considerations	111
	6.5	Design Procedures	114
7		**DESIGN EXAMPLES**	**116**
	7.1	Summary	116
	7.2	Wall Design Program Using Mathcad	116
	7.3	Wall Subjected To Mining Subsidence	126
	7.4	Wall Subjected To Soil Expansion	140
	7.5	Wall Subjected To Washout Between Pilings Or Piers	143
8		**RECOMMENDATIONS FOR ADDITIONAL RESEARCH**	**155**
	8.1	General	155
	8.2	Recommendations For Parametric Studies	156
	8.3	Recommendations Related To Masonry Behavior	157
		REFERENCES	**159**
		APPENDIX TABLES AND FIGURES	**164**
		VITA	**217**

LIST OF TABLES

Table Designation	Table Title	Page
Table 2.1	Coefficient Of Friction Of Joint At Bottom Of Brick Wall Normal Load On Joint Due To Weight Of Wall	165
Table 3.1	System Noise Measurements	166
Table 4.1	Summary Of Shear Specimen Results	167
Table 5.1	Description Of LVDT Measurements On Wall Specimens	168

LIST OF FIGURES

Figure Designation	Figure Title	Page
Figure 1.1	Schematic Sketch Of Suprking Brick	169
Figure 1.2	Photographs Of Suprking Brick Units	170
Figure 2.1	Schematic Sketch Of Suprking Brick Wall System	171
Figure 2.2	Small Industrial Building Constructed With Suprking Brick System	172
Figure 2.3	Idealized Pull-Out Failure Cone For Dowel In Hollow Brick Wall Flashing Joint	173
Figure 2.4	Comparison Of Shear Friction, Dowel, #4 Full Grouted Shear Specimen, And Idealized Flashing Joint Behavior	174
Figure 2.5	Shear Specimen And Free Body Diagram Of Left Side Of Shear Specimen	175
Figure 2.6	Flashing Joint Shear Capacity For Each Dowel Versus Projected Length Estimated From ACI 530 (Building,1992)	176
Figure 3.1	Component Testing Equipment Arrangement	177
Figure 3.2	Test Equipment	178
Figure 3.3	Component Test Instrumentation Arrangement	179

Figure 3.4	Half Brick Compressive Strength Specimen	180
Figure 3.5	Splitting Tensile Strength Test Arrangement Suprking Brick	181
Figure 3.6	Photograph Of Grout Specimens After Failure	182
Figure 3.7	Brick Prism Specimen For Compression Testing	183
Figure 3.8	Photograph Of Ungrouted Brick Prism Specimens In Test Machine After Specimen Failure	184
Figure 3.9	Ungrouted Brick Prism #2 Stress Strain Curves	185
Figure 3.10	Ungrouted Prism Specimen #2 Deformation Of Components	186
Figure 3.11	Ungrouted Prism Specimen #2 Stress Versus Strain Of Components	187
Figure 3.12	Ungrouted Prism Stress Strain Curves	188
Figure 3.13	Photograph Of 10K Grouted Brick Prism Specimens In Test Machine After Specimen Failure	189
Figure 3.14	10K Grouted Brick Prism #1 Stress Strain Curves	190
Figure 3.15	10K Grouted Prism Stress Strain Curves	191
Figure 3.16	Type N Mortar Grouted Prism Stress Strain Curves	192
Figure 4.1	Plot Of Shear Specimen Test Results On Curves For Flashing Joint Shear Capacity For Each Dowel Versus Projected Length	193

Figure 4.2	Flashing Joint Shear Capacity For #4 Dowel Versus Dowel Spacing	194
Figure 4.3	Shear Joint Specimen	195
Figure 4.4	Failed Shear Specimen With 10K Grout In Reinforced Cells	196
Figure 4.5	Shear Test Of Joints With Vinyl Flashing, #4 Reinforcing Bar, 10K Grout In Reinforced Cells Specimen #3 Load Deformation Curves	197
Figure 4.6	Shear Test Of Joints With Vinyl Flashing, #4 Reinforcing Bar, 10K Grout In Reinforced Cells Load Deformation Curves	198
Figure 4.7	Shear Test Of Joints With Vinyl Flashing, #4 Reinforcing Bar, Mortar Grout In Reinforced Cells Load Deformation Curves	199
Figure 4.8	Section Of Grouted Bond Beam Brick Next To Vinyl Flashing	200
Figure 4.9	Shear Test Of Joints With Vinyl Flashing, #4 Reinforcing Bar, 10K Grout In All Cells Load Deformation Curves	201

Figure 4.10	Shear Test Of Joints With Vinyl Flashing, #6 Reinforcing Bar, 10K Grout In Reinforced Cells Or All Cells Load Deformation Curves	202
Figure 5.1	Sketch Of Wall Specimen elevations	203
Figure 5.2	Specimen Support And Loading Configuration	204
Figure 5.3	LVDT Locations On Wall Specimen	205
Figure 5.4	Photographs Of Wall Specimens	205
Figure 5.5	Photographs Of Specimen #2 And #3 Failures	206
Figure 5.6	Small Scale Test Wall Specimens Load Deflection Diagram	207
Figure 5.7	Load Deformation Curves For LVDTs At Center Of Specimen #2	208
Figure 5.8	Small Scale Test Wall Specimens Moment Versus Total Rotation Curves At Mid span	209
Figure 5.9	Comparison Of Idealized Joint Deformation Curve With Shear Test Results Divided By 2 For Joints With Vinyl Flashing, #4 Reinforcing Bar and 10K Grout In All Cells	210

Figure 5.10	10K Grouted Prism Stress Deformation Curves - Specimens 2 & 3, Linear Load Deformation Curve For Brick Wall, And Equivalent Stress Block For Ultimate Bending Strength Compression Load	211
Figure 5.11	Comparison Of Measured And Predicted Moment Versus Total Rotation Diagrams At Mid Span Of Wall Specimens	212
Figure 5.12	Comparison Of Measured And Predicted Load Versus Vertical Deflection Diagrams At Mid Span Of Wall Specimens	213
Figure 7.1	Moment And Deformation Of Wall As Subsidence Face Moves Under Wall	214
Figure 7.2	Sketch Of Example Brick Wall Subject To Concave Curvature Due To Subsidence	215
Figure 7.3	Diagram Of Moment Versus Curvature For Subsidence Example Wall	216

MATHCAD NOTATION USED IN CALCULATIONS

(Mathcad, 1995)

In this table:

A and B represent arrays, either vector or matrix.

x and y represent real numbers.

m and n represent integers.

i represents a range variable.

t represents any variable name.

f represents a function.

X and Y represent variables or expressions of any type.

file is either a filename or a variable associated with a filename.

Operation	Appearance	Description
Parentheses	(X)	Grouping Operator
Subscript	A_n	Returns indicated element of an array
Superscript	$A^{<n>}$	Extracts column n from array A. Returns a vector.
Vectorize	$\vec{X}$	Forces operations in expression X to take place element by element.
Power	x^y	Raises x to the power y.

Square Root	$\sqrt{x}$	Returns square root of x
Division	$\frac{X}{y}$	Divides the expression X by the non-zero scalar y.
Multiplication	$X \cdot Y$	Returns the product of X and Y if both X and Y are scalars. Multiplies each element of Y by X if Y is an array and X is a scalar.
Addition	$X + Y$	Performs scalar addition if X,Y, or both are scalar. Performs element by element addition if X and Y are vectors or matrices of the same size. If X is an array and Y is a scalar, adds Y to each element of X.
Subtraction	$X - Y$	Performs scalar subtraction if X, Y, or both are scalar. Performs element by element subtraction if X and Y are vectors or matrices of the same size. If X is an array and Y is a scalar, subtracts Y from each element of X.
Less than or equal	$x \leq y$	returns 1 if $x \leq y$, 0 otherwise. x and y must be real scalars.
Conditional function	**if(cond ,x ,y)**	Returns x or y depending on value of cond. If cond is true (non-zero), returns x. If cond is false (zero), returns y.
Maximum	max(A)	Returns largest element in A. Returns a scalar.
Mean	mean(A)	Returns the mean of array A. Returns a scalar.

Median	median(A)	Returns the median of array A. Returns a scalar.
Read file	READPRN(file)	Matrix read from structured data file file.
Defining a variable	t := X	Defines t as the variable or expression X.
Defining a function	f := X	Defines f as the variable or expression X.
Defining a range variable	i := m .. n	Defines i as a range variable with the values m, m+1, m+2, ... n.
Defining an array	$A := \begin{pmatrix} \blacksquare & \blacksquare & \blacksquare \\ \blacksquare & \blacksquare & \blacksquare \\ \blacksquare & \blacksquare & \blacksquare \end{pmatrix}$	Defines A as an array consisting of the values, variables or expressions shown.
Evaluating a variable or expression	X =	Returns the scalar value of X.

LIST OF SYMBOLS

This list identifies and describes symbols for variables used as data input and the summary of results for calculations. File names, functions, and variables identified within calculations and used to simplify the computational process are described or identified symbolically as part of the computation process.

Symbol	Description
A	Net cross-sectional area of specimen
AsN	Cross-sectional area of a #N reinforcing bar
b	Section width for bending calculations
BaN	Pull-out strength of #N reinforcing bar based on masonry or steel strength, whichever is less
BamN	Pull-out strength of #N reinforcing bar determined based on masonry strength. Strength is estimated by using the ACI 530 (Building, 1992) code method and multiplying the resulting value by five
BasN	Pull-out strength of #N reinforcing bar determined based on steel yield strength and area of the reinforcing steel
c	Distance from the outermost compression fiber to the neutral axis of a beam
cfM	Coefficient of friction for flashing material M. If M is omitted, value

	applies to PVC flashing
cfratio	Coefficient of friction correction factor for the use of Copper flashing in lieu of PVC flashing in the joint
d	Section depth for bending calculations. Depth is defined as the distance from the centroid of the section tensile force element to the outermost member fiber in compression.
E(cond)	Modulus of Elasticity corresponding to conditions indicated by (cond)
f(cond)	Stress corresponding to conditions indicated by (cond)
Fm	Compressive strength of masonry
FyN	Tensile yield strength of #N reinforcing bar used based on test reports. If N is omitted, data for a #4 reinforcing bar is used
h	Brick wall height from the flashing joint at the bottom of the wall to the top of the bond beam at the top of the wall
I(cond)	Moment of inertia corresponding to conditions indicated by (cond)
j(cond)	Ratio of the distance between the centroid of compressive and tensile forces to the depth d corresponding to conditions indicated by (cond)
JtN	Flashing joint shear capacity for each #N reinforcing steel dowel crossing the joint
k(cond)	Ratio determined by the distance from the neutral axis of a beam to the outermost fiber in compression divided by the depth d corresponding to conditions indicated by (cond)
L(cond)	Span length corresponding to conditions indicated by (cond)

LbtN	The edge distance used in estimating pull-out strength for #N reinforcing bars
M(cond)	Moment corresponding to conditions indicated by (cond)
n(cond)	Stiffness ratio corresponding to conditions indicated by (cond)
N(cond)	Number of reinforcing steel corresponding to conditions indicated by (cond)
p(cond)	Area ratio of compression and tension elements indicated by (cond)
P(cond)	Load corresponding to conditions indicated by (cond)
tmj	Mortar joint thickness
T(cond)	Tensile force corresponding to conditions indicated by (cond)
Tubrick	Tensile strength of brick
Twallbrick	Net thickness of the brick wall
$\beta 1$	Equivalent stress block width factor
$\beta 3$	Equivalent stress block stress amplification factor
δ(cond)	Change corresponding to conditions indicated by (cond)
Δ(cond)	Deflection corresponding to conditions indicated by (cond)
ϕ(cond)	Section rotation corresponding to conditions indicated by (cond)

Chapter 1

Introduction

1.1 Purpose

The purpose of this research is to determine how to use the compressive strength of a reinforced hollow brick wall and the tensile strength of its foundation, when they are separated by flashing, to create a composite wall with stiffness and/or strength capabilities significantly greater than the capabilities of the individual elements. This design problem can not be solved by literature reviews and computations without testing because the shear transfer behavior of the structural system consisting of the flashing joint and the reinforcing steel crossing it has not been assessed. The process of developing a methodology to achieve and analyze the desired composite action involved developing answers to three questions:

1. What construction details are necessary, in addition to those normally used, to reliably transfer shear loads associated with in-plane bending from a reinforced hollow brick wall to a reinforced wall or concrete beam separated from the brick wall by flashing?

2. What numerical models are appropriate to (a) analyze shear transfer at a flashing joint and (b) analyze composite beam behavior for the reinforced hollow brick wall and its foundation?
3. What methodology, including assumptions and computational methods, is appropriate for design of composite reinforced hollow brick walls and their foundations for in-plane moments when they are separated by a flashing joint?

The hollow brick used in this research is the Suprking brick manufactured by the General Shale Co. of Johnson City, Tennessee. A sketch of the Suprking brick is shown in Figure 1.1.* In addition, photographs of the Suprking brick standard unit, both whole and split in half, and bond beam unit, both with and without flanges removed for use as a bond beam, are shown in Figure 1.2. The Suprking brick was used for this research because of (a) its availability, together with other masonry materials, from General Shale Co. without cost, and (b) its use as part of a self-supporting wall system with a flashing joint at its base to eliminate the need for exterior coatings and facilitate movement of moisture from the inside to the outside of the wall.

1.2 Summary

Several construction details were identified as necessary to provide ductile behavior of the composite system and assure predictable strengths are achieved. The details

were developed by testing alternative designs and developing details during the process to eliminate brittle failure modes and premature failure. The details and the tests associated with them are as follows.

1. Several preferred details associated with grouting the first two courses of the brick wall next to the flashing joint were identified by testing shear specimens with different grouting patterns. This dissertation identifies evaluation techniques for use in evaluating flashing joints where these details are not provided; however, using these details substantially increases ductility and load capacity of flashing joints. (a) The cells of the first two courses of the Suprking brick wall above the flashing joint must be grouted on either side of the vertical reinforcing steel crossing the flashing joint. (b) The grout must be continuous from the cells with reinforcing steel in them to their adjacent cells. This should be achieved by using a bond beam unit in the first course of the brick wall above the flashing joint. The bond beam unit should have appropriate flange pieces removed and be orientated with the open side down on either side of grouted cells with reinforcing steel. (c) The grout in the first two courses of brick next to the flashing in the reinforced cells and their adjacent cells should be Sonogrout 10K or similar grout with a 28 day strength of at least 4300 psi (pounds per square inch). Either thinned mortar grout or other grout may be used in the other cells around the vertical reinforcing bars provided anchorage of the bars on either side of the flashing joint is achieved.

---

* Figures and tables are included in the appendix.

2. The maximum size of reinforcing steel which should be used to transfer shear at the flashing joint is a #4. This requirement is based on comparison of results from testing shear specimens with #4 and #6 steel reinforcing bars. The #6 bars failed the brick before developing either the strengths or deformations expected for ductile behavior.
3. The preferred minimum spacing of reinforcing bars crossing the flashing joint is twenty (20) inches. This preference is based on failure of the small wall specimens with #4 bars at ten (10) inches center to center at smaller loads and deformations than would be expected based on results from testing of the walls with #4 bars at twenty (20) inches on center. Analysis indicates that reinforcing spacing of 15 inches center to center is also acceptable; however, this reduced spacing was not included in the testing performed as part of this research.

A numerical model which combines features of concrete beam strength design and hinged arch analysis was developed which predicted the behavior of the small scale test walls. The analysis procedure is broken into three related modeling steps.

1. The model used to estimate ultimate strength is similar to the one used for concrete beams except that the compression stress block for the brick wall is based on prism tests and the deformation properties of the shear joint based on shear specimen tests are used.

2. The model used to estimate deflections prior to initial tensile cracking of the brick wall uses the uncracked section moment of inertia and classic beam behavior to predict deflections.
3. The model for estimating deflection of a wall with tensile cracking assumes compression deformation consistent with prism tests and rigid body deformation at the shear joint based on data from the shear specimen tests.
4. Maximum deflections of the wall may be based on ultimate deformation of the shear joint based on shear specimen testing. This implies that brick joint strains will exceed values determined based on prism testing due to the relative stiffness of the flashing joint and the brick wall. This provision is considered acceptable because (a) wall tests confirm the large deflections associated with flashing joint deformations; and (b) the presumption that confinement of unevenly loaded mortar, which will occur in the joints between bricks in the top course of the wall, will facilitate greater joint deformations than observed during prism tests.

The design methodology developed to implement these findings is presented using a series of requirement statements, a computer program which automates the computation process, and a series of examples based on problems reported in literature or experienced by this author. The examples include a case of extreme loading associated with mining subsidence, a text book example of preventing damage due to expansive soil conditions by concentrating loads using a wall footing

spanning between areas of concentrated load, and an abnormal, but expected, condition associated with coastal storm damage.

1.3 Conclusion

This research develops and demonstrates a methodology for the composite design of steel reinforced brick masonry walls and concrete beams separated by a flashing joint for in-plane bending loads. The availability of this methodology enables the designer to select between (a) using the inherent strength of the flashing joint or (b) providing horizontal reinforcing in a hollow brick wall to resist moments resulting from in-plane forces. Using the inherent strength of the system offers an opportunity to accommodate extreme or abnormal loads associated with unlikely events at minimal cost. This is most effective when governing codes do not address the design conditions being considered allowing the designer to assign margin appropriate to the risk involved. For conditions which require large margins, such as those stipulated by ACI 530 (Building, 1992), the installation of horizontal reinforcing to resist loads may be more appropriate.

Chapter 2

Background

2.1 Introduction

Brick is one of the oldest building materials. One of its primary uses in modern construction is as solid masonry functioning as a veneer to cover and protect structural building elements while providing a pleasing appearance. This use has gained wide acceptance based on the pleasing appearance of the material and the ability of the veneer, when used with a drained gap behind the veneer, to resist the elements with minimal maintenance. Brick, when used as a veneer, is anchored to building structural elements to transfer lateral loads and eliminate brick wall instability problems. The only functions of a brick veneer are thus to support its self weight in axial compression and satisfy architectural requirements related to appearance, low maintenance and permanence, and resistance to weather.

As discussed by Schneider and Dickey (1994), hollow bricks were developed in the 1940s. Hollow bricks were originally conceived as hollow clay units similar in size and shape to hollow concrete block except they were made of fired clay. The use of fired clay in hollow unit masonry offers several advantages including:

a) The ability to develop compressive strengths much higher than concrete masonry

b) Face shell thickness and cross web dimensions similar to concrete block

c) Cell sizes and areas appropriate for placement of grouted reinforcement

d) Significant fire ratings for the wall system.

ASTM C652 (Standard, 1991) provides requirements for hollow brick. Hollow bricks may have a void ratio, measured as the ratio of the area of cells and/or cores to gross area, of 25% to 60%. Units with less than a 25% void ratio are classified as solid, units with more than a 60% void ration are classified as tiles. Hollow brick units also have more stringent physical property requirements for shell and web dimensions and compressive strength than structural clay tile.

Schneider and Dickey (1994) provide several examples demonstrating the design of reinforced brick walls using hollow bricks. Two common sets of hollow brick dimensions are provided in this text and used in the examples, a 4 ½ inch thick unit and a 7 ½ inch thick unit. Both units are 3 ½ inches high and 11 ½ inches long and are available in regular or bond beam units. A second feature of the examples provided is that the base of the brick walls are constructed directly on top of their foundation with no provision for flashing or removal of water from the inside of the wall at the base of the wall. In one example, based on a warehouse, the brick is founded on a concrete foundation four feet below grade.

The General Shale Company of Johnson City, Tennessee, is one of the largest manufacturers of bricks in the United States. Most of their production consists of solid brick generally used in veneer wall construction. In an effort to expand their market, they developed and began marketing a hollow brick which they designate a Suprking brick. General Shale's intent in developing the Suprking brick was to create a product which would be competitive with other wall systems for use in residences and light industrial buildings.

The Suprking system is different from the hollow brick system considered by Schneider and Dickey (1994) in several significant ways associated with perceived goals of the Suprking system. The major goals implicit in the design of the Suprking system include (a) the desire to make the Suprking wall look like a brick veneer wall, (b) the recognition that brick cannot be permanently waterproofed from the outside without significant expense and change in appearance, and (c) the objective that the use of the Suprking brick system eliminate the need for redundant wall systems. The brick dimensions, which are shown in figure 1.1, were selected such that the length of individual bricks is slightly greater than the dimension of a common building brick. The height of the brick is the same as an engineer or queen size brick. This size results in a brick wall having the same appearance as a common brick veneer wall. Waterproofing of the Suprking wall system is achieved using insulation with a moisture barrier facing the brick wall against the inside face of the wall. Any water or moisture collected between the insulation's moisture barrier and the inside face of the brick wall is drained at the bottom of the wall using flashing. The flashing,

which is commonly vinyl flashing, is attached to the insulation and passed under the bottom of the wall so that moisture moves from the inside to the outside of the wall.

The hollow bricks used in the Suprking wall system support both environmental and gravity loads associated with the building structure thus eliminating the need for a separate supporting wall as is used in brick veneer construction. References, such as Schneider and Dickey (1994), provide design details and methodologies which may be used to design and construct the various elements of the Suprking system with the exception of the flashing joint at the bottom of the wall.

This research has two primary goals focused on the structural capability of the flashing joint used at the bottom of the Suprking brick wall system. The first goal is to develop details for vertical reinforcing steel which crosses the flashing joint and which is used to develop wall strength. As part of this goal, (a) bar size, (b) the use of grouting, and (c) the need for bond beam bricks at the flashing joint are evaluated. The second goal is to develop a methodology to assess the structural behavior of a flashing joint with reinforcing bars crossing it. Specifically, this goal is focused on (a) determination of the shear load and deformation characteristics of the flashing joint and (b) the use of this information to assess wall response to in-plane bending loads.

2.2 Flashing Joint Forces Associated With In-plane Bending Due To Vertical Displacements

In-plane bending loads occur in a wall as a result of lateral loads on the structure, such as those due to wind and seismic activity, and vertical displacements, such as those due to subsidence, expansive soils, and loss of support under foundations. The lateral loads are resisted by vertical loads in the ends of the wall elements and horizontal shear in the wall. The in-plane moments associated with vertical movement result in horizontal forces at the top and bottom of the wall and vertical shear. The focus of this research is horizontal loading occurring in the flashing joint at the bottom of the wall due to the transfer of horizontal tension forces from the wall to the foundation. Horizontal tension forces at the bottom of the wall due to vertical displacements must be resisted by either additional horizontal steel in the wall above the flashing joint or transfer of forces through the flashing joint if they are to be resisted. This research develops the methodology necessary to use the flashing joint to resist the horizontal tension forces due to vertical displacements causing in-plane bending.

2.3 Suprking Brick Wall System

A sketch of the wall system proposed by the General Shale Company, Johnson City, Tennessee, is shown if figure 2.1. A picture of a small industrial building using this system is shown in figure 2.2. The major features of the wall system and their functions are as follows.

a) The wall exterior is Suprking brick which does not require coating. The mortar and grout used in the brick wall also do not require coating since moisture which may penetrate the wall is removed from behind the wall surface by the vinyl flashing.

b) The reinforcing steel bar is located in a brick cell and grouted. The construction method for the wall includes special provisions to facilitate grouting of cells with reinforcing steel after the wall is constructed. This eliminates the need to slip bricks over steel bars during construction.

c) Sheet metal "z" shaped beams are attached to the back side of the brick wall. Insulation, with its moisture barrier facing the brick, and fiberglass studs are supported by the sheet metal "z" beams.

d) A flashing joint with weep holes is provided to assure drainage of moisture collected in the air gap to the outside of the wall. The vinyl flashing is taped to the insulation to contain moisture and prevent it from entering the building.

e) Insulation is provided with damp proofing to prevent migration of moisture into the building and to improve the thermal resistance of the wall system.

f) Fiberglass studs attached to the sheet metal supports provide access space for electrical distribution systems and other utilities.

g) Wall board provides a finished architectural surface for the interior of the building and protects the insulation and other materials from fire.

This wall system provides structural support for building components and resists environmental loads such as wind and seismic effects if properly designed. Based on

marketing studies by General Shale Co., this wall system is competitive with wood wall systems and substantially less expensive than brick veneer and wood wall systems due to the combined structural and architectural functions of the Suprking brick wall.

2.4 Brick Prism Strength

Brick prism strength is an important variable is determining wall strength. For this research, it is determined for the Suprking brick system by testing. The values determined by test are used in evaluating wall bending capacity related to compression in the top course of brick in the wall.

The mechanism for failure of masonry prisms is a tensile rupture at right angles to the direction of compressive strain Mayes and Clough (1975). Based on this observation, numerical models have been developed to estimate prism strength. Paulay and Priestley (1992) presents a methodology, which is also discussed in Mayes and Clough (1975), in which prism strength is related to brick compressive strength and mortar strength. Mortar and brick compressive strength are determined by test for the materials used in this research. This method is demonstrated in chapter 3 as a procedure to estimate prism strength.

2.5 Flashing Joints, Shear Friction and Shear Dowels

Flashing joints are normally used at the bottom of brick veneer walls to transfer moisture from behind the wall to outside the building. For the Suprking brick wall system they are used for the same purpose as shown in figure 2.1.

Flashing joints may be constructed with vinyl sheeting, as was used for this research, or with sheet metal. When sheet metal is used, it is commonly copper sheet often with a paper backing or lead coating to assure its use as flashing. Flashing may be galvanized steel sheet metal; however, this is less desirable than copper due to corrosion over the life of the building.

Flashed joints have minimal structural function in a veneer wall. Veneer walls may be adhered directly to the building or tied to the building with anchors. Anchored brick veneer walls are constructed assuming that vertical loads are transferred through the flashing joints. The veneer ties between the building and the veneer resist all lateral loads. Probably due to the fact that flashing joints have minimal structural requirements and have functioned will for many years, very little testing on the shear behavior of joints with flashing has been performed.

During the planning of the laboratory research associated with this dissertation, it became evident that data on the behavior of a flashing joint with reinforcing steel dowels was not available. In order to assist in understanding the overall behavior of

the flashing shear joint, the major issues identified and associated findings of the research are summarized as follows.

a) The basic mechanism of shear transfer was not understood. It is important to identify the mechanism of shear transfer because it impacts the design and evaluation of the dowels. The three mechanisms possible for shear joints in general are bond, dowel action, and friction. Bond is not considered viable for the flashing joint because the flashing interrupts the masonry such that virtually no bond exists. Thus, only dowel action and friction are considered viable possibilities for shear transfer. As discussed, flashing joint strength and ductility are such that it is concluded that the basic mechanism of behavior is shear friction and not dowel action.

b) The basic mechanism of load resistance for the dowels was not understood because the mechanism of shear transfer was unclear. Based on the recognition that shear transfer is by shear friction, and not dowel action, it is concluded that the primary mechanism of load resistance required for the dowels is tensile pull-out, not shear. This provides a basis for the focus of subsequent evaluations on the tensile capacity of anchors as influenced by edge distance.

c) As discussed in Schneider and Dickey (1994), embedment capacity is generally based on a pull out of a conical section of the masonry. However, since hollow brick masonry is heterogeneous, actual values for pull out have been determined by test

or judgment. The consensus judgment prescribed by ACI 530 (Building, 1992) indicates very low dowel tensile capacities based on edge distance to the side of the brick wall adjacent to the reinforcing bar dowels. Concern about the effect of this small edge distance created doubt before the first tests were conducted as to whether or not flashing shear joints are a viable method for transfer of significant shear loads. The first shear test, as well as all the other tests, demonstrated that this concern was unfounded for #4 reinforcing bars and that tensile capacity significantly exceeds predictions based on edge distance to the side of the wall. Testing eventually demonstrated that a Suprking brick wall can develop the steel tensile yield strength of a #4 reinforcing bar if the bars are spaced far enough apart. Additional testing to assess the behavior of bars larger than #4 demonstrated that the steel yield strength of a #6 reinforcing bar cannot be developed no matter what spacing is provided due to the fact that failure by bursting toward the sides of the wall occurs as would be expected due to small edge distance. Based on these data, it was concluded that only longitudinal spacing of #4 reinforcing bar dowels needed to be considered when determining edge distance for Suprking walls.

The results comparing shear tests results and edge distance imply that the model associated with the pull-out behavior of the dowels crossing a flashing joint is different from the model implied by ACI 530 (Building, 1992) design equations. The pull-out failure mode may be represented by a cone if the material is homogenous. However, as discussed by Schneider and Dickey (1994), masonry is a heterogeneous assemblage of masonry unit material, mortar, and grout. Thus, pull-out capacity

should be based on tests or judgment. Based on the shear and beam tests reported by this research, the failure mode for the Suprking hollow brick system may be represented by cropped cone as sketched in Figure 2.3. The cropped cone failure mode results from the substantially greater strength of the brick as compared to the grout used in the Suprking assemblage.

d) When comparing shear specimen edge distance and shear joint dowel spacing to assess edge distance requirements, it must be recognized that the configuration of the shear specimen results in substantially greater confinement of the masonry above the dowel than below the dowel on the outer pairs of bricks. Since flashing shear joints will provide little confinement to prevent pull out of the masonry around the dowel, spacing requirements should be based on the edge distance below the dowel in the shear specimens. Based on the symmetry of the cropped cone failure mode, it is concluded that the longitudinal distance should be assumed symmetrical about the dowel in a flashing joint. Thus, spacing requirements for different edge distances are established by doubling the distance below the dowel of the shear specimen used to determine flashing joint behavior for different dowel spacing.

e) Based on these evaluations, the numerical model for the flashing shear joint was determined to include: a) basic joint behavior is shear friction, b) dowel tensile capacity governs joint behavior, c) edge distance for dowels is based on longitudinal dowel spacing, not the distance to the sides of the wall, and d) longitudinal spacing

requirements should be based on twice the distance from the dowel to the bottom of the outside pairs of bricks of the shear specimen.

As shown in subsequent sections, the behavior of wall specimen flashing joints is reasonably well predicted using the model summarized above with the coefficient of friction for PVC joints measured by McGinley and Borchelt (1989) and tensile yield strength test reports for the #4 reinforcing bars used in the specimens. Published test results and calculations associated with developing and quantifying this model of flashing joint behavior are discussed in the following sections. Comparison of test results and model predictions are provided in subsequent chapters.

2.5.1 Mechanism Of Shear Transfer

As previously discussed there are two possible methods of shear transfer at a flashing joint with reinforcing steel crossing the joint: (a) friction and (b) dowel bending, shear or kinking. Shear friction, which is limited by the flashing materials, results in small displacements until friction capacity is achieved. Dowel action is usually of limited structural significance because of the large displacements required to develop shear capacity Park and Paulay (1975).

Shear friction in concrete materials is associated with interlocking of materials on the two sides of the construction joint as discussed by Park and Paulay (1975). This mechanism is prevented by the placement of flashing at the base of a brick wall.

Thus test results generally available on joint behavior are inapplicable to the flashing joint.

McGinley and Borchelt (1989) reported a series of tests on the shear behavior of flashing joints with small normal forces associated with weight of veneer walls. The joints tested had no reinforcing or other ties connecting the brick wall above the flashing joint to the structure below. The tests were intended to simulate a one story brick wall resting on a flashing joint and subject to normal loads due to the weight of the wall and an applied shear force. The tests represent substantially different conditions than the Suprking wall flashing joint due to the large forces which are mobilized by the reinforcing steel crossing the shear joints. However, subsequent tests performed as part of this research indicate that the coefficient of friction remains relatively constant for PVC flashing both with and without dowels.

The tests reported by (McGinley and Borchelt,1989) determined that the coefficient of friction measured in all directions for a joint with flashing was approximately 0.5. The results of the testing are summarized in table 2.1. The use of PVC (vinyl) flashing resulted in slightly higher values of coefficients of friction, however, all the values result in low horizontal shear stress capacity of approximately 4 pounds per square inch (psi). This is not an issue in the design of anchored veneer walls since lateral load is transferred to the building by the anchors.

Park and Paulay (1975) report results of #4 shear dowel behavior tests consisting of applying load on a concrete construction joint which is waxed to prevent bond and has dowels crossing the joint. Based on these tests, Paulay and Priestley (1992) conclude that dowel action is capable of developing 25% of the axial strength of the dowel as a shear force. Figure 2.4 compares flashing joint load deformation estimates for #4 dowels associated with several different modes of behavior as follows.

a) The behavior of steel shear dowels is estimated based on test results summarized by Park and Paulay (1975).

b) Shear friction behavior is estimated using (i) results reported by McGinley and Borchelt (1989) for the in-plane coefficient of friction for flashing joints using PVC with small normal loads and (ii) normal loads associated with the yield strength of the #4 reinforcing bars as reported in section 3.14 . The coefficient of friction used in this estimate is 0.471.

c) Results from testing a fully grouted shear specimen with a #4 reinforcing bar, divided by 2 to account for the two shear faces of the shear specimen, are plotted.

d) The idealized curve for flashing joint design, which is developed in Chapter 5 and shown in figure 5.9, is plotted.

Review of figure 2.4 shows that flashing joint behavior is controlled by dowel behavior at forces up to the yield, or change in the load deflection behavior, of the dowel at approximately 25% of the #4 dowel axial capacity. At higher loads, the

behavior is controlled by a combination of friction and dowel behavior. Strength and deformation of the flashing joint are significantly greater than would be associated with dowel behavior. Thus, joint behavior at ultimate strength is controlled by shear friction behavior.

2.5.2 Effect Of Dowel Spacing On Flashing Joint Shear Capacity

As discussed, shear capacity of the flashing joint is controlled by friction behavior. The tensile capacity of the reinforcing bars crossing the joint thus determines the ultimate shear load on the joint because shear friction is dependent on normal loads associated with tensile capacity of the reinforcing steel.

The provisions of ACI 530 (Building, 1992) were used to make a preliminary estimate of tensile capacity of the reinforcing steel dowels neglecting the effects of hollow brick wall heterogeneity. Since the code provisions are written with a factor of safety of 5, the equations provided in ACI 530 are increased by a factor of five when used to estimate ultimate strength. The ultimate strength of the flashing shear joint for each reinforcing steel dowel assuming different edge distances is estimated as follows.

a) Symbols used in this calculation are assigned as described as follows. Numerical values associated with the constants are then assigned based on test data or physical dimensions of the Suprking hollow brick.

Fm = ultimate strength of the grouted masonry

Fb = strength of the hollow bricks

Fg = strength of the 10K grout

Fy4 = yield strength of the #4 reinforcing bar

As4 = cross sectional area of a #4 reinforcing bar

Fy6 = yield strength of the #6 reinforcing bar

As6 = cross sectional area of a #6 reinforcing bar

cf = Coefficient of friction based on the value shown in table 2.1 for PVC in-plane average static conditions. This coefficient of friction is adjusted using test results to develop a similar curve for design as shown in figure 4.1.

$Fm := 4400\,psi$ $Fy4 := 69.8\,ksi$ $As4 := .2\,in^2$ $Fy6 := 80.2\,ksi$

$As6 := .44\,in^2$ $cf := .521$

b) Length vectors, Lbt4 and Lbt6 for #4 and #6 bars respectively are calculated to generate a smooth curve. The expected joint capacity vectors, Jt4 and Jt6, are then calculated using the length vectors. The capacity vectors for the #4 reinforcing bar are calculated as follows. The calculations for the #6 reinforcing are performed similarly.

The pull-out strength of the dowel considering masonry strength, Bam4, is estimated as follows. $Bam4 := 0.5 \cdot \pi \cdot \overrightarrow{Lbt4^2} \cdot \sqrt{Fm \cdot psi} \cdot 5$

The pull-out strength of the dowel considering steel yield strength, Bas4, is estimated as follows. $Bas4 := As4\ Fy4$

The pull-out strength of the dowel, Ba4, is estimated using an "if" statement to select the smaller of the two values Bam4 and Bas4. This is identical to the procedure used in ACI 530 (Building, 1992).

$$Ba4_{n4} := if\left(Bam4_{n4} \le Bas4, Bam4_{n4}, Bas4\right)$$

The flashing joint shear capacity for each dowel is then calculated by multiplying the dowel pull-out load by the coefficient of friction.

$$Jt4 := Ba4 \cdot cf$$

c) The results obtained by these calculations are based on edge distance in the longitudinal direction of the wall. In order to account for the effect of shear model behavior versus the effective length in a wall joint, the confinement at the top of the outside portion of the shear specimen must be considered. Figure 2.5 shows a sketch of the shear specimen and a free body diagram of the left side of the shear specimen during loading. As shown in the free body diagram, as load is increased on the inside two bricks, shear friction forces will be developed on the PVC flashing interface between the inner and outer pairs of bricks. A normal force will develop due to reinforcing bar tension offset by distributed normal forces on the joint. The shear friction force will off set upward distributed forces on the outside pair of bricks due to the load. Due to the geometry of the specimen, an area of confined masonry will develop at the top of the outer two bricks. As a result, tension failure of the reinforcing steel will result from the edge distance from the steel dowel to the end of the grouted brick masonry in the downward direction of the free body diagram. Since there will be no area of confined masonry in a shear joint with flashing, there

will need to be an equal length of grouted brick masonry on both sides of the dowel. In summary, it is judged that an equal length of grouted brick masonry is required on both sides of the dowel to develop the tensile forces, and associated shear friction forces, observed during shear specimen testing. To account for this judgment and minimize possible confusion in the use of related figures, the distances calculated as Lbr4 and Lbr6 are doubled in figure 2.6 and associated figures and data developed in subsequent sections.

The results of these calculations assuming projected lengths are doubled to account for confinement of the shear specimens are shown in figure 2.6. Using this figure, the capacity attributable to each steel reinforcing bar crossing a shear joint with flashing may be estimated based on the projected length of the wall attributable to each reinforcing bar.

2.5.3 Effect Of Flashing Material On Flashing Joint Shear Capacity

Table 2.1 provides coefficient of friction values for PVC and Copper flashing. Flashing joint dowel capacity may be estimated using this data since dowel capacity is dependent on the coefficient of friction at the joint. As shown by shear specimen testing, the data presented by McGinley and Borchelt (1989) may be used with the higher loads associated with the tensile yield strength reinforcing steel dowels. The data for the coefficient of friction for PVC, cfpvc, and Copper, cfcu, flashing were used to determine the minimum coefficient of friction ratio, cfratio, for use as a

correction factor for flashing joints using Copper flashing in lieu of PVC flashing. The minimum value of cfratio is calculated as follows.

$$n = 0..3 \qquad cfpvc := \begin{bmatrix} .521 \\ .695 \\ .471 \\ .650 \end{bmatrix} \qquad cfcu := \begin{bmatrix} .430 \\ .454 \\ .397 \\ .428 \end{bmatrix}$$

$$cfratio_n := \frac{cfcu_n}{cfpvc_n} \qquad cfratio = \begin{bmatrix} 0.825 \\ 0.653 \\ 0.843 \\ 0.658 \end{bmatrix} \qquad \min(cfratio) = 0.653$$

Based on these calculations, the effect of Copper flashing on flashing joint dowel capacity may be determined by multiplying the appropriate dowel capacity by the minimum value of cfratio, 0.653.

2.6 Masonry Wall In-plane Bending

The structural behavior of a masonry in response to in-plane bending can be described by three stages: uncracked section, cracked section, and ultimate capacity (Schneider and Dickey 1994). These three stages are used in the calculations to model the behavior of small scale test walls in chapter 5 and to assess the behavior of example walls in chapter 7. The stages of bending described by Schneider and Dickey (1994) are similar to the stages suggested in other texts for design of concrete, such as Winter et. al. (1964) and Park and Paulay (1975), and masonry Paulay and Priestley (1992).

2.6.1 Uncracked Section Bending

A masonry beam in bending behaves as an uncracked section when tensile stresses in the materials, including steel reinforcing, are less than the tensile strength of the respective materials. This may be described with the following three conditions.

a) Strains are linear over the beam cross section. Sections that are a plane before bending remain plane after bending.

b) Stresses are proportional to their distance from the neutral axis.

c) Strain is small enough that masonry, as well as steel, resists tensile loads below the neutral axis.

2.6.2 Cracked Section Bending

A masonry beam in bending behaves as a cracked section when the following four conditions may be assumed to exist. These conditions are associated with moderate bending loads which result in tension strains large enough to crack, or fail, the masonry in the tension region of the beam thus transferring tensile load to reinforcing steel.

a) The neutral axis of the section moves upward causing a reduction in masonry compression area.

b) Strains remain linear over the cross section

c) Compressive stresses, which are developed entirely in the uncracked compressive section of the beam, remain elastic.

d) Tensile stresses, which are resisted entirely by reinforcing steel, are proportional to their distance from the neutral axis. Tensile stresses in uncracked concrete or masonry near the neutral axis of the section are neglected in this analysis.

2.6.3. Ultimate Capacity

Ultimate capacity for in-plane bending is the load at which failure is predicted to occur. The failure may be due to compression of the masonry or yielding of the reinforcing steel in tension. In either case, eventually failure will occur due to masonry compression due to large inelastic strains in the tension steel. However, the structure will deform substantially before failure if the tension steel yields prior to failure of the masonry. At the ultimate capacity of a masonry beam conditions may be described as follows (Schneider and Dickey, 1994).

a) The neutral axis moves further upward reducing the masonry compression area even further.

b) Strains are assumed to remain linear throughout the section.

c) If the tension steel yields before the ultimate capacity of the masonry is reached, the steel will yield thus governing the capacity of the section.

d) If the compressive capacity of the masonry is reached first, the stresses will no longer be proportional to the distance from the neutral axis and masonry compression will govern the capacity of the section.

2.6.4 Compression Stress Block For Masonry

The compressive stress block used to evaluate the ultimate bending behavior of masonry may be developed using the same techniques as are used for concrete beams (Paulay and Priestley, 1994). Using the results of prism tests, the stress-strain curves are used to develop equivalent parameters. A rectangular stress block

configuration is used to develop an equivalent stress block in Paulay and Priestley (1994). A similar method is used in Tawresey (1993) to develop a trapezoidal shaped stress block for concrete masonry. For this dissertation a rectangular stress block is developed because of (a) its ease of use and (b) the observation that ultimate moments are relatively insensitive to the location of the centroid of masonry compression due to the large section heights and small compressive regions associated with masonry walls.

2.6.5 Effect Of Flashing Joint On Beam Behavior

The results of this research show that several of the assumptions described above must be modified for analysis of hollow brick walls subjected to in-plane bending moments where tensile capacity of the wall is provided by shear at a flashing joint. Assumptions associated with uncracked sections provided reasonable results when compared with wall test results for initial loading prior to wall cracking.

The major changes to the cracked section and ultimate capacity analysis were as follows.

a) Due to the low relative stiffness of the shear joint when compared to the masonry, compressive yielding of the masonry is usually reached at moments only slightly larger than moments required for initial section cracking.

b) Displacement is determined by rigid body rotation at the cracked section. The procedure used for concrete beams, where displacements may be calculated

by estimating an equivalent moment of inertia and using homogeneous beam theory to predict displacements (Building, 1989), is inappropriate.

c) Joint mortar strains, in lieu to global masonry prism strains, should be used to estimate masonry compressive behavior. This is because the joint has substantially less compressive strength and more inelastic strain than the hollow brick units included in the masonry.

d) The shear capacity associated with all the vertical reinforcing steel crossing the flashing joint will be developed. This is similar to the behavior observed for shear dowels used in composite concrete and steel beam design as described in Salmon and Johnson (1990) and the AISC code (Manual, 1986).

e) Wall failure occurs due to shear deformation at the flashing joint exceeding limits for the vertical reinforcing bars and causing failure of the masonry around the bars. Compressive joint mortar failure is not a cause of wall failure because of confinement of the joint mortar by surrounding bricks and the insensitivity of moments capacity due to small compressive area and large wall height.

Chapter 3

Mechanical Behavior of Wall Components

3.1 Introduction

A reinforced brick and reinforced concrete beam composite wall consists of several individual components including brick, mortar, grout, reinforcing steel, concrete, and vinyl flashing. These components act individually and in conjunction with adjacent components to determine the overall global behavior of the composite wall. In order to construct a model of the behavior of the composite structure, the mechanical properties of the individual components and their behavior in conjunction with adjacent components were determined. The tests performed consisted of compressive strength of bricks, splitting strength of bricks, compressive strength of type N mortar used in wall, compressive strength of premixed 10K grout, compressive strength of grout made by thinning mortar (called mortar grout), compressive strength of ungrouted brick prisms, compressive strength brick prisms grouted with 10K grout, compressive strength of brick prisms grouted with mortar grout, bond beam compressive strength, compressive strength of concrete used in the wall specimens, splitting tension tests of the concrete used in the wall specimens,

tension tests of #5 reinforcing bar from the same heat as the bar used in the wall specimens, and numerous shear joint tests

3.2 Summary

These tests provided data on mechanical properties of wall components including maximum strength and load/deformation characteristics. Test results are used to develop numerical models to predict relevant mechanical properties. Specific design parameters are provided for the various components.

3.3 Component Testing Equipment and Data Evaluation

Component testing was performed using commercial testing machines for loading the specimens and linear variable differential transducers (LVDT) to measure deformations. All the component tests, except those used to determine concrete compressive strength and splitting tension strength, were performed on a Tinius Olsen universal testing machine. The concrete strength tests were performed on a Forney testing machine. Deformations were measured for several of the specimens tested using the Tinius Olsen universal testing machine as indicated by the test results presented.

3.3.1 Test Equipment

A sketch showing component testing equipment arrangement using the Tinius Olsen Universal Testing Machine, 120,000 pound model super L, and LVDTs to measure

deformations is shown in figure 3.1. For testing using the Forney Testing Machine, model LT-350, the equipment arrangement is similar except the LVDTs were not used. Photographs of the Tinius Olsen Universal Testing Machine and the Forney Testing Machine are shown in figure 3.2. The arrangement consists of placing the specimen between the movable base and the fixed head of the machine. The movable base is then hydraulically raised loading the specimen in compression. Load was applied based on controlling the rate of pumping oil into the machine piston. Deflections were not used to control loading. The calibrations of both testing machines were verified in July, 1995. The Tinius Olsen machine was found to have a accuracy tolerance of 0.33% to 0.50% from 600 pounds (lb.) to 120,000 lb., the Forney machine was found to have an accuracy tolerance of 0.97% from 35,000 lb. to 350,000 lb.

3.3.2 Data Collection

Visual observation of load indicating instruments was used to determine ultimate load for component tests when deformations were not measured. When deformations were measured, analog data from the LVDT and the Tinius Olsen universal testing machine load cell were digitized and recorded using a Optim Megadac 3008 data collection unit and an IBM PS/2 Model 80 personal computer. The data collection equipment is shown on the left hand side of the photograph of the Tinius Olsen testing machine shown in figure 3.2. A schematic drawing of the component test instrumentation arrangement is shown in figure 3.3. Electrical characteristics of the individual LVDTs were determined by the device supplier. The

electrical characteristics of the Tinius Olsen universal testing machine load cell were determined by comparing changes in voltage with various load levels as indicated by the machine load indicating gage.

3.3.3 Data Evaluation

Data evaluation was performed by transferring files from the IBM PS/2 Model 80 personal computer to an IBM compatible personal computer and performing computations using the Mathcad Plus 6.0 program (Mathcad, 1995). This process facilitated both the preparation of calculations and the graphical presentation of results. Examples are provided as part of the discussion of test results demonstrating the details of this evaluation.

The use of LVDTs to measure both specimen and machine movements facilitates the determination of specimen behavior at deformations exceeding those associated with ultimate strength. Using LVDTs it is possible to measure both machine movements and specimen deformations using the arrangement shown. The LVDTs used to measure specimen deformation are expected to provide reasonable data on the behavior of the specimen in the area where the LVDTs are attached. Unfortunately, the LVDTs become unreliable as ultimate strength is approached due to disruption of the brick face shells due to splitting failure of the bricks. The LVDTs often "fell off" the specimens near ultimate load. In order to establish behavior of the specimen after failure, it is necessary to measure machine movements and correct them to

provide data representative of the behavior of the specimens in the area where the LVDTs are attached to the specimens.

The use of machine deformation data involves calibrating machine deformation measurements with specimen deformation measurements in order to quantify effects due to machine and component elastic deformations, initial bearing displacements associated with specimen capping irregularities, differing distances between LVDT mounting locations, and the effects of end restraint.

Priestley and Elder (1983). used both machine and specimen measurements to determine post-failure behavior of masonry prisms. Their measurements and calculations demonstrated the viability of this technique for grouted concrete masonry prisms. For this research, the specific procedure used for the different types of specimens varies based on the type of specimen being considered because of changing specimen behavior and end bearing conditions. The correction procedure consists of three general steps as follows:

First, machine measured deformations are multiplied by a constant factor. This linear adjustment factor is selected to adjust the slope of the machine measured stress strain curve to make the initial slopes of the machine and specimen stress strain curves approximately equal. Use of this factor adjusts results for machine and component elastic deformation differences such as machine and bearing surface elastic deformations and differences in gage length between the machine and

specimen mounted LVDTs. The method of determining the factor assumes that the measurements of deformation of the specimen are correct at loads below initial failure.

Second, the machine measured strains are adjusted so that machine measured strains and specimen measured strains are equal at a stress value of approximately 25 percent of ultimate stress. This constant adjustment factor accounts for any initial displacements due to irregularities in specimen capping and similar anomalies which can effect machine displacements during initial loading of the specimen. This adjustment assumes that initial measurements made on the specimen are more representative of specimen strains than initial machine measurements.

Third, the machine measured strains at displacements beyond ultimate load are modified by a linear factor to account for the influence of machine bearing area on the specimen. The adjustment factor is estimated based on the assumption that failure of the specimen is prevented near machine bearing due to friction between the specimen and the machine bearing surfaces. During specimen unloading, it is assumed that deformations of the specimen near the machine bearing are linear elastic with the same slope as the initial stress strain curve of the specimen near the end bearing. For the concrete masonry prisms being tested, the referenced paper [Priestley, 1983] used initial prism elastic stiffness measurements for this adjustment. This is inappropriate for the brick and mortar specimens used in this testing because the brick is significantly stiffer than the mortar joints. For evaluation

of results using brick, elastic properties of brick are based on structural clay tile component behavior data described by Columber (1994). Deflections in the failing portion of the specimen are assumed equal to the displacements from the machine LVDTs adjusted as in steps 1 and 2 above less elastic displacements for the portion of the specimen outside the specimen mounted gage length. Calculations using this procedure are shown as part of the description of testing and test results for the various component tests.

3.3.4 System Noise

Deformation and load data provided by the LVDTs and Megadac were used directly for analysis and evaluation of data. This was deemed appropriate because the variations in readings caused by inherent system response to outside factors, such as alternating current electrical supply and the digitizing process, were small. This conclusion was verified by reviewing the test data for periods prior to application of load. The results of this review are summarized in table 3.1. The data indicate that LVDT measurements vary by less than ½ %, the Tinius Olsen load cell varies by 2.9%, and the load cell of the ram used for wall testing varies by 0.1 %.

3.4 Compressive Strength of Bricks

Compressive strength of brick facilitates the evaluation of masonry construction using the brick tested. Compressive strength may be used to define overall wall behavior in accordance with code requirements. For example, ACI 530-92, section 5.5 (Building, 1992) uses net compressive strength of units to estimate modulus of

elasticity of masonry; ACI 530.1-92, section 1.6.2 (Specifications, 1992) uses net compressive strength of units to estimate compressive prism strength of masonry. This section describes the compressive strength testing of Suprking brick specimens using methods described in ASTM C 67-91 (Standard, 1991).

3.4.1 Specimen Preparation

Suprking bricks were selected from the stock of bricks being used to construct other specimens. Each of the four specimens tested was prepared from a different brick. The specimens were prepared by cutting the Suprking bricks in half length-wise at the center through the drainage cell. Since the width of the saw blade was approximately the same as the width of the drainage cell, the ends of the two half bricks were flush. The resulting half-brick specimen is shown in figure 3.4. A photograph of a half brick similar to the specimen is shown in figure 1.2.

The specimen was capped with sulfur based capping compound using a steel mold slightly larger than the face of the half-brick specimen. The specimen was then placed in the universal testing machine and loaded as indicated in figure 3.4.

3.4.2 Test Equipment

The test was performed on the Forney compression test machine. The specimen was placed on the movable base. A bearing plate with a spherical bearing was used to transfer load from the fixed head to the specimen. Deformations were not

measured. Applied load at failure was observed on the testing machine dial indicator and recorded.

3.4.3 Results

The four specimens failed in a brittle manner accompanied by loud noise and shattering of the brick specimens. Examination of the pieces of the failed specimens indicated that failure occurred by splitting tension parallel to the direction of load. The mean compressive strength of the brick based on the net area of the specimens was 14900 psi.

3.4.4 Evaluation of results

A summary of the material properties of brick currently used in the United States is reported by Subasic and Borchelt (1993). This report summarizes qualification test results provided by brick manufacturers representing over sixty percent of US manufacturers. The results are collected and statistically analyzed to provide a comparison with ASTM requirements. The mean compressive strength of solid extruded facing brick satisfying the requirements of ASTM C216 - 91c (Standard, 1991) was 11,305 psi with a standard deviation of 4464 psi. The results of tests performed as part of this Suprking research are consistent with these results.

3.5 Splitting Strength Of Bricks

Splitting strength of bricks provides data related to the failure mechanism of bricks. This section describes the testing of Suprking brick specimens using methods described in ASTM C1006-84 (Standard, 1984).

3.5.1 Specimen Preparation

Two Suprking bricks were selected from the stock of bricks being used to construct other specimens. Two splitting tension tests were performed on each brick. Figure 3.5 shows the test arrangement for the two ends of the brick. The tests were performed at one end of each brick and then at the other end. The 1/4" steel rods used to apply load were held in position using capping compound consisting of a 1 to 1 mix by weight of Plaster of Paris and Type II Portland Hydraulic Cement mixed with water to result in a thick paste.

3.5.2 Test Equipment

Load was applied perpendicular to the top and bottom face of the brick on the 1/4 inch steel rods using the Tinius Olsen test machine. A bearing plate with a spherical bearing was used to transfer load from the fixed head to the specimen. Deformations were not measured. Applied load at failure was observed on the testing machine dial indicator. Load was recorded when the brick split apart.

3.5.3 Results

The bricks split in a brittle manner accompanied by loud noise and movement of the brick pieces apart. The splitting went from the rods at the top of the specimen to the rods at the bottom of the specimen in three out of four of the tests. In the first test performed, the split went from (a) rod to rod on one side of the brick and from (b) the rod to a point approximately 1 inch from the rod on the bottom of the brick on one side. Review of the results indicated that this change in brick splitting failure did not effect splitting stress significantly. The observed loads were 5950, 4550, 5900 and 9450 lb. The mean tensile strength was 835 psi.

3.5.4 Evaluation of Results

As demonstrated by these data, the tensile strength of the brick varies significantly. For these data, the variation in load was from 4550 to 9450 lb. This demonstrates the susceptibility of brick tensile strength to imperfections which exist in the brick. This variation makes the prediction of tensile cracking strength of bricks and brick structures imprecise.

3.6 Compressive Strength Of Type N Mortar Used In Specimens

The compressive strength of the type N mortar used in the joints for the test specimens is used to develop methods to estimate prism and structural strength. Type N mortar was selected for this research based on its general use in masonry construction and input from representatives of the General Shale Company, the manufacturer of the Suprking bricks used in this experimentation.

3.6.1 Specimen Preparation

Specimen preparation consisted of estimating mix proportions of dry materials by weight, mixing dry materials, mixing dry materials with water to obtain workable mortar as appropriate for use in masonry construction and similar to the consistency used in construction of specimens, casting specimens in standard molds and curing the specimens in a moist room. The procedure for casting and curing the specimens used methods described in ASTM C 109 - 90 (Standard, 1990). The specimens were 2 inch cube specimens.

The Type N mortar mix design, used for these specimens as well as all others constructed as part of this research, was determined based on ASTM C270-91a (Standard, 1991). This specification requires that type N cement-lime mortar contain the following proportions by volume of materials: cement = 1 part, hydrated lime = over 1/4 to 1 1/4, aggregate (measured in damp, loose conditions) = not less than 2 1/4 and not more than three times the sum of the separate volumes of cementitious materials (cement and lime).

Based on these requirements, a mix ratio by volume of 1 part cement, 3/4 parts hydraulic lime, and 4 3/4 parts sand was selected. These volume proportions were converted to weight proportions for use in this research to improve consistency of laboratory results and to satisfy the requirements of ASTM C270-91a, section 5.1 (Standard, 1991). The conversion from volume proportions was performed as described in this standard.

The 2 inch cube specimens were tested after 28 days of curing in a moist room. Specimens were tested using sides which were cast against the metal forms as bearing surfaces.

3.6.2 Test Equipment

The tests were performed on the Tinius Olsen Universal testing machine. A bearing plate with a spherical bearing was used to transfer load from the fixed head to the specimens. Deformations were not measured. Applied load at failure was observed on the testing machine dial indicator and recorded.

3.6.3 Results

The failure mode of the mortar specimens was substantially less brittle than the failure of the bricks. The failure surfaces were generally on 45 degree planes creating cone type pieces with the bearing surfaces still intact. The mean compressive strengths of the cubes was 1475 psi.

3.6.4 Evaluation of Results

These results show that the strength of the type N mortar used in this research is approximately 1500 psi. The standard deviation of the strength results is about 10% of the strength. This variation was associated with the fact that the specimens were cast on three separate days. This result is not unexpected given the inexact method of measuring mix water by adding water until mix consistency is judged acceptable

for use as masonry mortar. These results demonstrate that mortar strength is relatively consistent provided that dry mix are consistent from batch to batch.

3.7 Compressive Strength Of Premixed 10K Grout

The compressive strength of 10K grout used to grout test specimens is used to develop methods to estimate prism and structural grout. 10K grout is a proprietary material manufactured by the Sonneborn Corporation (Sonogrout, 1992). 10K grout mix, when combined with water, is used in numerous construction applications. This material is recommended by the General Shale Corporation, the manufacturer of the Suprking bricks used in this research, for use when the contractor wishes to use a premixed grout in lieu of mixing his own materials.

3.7.1 Specimen Preparation

Specimen preparation consisted of mixing dry 10K grout mix with water to develop a consistency of very heavy cream suitable for pouring into brick cavities, casting 3 x 3 x 6 inch specimens using molds built with bricks, and curing the specimens in a moist room. The procedure for casting and curing the specimens used methods described in ASTM C1019-89a (Standard, 1989).

The specimens were tested after 28 days of curing in the moist room. The specimens were capped with Sulfur capping compound before testing.

3.7.2 Test Equipment

The compression tests were performed on the Tinius Olsen Universal testing machine. A bearing plate with a spherical bearing was used to transfer load from the fixed head to the specimens. Deformations were not measured. Applied load at failure was observed on the testing machine dial indicator and recorded.

3.7.3 Results

The failure mode for the grout specimens was substantially less brittle than the failure of the bricks. The failure surfaces were generally slopped from the top corner of the specimen to the opposite bottom corner resulting in either two pieces on each side of the crack going from the top to bottom surface or double cones. A photograph showing the failed 10K grout specimens, on the left and right sides, and a failed mortar grout specimen, in the center, is shown in figure 3.6. The mean strength of the grout was 4284 psi.

3.7.4 Evaluation of Results

These results show that the approximate strength of 10K grout used in this research is 4300 psi. This is about three times the compressive strength of the mortar used in the research and about 1/3 the compressive strength of the Suprking bricks.

3.8 Compressive Strength Of Grout Made By Thinning Mortar (Called Mortar Grout)

The compressive strength of grout made by thinning mortar, so that it will flow into Suprking brick cells, is used to develop methods to estimate prism and structural strength. Consultation with the General Shale Corporation, the manufacturer of Suprking brick, indicated that masons sometimes use grout made by thinning mortar being used on the job. Since this grout may be substantially weaker than grout made with 10K grout mix or other grouts obtained from batch plants, it was added to the research as a "worst case" material.

3.8.1 Specimen Preparation

Specimen preparation consisted of adding water to type N mortar until it had a consistency of very thick cream suitable for pouring into Suprking brick cavities, casting 3 x 3 x 6 inch specimens using molds built with bricks, and curing the specimens in a moist room. The procedure for casting and curing the specimens used methods described in the American Society for Testing Materials (ASTM) "Standard Method of Sampling and Testing Grout" [ASTM C1019-89a].

A total of three specimens were cast, one on the first day and two on the second day. The specimens were tested after 28 days of curing in the moist room. The specimens were capped with Sulfur capping compound before testing.

3.8.2 Test Equipment

The compression tests were performed on the Tinius Olsen Universal testing machine. A bearing plate with a spherical bearing was used to transfer load from the fixed head to the specimens. Deformations were not measured. Applied load at failure was observed on the testing machine dial indicator and recorded.

3.8.3 Results

The failure mode for the mortar grout specimens was substantially less brittle than the failure of the bricks and similar to the failure mode of the 10K grout specimens. A photograph showing a grout specimen after failure is shown in figure 3.6. Test results indicate that the specimen cast the first day had a compressive strength of 2175 psi. The specimens cast the second day had compressive strengths of 1310 and 1520 psi. These results show that substantial variation in mortar grout strength may occur. The mean strength of the three mortar grout specimens was 1670 psi.

3.8.4 Evaluation of Results

These results show that the strength of grout made by thinning mortar may vary substantially. This variation is probably due to changes in water. For use in evaluating the behavior of other specimens used in this research, the strength of mortar grout used in this research is 1600 psi. This is about the same as the compressive strength of the mortar used in the research and about 1/10 the compressive strength of the Suprking bricks.

3.9 Compressive Strength Of Ungrouted Brick Prisms

The compressive strength of ungrouted prisms is used to estimate the compressive strength of brick masonry in areas where the bricks are not grouted. This test also provides data on the interaction of the brick and mortar without additional variables resulting from the use of various types of grout in the brick cells. This section describes testing of Suprking brick prisms using methods similar to those described in the ASTM E 477 - 84 (Standard, 1991).

3.9.1 Specimen Preparation

Suprking bricks were selected from the stock of bricks being used to construct other specimens. The prisms used ½ bricks made by cutting Suprking bricks in half length-wise at the center through the drainage cell as was done for the half brick compressive strength specimen. The specimen was constructed using four ½ bricks and type N mortar. An elevation of the specimen is shown in Figure 3.7.

After curing for at least four weeks after completion of the prism specimen, the specimen was capped with sulfur based capping compound using a steel mold slightly larger than the face of the prism specimen. The specimen was then placed in the universal testing machine and loaded as indicated in figure 3.7. The LVDTs in figure 3.7 were attached to the bricks using supports next to the mortar joints as shown.

3.9.2 Test Equipment

The test was performed on the Tinius Olsen Universal test machine. The specimen was placed on the movable base. A bearing plate with a spherical bearing was used to transfer load from the fixed head to the specimen. Deformations were measured using the component test instrumentation arrangement shown in figure 3.2. LVDTs were used on the specimen in all four tests performed, they were used on the machine on three of the four tests performed.

3.9.3 Results

The four specimens failed by longitudinal splitting. Specimen failure was brittle; however, it was observed during the test that failure was preceded by considerable nonlinear deformation. Examination of the pieces of the failed prism specimens indicated that failure occurred by splitting tension parallel to the direction of load. Photographs of two of the specimens after failure are shown in figure 3.8. The failure mode was consistent with the concept summarized by Paulay and Priestley (1992) for the failure mechanism of brick prisms. This theory is that failure is the result of friction between the mortar and the brick associated with inelastic deformation of the mortar perpendicular to the direction of loading.

Load deformation curves were developed from data using methods described in section 3.3.4. The load deformation data reduction for the second set of data collected is as follows:

a) The raw data are read and stored in the form of the matrix P2. The vectors of the matrix represent different types of data. Each row in the matrix is the data for a specific event time during the test.

P2 = READPRN(upr2)

b) Assign names to the vectors from the matrix P2. Each of the vectors represents a different type of data. The location of LVDTs located on the specimen and the machine are shown in figures 3.1 and 3.7.

d1hp2 = LVDT number 1 displacement measurements on specimen

d2hp2 = LVDT number 2 displacement measurements on specimen

d3hp2 = LVDT number 3 displacement measurements on machine

d4hp2 = LVDT number 4 displacement measurements on machine

Lrhp2 = Load cell measurement from machine

$d1hp2 := P2^{\langle 1 \rangle} \cdot in$ $d2hp2 := P2^{\langle 2 \rangle} \cdot in$ $d3hp2 := P2^{\langle 3 \rangle} \cdot in$

$d4hp2 := P2^{\langle 4 \rangle} \cdot in$ $Lrhp2 := P2^{\langle 5 \rangle} \cdot kip$

c) Assign a value to the variable ini2 = data row number used as the initial data point for LVDTs attached to the specimen. This value is established by plotting data points versus data row number for data collected before load is applied. Due to system noise, data values will vary prior to load application. An initial row number value is selected at a data point with maximum noise based on the observation that system noise is substantially smaller than system response to load. The initial value selected is ini2 := 15

d) Values of variables based on measurements of the specimen prior to testing are as follows where:

A = The net cross-section area of the specimen $A = 13.922 \cdot in^2$

g2 = The gage length of the LVDTs measured as the distance between the centers of the LVDT support blocks shown on figure 3.5. $g2 := 7 \cdot in$

e) Calculate values for the stress versus strain using values from the LVDTs attached to the specimen. Also calculate values for other variables used in evaluating performance of the prism. The variables calculated are defined as:

σhp2 = stress on the net cross-section of the prism

εhp2 = strain of the prism based on measurements between LVDT support blocks attached to the specimen

σhp2ult = ultimate stress of prism before failure

Ehp2 = modulus of elasticity, or change in stress/strain, measured between initial load and approximately 1500 psi stress in the mortar.

$$\sigma hp2 := \frac{\overrightarrow{Lrhp2} - Lrhp2_{ini2}}{A}$$

$$\sigma hp2ult := \max(\sigma hp2) \qquad \sigma hp2ult = 5.251 \cdot ksi$$

$$\varepsilon hp2 := \frac{\left(d1hp2_{ini2} + d2hp2_{ini2}\right) - \left(\overrightarrow{d1hp2} + \overrightarrow{d2hp2}\right)}{2 \cdot g2}$$

Based on trial and error, it was determined that σhp2 is approximately 1500 psi for the 118th set of values in the data set. This is confirmed by:

$$\sigma hp2_{118} = 1517.94 \cdot psi$$

Based on trial and error, a range variable, i2, is established to include data sets which are valid for determining εhp2. Data beyond the upper limit of this range is inappropriate due to specimen failure or dislocation of LVDTs.

$i2 = ini2 .. 421$

$$Ehp2_{i2} := \frac{\sigma hp2_{i2}}{\varepsilon hp2_{i2}}$$

$Ehp2_{118} = 3629.835 \cdot ksi$

f) In order to facilitate interpretation of results, the stiffness of the bricks must be determined. Data on the modulus of elasticity of clay tile coupons, which are similar to brick, and type N mortar, which is used in these prisms, is provided by Columber (1994). These data demonstrate that the modulus of elasticity of brick will remain constant at stresses up to the ultimate strength of the brick prisms tested. The data on type N mortar shows that the stress strain relationship above approximately 1500 psi is nonlinear. To determine Eclay, the average value of Eclay reported in Columber (1994) is used.

$Eclay := 3760\,ksi$

g) Calculate the values of strains using the data from the LVDTs attached to the machine. These values are then corrected for compression of the specimen capping, the effect of machine deformations, and the effect of elastic rebound of specimen bricks after ultimate strength is achieved. The variables used in the analysis are as follows.

εmhp2 = uncorrected strain of prism based on LVDTs attached to the machine

εcmhp2 = corrected strain of the prism including the effects of capping, machine flexibility, and elastic rebound of the brick.

cchp2 = correction for cap thickness change and seating of load on caps

cehp2 = correction for machine deformation effects

cbhp2 = correction for elastic rebound of prism bricks after ultimate strength is reached

jni2 = data row number used as the initial data point for LVDTs attached to the testing machine. This variable is determined similarly to ini2 except that data from LVDTs attached to the machine, instead of the specimen, are used.

j2 = a range variable based on trial and error established to include data sets which are valid for determining ecmhp2. Data beyond the upper limit of this range is inappropriate due to specimen failure.

$$\varepsilon mhp2 := \frac{\left(d3hp2_{ini2} + d4hp2_{ini2}\right) - \left(\overrightarrow{d3hp2} + \overrightarrow{d4hp2}\right)}{2 \cdot g2}$$

jni2 := 40 j2 := jni2 .. 423

$$cchp2 := \varepsilon mhp2_{jni2} - \varepsilon hp2_{jni2}$$

The value of cehp2 was estimated based on trial and error:

cehp2 := .583

The value of cbhp2 is estimated based on the length of brick in the specimen beyond the gage length.

$$cbhp2 := \frac{\sigma hp2ult - \sigma hp2}{Eclay} \cdot \frac{(2.6254) \cdot in}{g2}$$

To facilitate the use of cbhp2, a conditional statement must be constructed to find the index variable, jult2, associated with ultimate strength data.

$jjult2_{j2} := if\left(\sigma hp2_{j2} = \sigma hp2ult, j2, 0\right)$ $\quad$ $jult2 := max(jjult2)$

jult2 = 323

The three correction factors to determine corrected strains from machine LVDTs are used in a conditional statement to determine corrected strain ecmhp2

$\varepsilon ccmhp2_{j2} := \left(\varepsilon mhp2_{j2} - cchp2\right) \cdot cehp2$

$\varepsilon cmhp2_{j2} := if\left(j2 \le jult2, \varepsilon ccmhp2_{j2}, \varepsilon ccmhp2_{j2} + cbhp2_{j2}\right)$

Figure 3.9 shows a comparison of the prism number 2 stress strain curves based on LVDTs attached to the specimen, LVDTs attached to the machine, and corrected data from the LVDTs attached to the machine. As shown, the corrected machine data is virtually identical to the data from the specimen. Thus the correction process is successful in predicting specimen displacements from machine measurements.

h) Assuming that the brick modulus of elasticity is Eclay, and using prism stress σhp2, and the corrected machine strains εcmhp2; the stress and strain curve for the mortar in the joints may be calculated. The following additional symbols are used for this calculation.

tmj = the average prism joint thickness $\quad$ $tmj := \frac{3}{8} \cdot in$

εjmhp2 = joint mortar strain for prism specimen 2

Stress and strain are calculated and graphed as follows.

$$\varepsilon jmhp2_{j2} := \frac{\varepsilon cmhp2_{j2} \cdot g2 - \frac{\sigma hp2_{j2}}{Eclay} \cdot (g2 - 3 \cdot tmj)}{3 \cdot tmj}$$

Figure 3.10 shows the deformation of the prism over the gage length due to prism strain, brick strain and mortar strain. As can be seen from this figure, the deformation of the bricks and the three mortar joints are approximately equal at stress levels up to 3500 psi. Above 3500 psi, virtually all deformations observed during prism testing are due to mortar joint deformation. Figure 3.11 shows the strain of the various components.

In order to assure repeatability of these results, a total of four brick prisms were constructed and tested. Deformation of the first specimen was determined using LVDTs attached to the prism. Deformation of the other three specimens was determined from gages attached to both the specimen and the testing machine. The specimen determined stress strain diagram for specimen 1 and the corrected machine based stress strain diagram for specimens 2,3 and 4 are shown in Figure 3.12. As shown by this figure, the performance of all four specimens was similar to the behavior of specimen 2 which is described in detail.

3.9.4 Evaluation of Results

The results of these ungrouted brick prism tests and associated computations support the following assumptions for use in design of Suprking brick walls.

a) Prism strength is approximately 5250 psi. Prism strain when stress is at ultimate strength is approximately 0.0035 inches/inch. Prism strain in the plastic range when stress is at 85% of ultimate strength is approximately 0.005 inches/inch.

b) Brick and mortar deformations contribute approximately equally to prism deformations at stresses below approximately 3500 psi. At higher stress levels, deformation results primarily from deformation of the mortar joints between the bricks.

c) The relationship between stress and strain for bricks within the prism is linear.

d) The relationship between stress and strain for mortar is nonlinear. Mortar strain at ultimate strength is approximately 0.015 inches/inch. Mortar strain in the plastic range at 85% of ultimate strength is approximately 0.025 inches/inch.

3.10 Compressive Strength Of Brick Prisms Grouted With 10K Grout

The compressive strength of brick prisms grouted with 10K grout is used to estimate the strength of grouted masonry. 10K grout was used for testing based on recommendations from the manufacturer of Suprking bricks. This test also adds data for 10K grout for use with brick and mortar data in evaluating the interaction of various components of brick prisms. This section describes testing of Suprking brick prisms using methods similar to those described in ASTM E447-84 (Standard, 1991).

3.10.1 Specimen Preparation

Suprking bricks were selected from the stock of bricks being used to construct other specimens. The prisms were constructed using ½ bricks made by cutting Suprking bricks in half length-wise and type N mortar. An elevation of the specimen is shown in Figure 3.7. After curing for at least 2 days, the prism specimens were grouted using 10K grout (Sonogrout, 1992).

After curing at least four weeks after the completion of grouting, the specimen was capped with sulfur based capping compound using a steel mold slightly larger than the face of the prism specimen. The specimen was then placed is a universal testing machine and loaded as indicated in figure 3.1. LVDTs were attached to the bricks as shown in figure 3.7.

3.10.2 Test Equipment

The test was performed on the Tinius Olsen universal test machine. The specimen was placed on the movable base. A bearing plate with a spherical bearing was used to transfer load from the fixed head to the specimen. Four LVDTs, two attached to the specimen and two attached to the machine, were used for all four of the tests performed.

3.10.3 Results

The specimens failed by longitudinal splitting of the brick face shells. The face shells then fell off the inner grout core leaving it exposed. Specimen failure was brittle; however, it was observed during the tests that failure was preceded by considerable nonlinear deformation. The failure mode was consistent with the mode of failure summarized in Paulay and Priestley (1992). Photographs of failed specimens are shown in figure 3.13.

Load deformation curves were developed from data using methods described in section 3.3.4. The detailed calculations are almost identical to the calculations shown in section 3.9.3 except that the effect of the grout is included. Figure 3.14 shows a comparison of grouted prism number 1 stress strain curves based on LVDTs attached to the specimen, LVDTs attached to the machine, and corrected data from the LVDTs attached to the machine. As shown, the corrected machine data is virtually identical to the data from the specimen. Thus the correction process used for the grouted specimens is successful in predicting specimen displacements from machine measurements.

In order to assure repeatability, a total of four brick prisms grouted with 10K grout were constructed and tested. The stress strain curves based on corrected machine measurements for these specimens are shown in Figure 3.15.

3.10.4 Evaluation of Results

The results of these 10K grouted brick prism tests and associated computations support the use of a prism strength of 4400 psi and a prism strain at ultimate strength of 0.002 inches/inch for use in design of Suprking brick walls.

3.11 Compressive Strength Of Brick Prisms Grouted With Mortar Grout

The compressive strength of brick prisms grouted with type N mortar grout is used to estimate the strength of grouted masonry. Type N mortar grout was used for testing based on questions from the manufacturer of Suprking bricks. Specifically, the manufacturer was asked by contractors if the use of thinned leftover type N mortar for grouting was acceptable. The process used for construction and testing of specimens was identical to the process used for specimens using 10K grout except that a different grout was used.

3.11.1 Specimen Preparation

Type N mortar grout was made by combining dry materials used for making type N mortar and water. Water was added until the mix had a thick cream consistency appropriate for use as grout. The grout was then poured into Suprking brick prisms using the same method as was used for the 10K grout specimens. The specimen was then tested and instrumented as indicated in figures 3.3 and 3.5.

3.11.2 Test Equipment

The test was performed on the Tinius Olsen universal test machine. Specimen #1 had LVDTs attached to the specimen only. LVDTs were used on both the machine and the specimen for specimens #2 and #3.

3.11.3 Results

The specimens failed by longitudinal splitting of the brick face shells. The face shells then fell off the inner grout core leaving it exposed. The failure mode was the same as for the prisms grouted with 10K grout.

Load deformation curves were developed using the same methods as were used for the prism specimens grouted with 10K grout. The stress strain curves based on corrected machine measurements for the three specimens using mortar grout are shown in Figure 3.16.

3.11.4 Evaluation of results

The results of these mortar grouted brick prism tests and associated computations support the use of a prism strength of 3800 psi and a prism strain at ultimate strength of 0.002 inches/inch for use in design of Suprking brick walls.

3.12 Compressive Strength Of Concrete Used In Wall Specimens

The compressive strength of the concrete used in the beam at the bottom of the wall specimens was determined to facilitate evaluation of wall specimen behavior and to assure acceptable concrete mix proportions.

3.12.1 Specimen Preparation and Test Equipment

The concrete mix was designed using the US Bureau of Reclamation Concrete Manual method (Concrete, 1963). The mix design is based on Table 14 of the referenced manual and presumes ¾ inch normal weight course aggregate, non-air entrained concrete, 316 lb. of water per yard of concrete, and sand 45% of the total aggregate by volume. The resulting mix design for a yield of 1 cubic yard of concrete is:

Water	316 lb.
Cement	486 lb.
Course Aggregate (3/4 inch)	1559 lb.
Fine Aggregate (sand)	1575 lb.

Specimen casting, curing and preparation for testing were performed in accordance with ASTM specification C39 - 94 (Standard, 1994). The specimen was tested using the Forney compression testing machine. Deformation measurements were not made during specimen loading.

3.12.2 Results

The specimens failed by longitudinal splitting and formation of the "double cone" configuration expected for concrete cylinders. A total of 2 specimens were tested. The maximum loads, Pult, were 65,000 lb. and 65,800 lb. The mean ultimate stress was 2300 psi

3.12.3 Evaluation of Results

The concrete mix was found acceptable and used for constructing wall specimens based on these results. Concrete strength at 28 days was 2300 psi.

3.13 Splitting Tension Tests Of Concrete Used in Wall Specimens

The splitting tension strength of the concrete used in the beam at the bottom of the wall specimens was determined to facilitate evaluation of wall specimen behavior and to assure acceptable concrete mix proportions.

3.13.1 Specimen Preparation and Test Equipment

The concrete used for these specimens was the same as the concrete used for compression test specimens described in section 3.12. Specimen casting, curing and preparation for testing were performed in accordance with ASTM specification C 446 - 90 (Standard, 1990). The specimen was tested using the Forney compression testing machine. Deformation measurements were not made during specimen loading.

3.13.2 Results

The specimens failed by longitudinal splitting. A total of four specimens were tested. The maximum loads were 27700, 30500, 31100, and 26300 lb. The mean ultimate stress was 255 psi.

3.13.3 Evaluation of Results

The concrete mix was found acceptable and used for constructing wall specimens based on these results. Concrete splitting strength at 28 days was 255 psi.

3.14 Mill Test Reports For Reinforcing Steel Used In Wall Specimens

Reinforcing steel used in these tests was manufactured in accordance with ASTM A615-94 [ASTM A615-94]. It was purchased from a local supplier which maintains records associating individual steel reinforcing bars, heat numbers and certified mill test reports (cmtrs) for use by clients as required. All of the bars of each size came from the same heat number. The bar sizes and associated results from physical tests are summarized as follows:

Bar Size	Yield Strength P.S.I.	Tensile Strength P.S.I.	Elongation % in 8"
4	69,800	104,700	15 %
5	63,500	98,000	15 %
6	80,227	100,227	14 %

Chapter 4

Mechanical Behavior of Reinforced Shear Joints With PVC Flashing

4.1 Introduction

The reinforced brick and reinforced concrete beam used in a composite wall system are often separated by flashing. The flashing facilitates drainage of moisture from behind the brick wall. If the exterior of the masonry can be waterproofed, such as with concrete unit masonry with an exterior coating, drainage from behind the wall is not required and the flashing may be eliminated. Since brick generally cannot be made waterproof due to architectural requirements, a vinyl flashing should generally be installed.

The installation of the flashing results in breaking the bond between the reinforced brick wall and reduced friction as discussed is Chapter 2. The tests documented in this chapter provide data on the strength and stiffness of joints between reinforced brick and concrete separated by flashing. The tests use a vinyl flashing material commonly used in East Tennessee for this purpose.

The shear joint tests included several shear joint configurations all using vinyl flashing. The various configurations considered the use of #4 and #6 steel reinforcing bars for dowels, the use of both 10K and mortar grout in the cells with reinforcing, and the effect of using 10K grout to grout cells adjacent to cells with reinforcing bar as well as the cells with reinforcing. When adjacent cells were grouted, a brick bond beam unit was used to assure continuous grout support next to the flashing.

4.2 Summary

These tests provide data on the strength and load/deformation characteristics of various configurations of shear joints with flashing and steel reinforcing bar dowels to transmit shear loads across the joint, subject to monotonically increasing load. Several specimen configurations were tested to determine which ones exhibit failure of the brick prior to development of dowel strength and ductility. The tests determined that to assure optimum behavior the brick cell in the direction of loading adjacent to the cell with the dowel in it must also be grouted to avoid premature failure of the brick. The shear tests also found that #6 dowels cause failure of the brick prior to the reinforcing steel developing its potential strength. The test results and the section describing the tests are shown in table 4.1. This table demonstrates the significant reduction of load which occurs due to premature failure of the brick.

To provide understanding of these results, the analysis of joint capacity shown in section 2.5.2 using dowel tensile strength to determine spacing was compared to the results from shear specimen tests. The same computational methodology based on ACI 530 (Building, 1992) was used in this evaluation and in section 2.5.2. The comparison was performed as follows.

a) The coefficient of friction, cf, determined from the shear specimen with a #4 reinforcing bar and 10K grout in all cells was used to recalculate the relationship between bar spacing and ultimate flashing joint capacity per dowel. The coefficient of friction from this test was used because this test was the only one that clearly developed the ultimate strength of the dowels.

cf = .544

$$Bam4 := 0.5 \cdot \pi \cdot \overrightarrow{Lbt4^2} \cdot \sqrt{Fm \cdot psi \cdot 5} \qquad Bas4 := Ab4 \cdot Fy4$$

$$Ba4_n := if\left(Bam4_n \le Bas4, Bam4_n, Bas4\right) \qquad Jt4 := Ba4 \cdot cf$$

The results from the #4 reinforcing steel shear specimens with 10K grout, divided by 2 in order to account for the two joint sections resisting shear in each specimen were then plotted as data points using vectors length, Ls4, and joint force, Jt4. Similar calculations were used to plot data from specimens with #6 reinforcing steel and mortar grout with #4 reinforcing steel.

Figure 4.1 summarizes the comparison shear specimen test results with predictions based on shear friction as discussed in section 2.5.2. For the specimens with #4

reinforcing bars the comparison is excellent. The model developed in section 2.5.2 predicts the behavior of specimens with #4 dowels.

For specimens with #6 dowels the comparison is not as close as for #4 dowels. The difference between predicted and measured values is probably due to the #6 bar being so large that failure is caused by side bursting observed during testing. Failure of the specimens with a #4 bar, which is less than ½ as large as a #6 bar, fail due to the length of the brick in the direction of load. No effect associated with the transverse edge distance, which would be indicative of side bursting, was observed. Based on these results, the use of #6 reinforcing steel as dowels for a flashing joint is not recommended and wall specimens using #6 bars were not tested.

Figure 4.2 uses the data shown in figure 4.1 to develop a flashing shear joint dowel design curve. The curve is only for #4 reinforcing bar since the use of #6 reinforcing steel for flashing shear joints is inappropriate. The curve for #4 dowels is developed by increasing the longitudinal edge distances to include (a) the diameter of the reinforcing steel and (b) the distance included in the drainage cell and the joints between bricks. The increased distances are then multiplied by two to obtain the appropriate center to center spacing associated with the original longitudinal edge distances.

4.3 Shear Test Specimen Configuration And Test Method

Shear specimen testing and data evaluation were the same as described in section 3.3 for brick wall component tests. All the shear tests used the Tinius Olsen Universal Testing Machine to apply monotonically increasing loads to failure.

Suprking bricks were selected from the stock of bricks being used to construct other specimens. The shear specimens used whole bricks for transmitting shear loads and testing joint configurations. Vinyl flashing was .020 inch thick Wascoseal concealed flashing manufactured by York Manufacturing Co., Sanford, Maine. An elevation of the specimen is shown in figure 4.3. A photograph of a failed specimen is shown in figure 4.4. LVDTs were placed on both faces of the specimen. Half bricks were used to provide additional grout anchorage of #6 reinforcing bars where prevent premature bond failure due to tension in steel reinforcing bars. Half bricks, which are not shown in figure 4.3, were used to provide additional grout anchorage of #6 reinforcing bars where prevent premature bond failure due to tension in steel reinforcing bars. Half bricks were not used for the specimens with #4 steel reinforcing bars. Four different configurations of this basic specimen were constructed and tested:

a) 5 specimens using #4 steel reinforcing bars with 10K grout in the cells with the reinforcing bars were tested.
b) 3 specimens using #4 steel reinforcing bars with mortar grout in the cells with reinforcing bars were tested.

c) 4 specimens using #4 steel reinforcing bars with 10K grout in all cells were tested. In addition, the bricks used in these specimens on the outer sides of the vinyl flashing were bond beam units with the ½ of the center flange removed and the resulting space grouted. The broken out side of the bond beam flange was orientated to face the vinyl membrane.

d) 3 specimens using #6 steel reinforcing bar with 10K grout in the cells with reinforcing bars were tested.

e) 1 specimen using #6 steel reinforcing bar with 10K grout in all cells was tested. In addition, the bricks used in this specimen on the outer sides of the vinyl flashing were bond beam units with the ½ of the center flange removed and the resulting space grouted. The broken out side of the bond beam flange was orientated to face the vinyl membrane.

After curing at least four weeks, the specimen was capped using grout containing 1 part Plaster of Paris and 1 part Portland Cement by weight, and water to make a thick paste. The specimens were then stored in dry conditions at least 1 day before testing. The specimen was then placed in the universal testing machine and loaded as indicated in figure 4.1. Load was controlled by the rate of pumping oil into the machine cylinder. Deformation was not used to control machine load. The LVDTs were attached to the bricks using supports crossing over the shear joints as shown in figure 4.1.

The load reported and graphed in succeeding sections of this chapter is the load on the entire specimen. This load was used in reviewing specimen behavior because specimens generally failed on one side of the specimen prior to failing on the other side and, as a result, loads on an individual shear joint could not be separately determined. When this data is used to develop load deformation data for single reinforcing steel dowels, the specimen loads may be divided by two to estimate the load on individual dowels. This methodology was used to calculate coefficients of friction for the data for comparison to other published data.

4.4 Shear Test Of Joint With Vinyl Flashing, #4 Reinforcing Bar, 10K Grout In Reinforced Cells

This test configuration is similar to that which would result from installation of vertical reinforcing in the wall without special provisions to enhance the behavior of the flashing joint. Specimen configuration and test method are described in section 4.3. Figure 4.4 shows a photograph of a failed shear specimen with grout in the reinforced cell mounted in the test machine.

4.4.1 Results

A total of five specimens with this configuration were tested. The first specimen failed by bending of the #4 reinforcing steel dowel, the dowel never pulled out of the grouted brick cell even though the center portion of the specimen was pushed down flush with the bottom of the side portions of the specimen. The other four specimens

failed by brittle failure of the outer pairs of bricks. These failures were due to braking the flange between the cells of the bricks and the face shells of the bricks.

Load deformation curves were developed from data using methods similar to those described in section 3.3.4. Specifically, elastic rebound at strains beyond ultimate strength were not considered since strains in the specimen (brick) outside the gage length are not significant compared to reinforcing steel dowel deformations. The calculation procedure consists of calculating load deformation data from gages mounted on the specimen and the test machine and then correcting machine measurements for the effects of machine deformations and initial displacements due to capping irregularities and similar anomalies. The load deformation data reduction is similar to the calculations shown in section 3.9.3.

Figure 4.3 shows a comparison of the shear specimen number three stress strain curves based of LVDTs attached to the specimen, LVDTs attached to the machine, and corrected data from the LVDTs attached to the machine.

In order to assure repeatability of results, a total of five shear specimens using #4 reinforcing steel and 10K grout in the reinforced cells were constructed and tested. The corrected machine based load deflection curves for the five specimens are shown in figure 4.4. The effect of brick failure versus bending failure of the steel reinforcing bar is shown by the difference between the load deflection diagram for specimen 1 and the rest of the specimens. Calculations to assess the behavior for this type of

joint are based on results from specimens 2,3,4 and 5. Specimen 1 behavior is not considered a reliable indication of the behavior of this joint configuration based on these tests. The mean ultimate strength of specimens 2,3,4 and 5 is 9.95 kip.

The coefficient of friction is determined in order to facilitate comparison of data for different sizes of reinforcing bar dowels and from tests by others. The coefficient of friction for a specimen is the maximum load on the specimen divided by two times the yield strength of the reinforcing bar dowel. The mean coefficient of friction for specimens 2,3,4 and 5 was 0.36.

4.4.2 Evaluation of Results.

The results of these shear joint tests and associated computations support the following assumptions for use of shear joints with vinyl flashing, #4 steel reinforcing bars and 10K grout in the cells with reinforcing bars.

a) Specimen strength is approximately 10,000 lb. for #4 steel reinforcing bar crossing the joint.
b) The joint usually fails in a brittle manner due to failure of brick flanges and brick shell walls around the ungrouted cell.
c) The joint may loose significant load capacity subsequent to deformations of 0.1 inches or less.

This type of joint should be used only where loads are well defined and a brittle joint failure mode is acceptable.

4.5 Shear Test Of Joint With Vinyl Flashing, #4 Reinforcing Bar, Mortar Grout In Reinforced Cells

This test configuration is identical to the configuration described in section 4.4 except that type N mortar thinned to grout consistency was used in lieu of 10K grout. This configuration was included to provide data on the effect of using mortar grout in lieu of 10K grout on the performance of shear joints with a vinyl membrane.

4.5.1 Results

A total of three specimens with this configuration were tested. All three specimens failed by brittle failure of the outer pairs of bricks. These failures were due to breaking the flange between the cells of bricks and the face shells of the bricks. Load deformation curves were developed from data using the same methods as were used in section 4.4.1. The corrected machine based load deformation curves for the three specimens are shown in figure 4.5.

The mean strength of this type specimen was 8.19 kip. The mean coefficient of friction was 0.293.

4.5.2 Evaluation of Results

The results of these shear joint tests and associated computations support the following assumptions for use of shear joints with vinyl flashing, #4 steel reinforcing

bars and grout made by thinning type N mortar and using it to grout cells with reinforcing bars.

a) Specimen strength is approximately 8000 lb. for #4 steel reinforcing bar crossing the joint.
b) The joint fails in a brittle manner due to failure of brick flanges and brick shell walls around the ungrouted cell.
c) The joint may loose significant load capacity subsequent to deformations of 0.2 inches.
d) Comparison of test results from specimens using 10K grout and mortar grout shows that the use of mortar grout, which has a strength of less than ½ of the strength of 10K grout, reduces shear joint strength 20% and doubles joint deformation prior to failure.

4.6 Shear Test Of Joint With Vinyl Flashing, #4 Reinforcing Bar, 10K Grout In All Cells

This test configuration was developed to eliminate the failure mode observed in the shear joint specimens without grout in cells adjacent to reinforced cells. The objective was to increase both strength and ductility of the joint. Elimination of the brittle failure observed in tests described in sections 4.4 and 4.5 is important to assuring distribution of shear load to all the shear dowels in a wall. Test method and overall specimen configuration are described in section 4.3. Details of grouting

adjacent cells and the use of bond beam bricks for this specimen are described in this section.

4.6.1 Test specimen Configuration

The test specimen for this configuration used six Suprking bricks as shown in figure 4.1. The load on the center two bricks of this specimen bears directly against the grouted cell containing the #4 reinforcing bar. Failure of these two bricks did not initiate specimen failure during tests described in sections 4.4 and 4.5. Thus, the configuration of these two bricks was not changed for this series of tests. Failure did occur in the ungrouted cell next to the load in the outer pairs of bricks. Thus, the intent of this specimen was to grout the brick cells in the outer pair of bricks next to the point of loading.

The Suprking brick contains two large cells which may be used for grouting and reinforcing steel. In addition a drainage cell is provided in the center flange of the brick as shown in Figure 1.1. To eliminate possible brick failure, the specimen was designed to provide continuous support for the steel reinforcing bar up to the point of load application. To provide continuous support, a bond beam brick with ½ of its flange removed was used next to the vinyl flashing in the outer pair of bricks. This permitted the placement of grout continuously between the cells next to the vinyl flashing. A section showing this configuration is shown in figure 4.8. The Suprking bricks shown in figure 4.6 is orientated as the shear plane would occur in a wall. For

the shear test specimens, the flashing and load are orientated in the vertical direction and the reinforcing steel is horizontal.

4.6.2 Results

A total of three specimens with this configuration were tested. All three specimens failed by bending and pulling of the steel reinforcing bar resulting in failure of the grout and brick surrounding the reinforcing steel. Failure occurred in either the center pair of bricks or one of the outer pairs of bricks depending on local conditions. The failures were all ductile enough that movement of the bricks on the two sides of the vinyl flashing could be observed prior to failure. Load deformation curves were developed from data using the same methods as were used in section 4.4.1. The corrected machine based load deformation curves for the three specimens are shown in figure 4.7.

The mean strength of this type of the three specimens was 15.2 kip.
The mean coefficient of friction was 0.544.

4.6.3 Evaluation of Results

The results of these shear joint tests and associated computations demonstrate that shear joints with vinyl flashing, #4 reinforcing steel dowels, and grout in the cells with reinforcing as well as adjacent cells in the direction of load are ductile and fail at a predictable load. These tests support the following assumptions.

a) Specimen strength is approximately 15,000 lb. for #4 steel reinforcing bar crossing the joint

b) The joint deforms in a predictable manner over a distance of substantial deformation after ultimate load is achieved.

c) The joint has significant capacity for deformations up to 0.35 inches.

d) After reaching ultimate strength, joint capacity decreases are approximately linearly related to increasing deformations.

e) Comparison of test results with results for specimens with only reinforced cell grouted indicates an increase in strength of approximately 50%.

f) The strength of specimens with all cells grouted are approximately equal to the strength of Specimen #1 shown in figure 4.3 for specimens with 10K grout only in reinforced cells. This indicates that Specimen #1, which behaved differently from similar specimens, failed by yielding the #4 reinforcing steel rather than failing brick flanges and walls as did other bricks in specimens without grout in adjacent cells.

4.7 Shear Test Of Joint With Vinyl Flashing, #6 Reinforcing Bar, 10K Grout In Reinforced Cells Or In All Cells

These test specimens are similar to the those described in sections 4.4 and 4.6 except that #6 steel reinforcing bars are used in lieu of #4 reinforcing steel bars. In addition, pairs of half bricks were placed over the extension of the #6 reinforcing bar and grouted to provide additional anchorage for #6 bars. These configurations were

developed to determine if increasing reinforcing area would proportionally increase joint capacity.

4.7.1 Results

A total of four specimens were tested. Three of the specimens had 10K grout only in the cells with reinforcing steel. One of the specimens had 10K grout in all the cells and was constructed as indicated in figure 4.5. The failure mode for all four specimens was brittle. The specimens with grout only in reinforced cells failed by breaking brick flanges and face shells next to the unreinforced cells as was observed for the specimens with #4 reinforcing bars. The fully grouted specimen failed by splitting one of the outer pairs of brick in half vertically. The failure appeared to result from splitting tension below the bearing of the #6 reinforcing bar. Load deformation curves were developed from the data using the same methods as were used in section 4.4.1. The corrected machine based load deformation curves for the four specimens are shown in figure 4.8.

The mean strength of specimens 1,2 and 3, which had grouting only in the reinforced cells, was 12.93 kip. The mean coefficient of friction for these three specimens was 0.183.

The strength of the specimen with grouting in all cells was 20.95 kip. The coefficient of friction was 0.297.

4.7.2 Evaluation of Results

The results of these shear tests and associated computations support the following assumptions for use of shear joints with #6 steel reinforcing bars.

a) Specimen strength is approximately 13,000 lb. for #6 reinforcing bar crossing the joint when adjacent joints are not grouted. Specimen strength is increased to approximately 21,000 lb. by grouting the adjacent cell in the direction of load and using a bond beam brick with ½ the flange removed next to the vinyl flashing.

b) The joint fails in a brittle manner. Load deformation curves show that grouting the cells adjacent to the #6 reinforcing bar increases deformations . The mode of failure changes from breaking of flanges and brick adjacent to the unreinforced cell to tension splitting of the specimen below the bearing area of the #6 reinforcing bar when all cells are grouted.

c) The joint may loose significant load capacity subsequent to deformations of 0.12 inches when adjacent cells are not grouted. Loss of load capacity occurs at approximately 0.17 inches when adjacent cells are grouted.

d) Comparison of test results from specimens using #4 reinforcing bars and #6 reinforcing bars indicates that load capacity increases approximately 25% when steel area is more than doubled. In addition, the deformation of the joint with #4 reinforcing steel and grout in all cells is at least twice as much as observed for all other shear joint specimens tested. This is due to the change in failure mode from (i) yielding of the #4 reinforcing bar when all cells are grouted to (ii) splitting failure of the grout and brick for the other types of joint configurations.

Chapter 5

Behavior Of Small Scale Test Walls

5.1 Introduction

Chapters 4 and 5 describe the testing of the individual components that are used in a reinforced Suprking brick wall and the testing of various joint configurations using vinyl flashing to eliminate cohesion at the joint. The tests described in this chapter provide data on the interaction of the brick wall components supported on a concrete beam with vinyl flashing in the joint between the wall and the concrete beam.

5.2 Summary

Four small scale brick walls attached to a reinforced concrete beam with #4 steel reinforcing bars were tested to assess the interaction of individual components. The brick walls were separated from the concrete beams supporting them by a vinyl flashing. The joint at the interface between the brick wall and concrete beam used #4 reinforcing steel dowels placed in cells grouted with 10K grout. In addition, bond beam bricks were placed on top of the vinyl flashing and the first two courses

of brick were grouted to produce a joint configuration similar to the joint described in section 4.6. The tests demonstrated the ability of the joint between the brick wall and the concrete beam to transmit shear loads from the brick wall to the concrete beam and develop substantial nonlinear displacements prior to collapse. They also showed that maximum flashing joint strength and ductility are achieved if steel dowels are placed 20 inches apart and that substantially less strength and ductility are developed by the flashing joint if the dowels are placed 10 inches apart. Calculations to evaluate wall specimen behavior show that section moment-rotation diagrams and beam load-displacement diagrams may be predicted using brick wall component load-deformation properties.

5.3 Wall Test Specimen Configuration

The four wall specimens tested were the same except for the number of vertical #4 steel reinforcing bars used to transmit shear load across the joint between the brick wall and the concrete beam supporting it. Two specimens used 2 #4 steel reinforcing bars placed on each side of the specimen centerline for a total of four bars. The other two specimens used four #4 steel reinforcing bars placed on each side of the specimen centerline for a total of eight bars. A sketch of the wall specimen is shown in figure 5.1. Photographs of the two types of wall specimens are shown in figure 5.4.

The concrete beam used to support the brick wall was constructed using wood forms and a #5 steel reinforcing bar longitudinally down the center. The form joints were

sealed with tape. The inside faces of the plywood form were oiled prior to placing reinforcing steel in the form. Vertical #4 steel reinforcing bars were installed with approximately five inches of bar protruding from the bottom of the form to facilitate installation the anchor blocks. Concrete mix proportions are identified in section 3.12. The same batch of concrete was used for the four wall beams as well as the test cylinders used to determine concrete strength.

Concrete was placed in the form and vibrated to assure consolidation. The top was struck off with the flat edge of a trowel. The top of the beam was then lightly troweled to provide a smooth finish. The intent of the finish was to approximate the finish provided on a finished floor adjacent to dowels where concrete finishing machines cannot be used. After placing of the concrete, the concrete beams were draped with burlap and kept wet for three days. They were then stripped and transferred to another laboratory for installation of the waterproof membrane and brick wall on top of the beam.

Before beginning construction of the brick wall, the concrete beams were turned upside down and anchor blocks to provide additional anchorage for the #4 vertical reinforcing bars were installed. The anchor blocks consisted of two half Suprking bricks centered on the reinforcing bars protruding from the bottom of the concrete beam and grouted with 10K grout. After curing of the anchor block grout for at least 1 day, the beams were turned right side up and construction of the brick wall was begun.

The wall consisted of a total of five courses of Suprking bricks. The first course consisted of a combination of bond beam bricks and regular bricks constructed to facilitate grouting similar to the configuration shown in figure 4.5. Load on the reinforcing bars was outward from the centerline of the wall specimen and thus provision for grouting was made for the cells on the outward side of the bars. Flanges and/or end walls of bond beam bricks were removed to allow continuity of the grout from the cell with the bar to the adjacent cell. After placing the second course of brick, the first and second course cells were grouted as required to simulate conditions shown in figure 4.6.

After placing of the third and fourth courses using regular brick, the fifth course was constructed using bond beam bricks with all flanges and end walls removed except for the outer walls at the ends of the specimen. After cells without reinforcing bars in them were blocked off at the bottom of the fifth course, 10K grout was placed in the bond beam bricks and the cells with reinforcing bars in them. The specimens were then stored in the laboratory for at least one month before testing.

The wall specimen support and loading configuration are shown in figure 5.2. At each of the three load points, a 1 inch thick plate 6 inches long and 5 inches wide was used to distribute load the specimen. Grout made using 1 part cement and 1 part Plaster of Paris was used to level the plates and assure full bearing between the plate and the wall. A 1 inch wide plate or a steel bar was used to simulate either

laterally restrained and pinned supports. The end supports were placed on the sides of steel tubes which were high enough to insure that the anchor blocks would not impinge on the floor before the specimen failed in bending.

5.4 Wall Specimen Testing and Data Collection Equipment

Wall specimen testing was performed using a hydraulic ram to apply load, a load cell to determine the load applied, and LVDTs to measure deformations.

5.4.1 Test Equipment

Loading of the specimen was provided by a hydraulic ram supplied by an electric pump. The ram was mounted on a structural steel frame anchored to the laboratory floor next to the specimen. The ram and the loading head had a pair of pin hinges aligned at right angles to each other to assure that the loading system applied axial loads. For the first wall specimen tested, control of the movement of the hydraulic ram was based on maintaining load. This resulted in rapid collapse of the specimen after yielding of the wall began. Deflection control of the ram was used for the other three tests. This resulted in collection of substantially more data related to wall load deformation behavior after yield for the last three specimens.

5.4.2 Data Collection Equipment

Analog load data was provided during the test by a load cell attached to the ram between the wall specimen and the loading cylinder. Analog data on displacements

were collected from the eight LVDTs located as indicated in figure 5.3. These locations and the purpose of each measurement are summarized in table 5.1

During the test, the analog data were digitized and stored using a Optim Megadac 3008 data collection system and an IBM PS/2 Model 80 personal computer. A schematic drawing of the component test instrumentation is shown in figure 3.2. Electrical characteristics of the individual LVDTs were determined by the device supplier. The electrical characteristics of the load cell were determined from data collected during previous experiments at the University of Tennessee.

5.5 In-plane Bending Test Of Wall Specimens With Vertical #4 Steel Reinforcing Bars Crossing PVC Flashing Joint

These tests were performed to assess wall behavior when a horizontal joint with vinyl flashing between the wall and the concrete beam is used. In order to facilitate the discussion of these tests, the specimens are named as follows.

Specimen Designation	Number of Vertical #4 Bars
1	4
2	4
3	8
4	8

5.5.1 Results

As increasing load was applied, a loud cracking noise could be heard as the bricks in the wall failed in tension and a vertical crack could be observed at the center of the wall starting at the flashing shear joint. Review of the video tapes made during testing confirms the impression during testing that wall specimens 1 and 2 were very ductile and that wall specimens 3 and 4 failed suddenly before any observable ductile movement occurred.

Specimen 1, which was loaded based on maintaining ram pressure, failed by dislodging the end couple of feet of wall from the rest of the specimen. Specimen 2 failed with a large shear crack starting approximately 1 foot from an end sloping toward the center of the specimen at approximately 45 degrees. Both specimens 1 and 2, with four vertical #4 bars, developed a wide vertical crack at the middle of the specimen and developed large center hinge rotations about a compression area in the top course of bricks.

Specimens 3 and 4, with eight vertical #4 bars, developed very little hinge rotation and small vertical cracks at the center of the specimen before failing by splitting near the end of the specimen. These two walls failed by splitting around vertical reinforcing bars near end of the wall and then becoming unstable and unable to resist further loading. Review of the video tapes made during testing showed that both walls failed at or very near to the left end vertical reinforcing bar. No significant ductility was observed during testing of these two specimens. This failure

is consistent with the reduction in dowel tensile capacity associated with the dowel spacing used in these specimens. The effect of dowel spacing is discussed in section 2.5.2 and in this chapter. Photographs showing the failure of specimens 2 and 3 are shown in figure 5.5

5.5.1.1 Load Deflection Curves

The data from the tests was processed using the Mathcad 6.0 plus [Mathcad 6.0 plus, 1995] computer program. Load deformation data reduction for the four specimens was similar. The load deflection diagram for the specimens is shown in figure 5.6.

5.5.1.2 Composite Behavior

The nature of the composite behavior of the brick wall and concrete beam must be evaluated in order to assess how external forces are being resisted by the specimens. If the two are acting together as one element, then plane sections should remain-plane during the application of load. To test this hypothesis, the deformations measured by the three horizontal LVDTs at the center of the specimen were compared. The results of the comparison for specimen #2 are plotted in figure 5.7.

Figure 5.7 shows that the brick is moving substantially more than the concrete beam. In addition, the top and bottom deformations for the brick wall show that the wall is acting in bending with compression at the top and tension at the bottom. The deformations of the other three specimens were similar. Based on this evaluation,

the wall may be considered two independent structures deflecting together when a flashing is used in the joint between the wall and the concrete beam.

5.5.1.3 Load Resisted by Concrete Beam

The load deflection curve for the concrete beam may be estimated using assumptions stipulated in the ACI 318 code [American Concrete Institute, ACI 318-89] together with concrete properties reported in sections 3.12 and 3.13. Based on this analysis, the bending stiffness of the concrete beam is neglected in evaluating the behavior of the wall specimen. The concrete beam will, however, contribute to the behavior of the wall as a tension member. From the data shown in figure 5.7, it is concluded that the concrete beam is much stiffer than the joint when subjected to loading. Thus the concrete beam is considered a rigid tension link between the vertical reinforcing bars on opposite sides of the center line of the specimen with no vertical bending stiffness.

5.5.1.4 Moment Rotation Curves for Specimen Brick Walls

Moment rotation curves may be plotted from experimental data obtained during the wall tests. Total specimen bending moment is obtained based on statics. Since the concrete beam will not resist any significant bending moments, the total specimen bending moment is resisted by the Suprking brick wall. Total rotation at mid span of the specimen is determined from the gage readings at the top and bottom of the wall. Total rotation, in lieu of rotation associated with each side of the center line of the crack at mid span of the specimen, is used since there was no attempt to differentiate

rotation associated with each of the two sides of the crack. The moment rotation curves for the four specimens are shown in figure 5.8

5.6 Modeling Of Small Scale Test Wall Behavior

The numerical modeling of the reinforced brick wall involves estimating values for applied external moment and associated section rotation for initial tension cracking of the brick wall and then at different load levels associated with changes in behavior of the joint between the wall and the concrete beam. The process of developing the model involves determining uncracked wall behavior, idealizing joint shear behavior, calculation of moments and section rotations at appropriate levels assuming plane sections remain plane, and comparing calculated and measured results.

5.6.1 Uncracked Section Behavior

The uncracked section analysis is based on classic beam theory assuming plane sections remain plane and that tension stress in the brick does not exceed the splitting tension strength of the Suprking bricks. Tensile strength of the bricks, Tubrick, is estimated based on the median test value reported in section 3.5. The modulus of elasticity of the brick wall, Ebrickwall, is estimated based on test results for 10K grouted prism specimen #1 reported in section 3.10.3 for stresses up to 1500 psi.

Tubrick := 750 psi Ebrickwall := 2800 ksi

The height, h, and brick wall thickness, twallbrick, of the brick wall are then used to calculate the uncracked section moment of inertia, Iuncrack, and moment, Muncrack, when stress will reach the tensile strength of the brick wall. Section rotation at mid span of the specimen, funcrack, is then calculated.

$h = 15 \cdot in$ $\quad$ $twallbrick := (4.625 - 2.625) \cdot in$ $\quad$ $Iuncrack := \frac{twallbrick \cdot h^3}{12}$

$Muncrack := \frac{Tubrick \cdot Iuncrack \cdot 2}{h}$ $\quad$ $Muncrack = 4.687 \cdot kip \cdot ft$

$\phi uncrack := \frac{Tubrick \cdot 2 \cdot in}{Ebrickwall \cdot h}$ $\quad$ $\phi uncrack \cdot 10^6 = 35.714$

Deflection of the specimen, Δuncrack, is calculated using the length, L, as the distance between the supports and assuming that the specimen is simply supported with a concentrated load at mid span. The load, Puncrack, is also calculated

$L = 90 \cdot in$

$Puncrack := \frac{4 \cdot Muncrack}{L}$ $\quad$ $Puncrack = 2.5 \cdot kip$

$\Delta uncrack := \frac{Muncrack \cdot L^2}{12 \cdot Ebrickwall \cdot Iuncrack}$ $\quad$ $\Delta uncrack = 0.024 \cdot in$

These estimates of specimen behavior were compared with test results plotted in figure 5.6. At a load of approximately 2.5 kips, test results indicate that specimens 1, 2, and 4 deflected approximately 0.02 inches and specimen 3 deflected 0.1 inches. The deflections of specimens 1,2 and 4, are approximately equal to the 0.024 estimate. The measured deflection of .1 inches for test 3 is not consistent with uncracked behavior. The larger deflection occurred because the specimen was

initially loaded and then unloaded due to vibration of the test specimen and the hydraulic ram applying load. The wall was probably cracked during this initial loading and unloading thus preventing the measurement of deflections prior to wall cracking.

These estimates of uncracked wall behavior are consistent with measured observations since (a) it is inappropriate to compare specimen #3 deflections with estimates to assess the validity of the uncracked section deflection and (b) the other test measurements are approximately equal to estimates.

5.6.2 Idealization of flashing joint shear deformation behavior

Adjusted results of testing joints with vinyl flashing and 10K grout in all cells are shown in figure 4.6. The results are adjusted by dividing the load applied to the specimen by 2 assuming that the specimen load was equally divided between the two shear planes during testing. Although this conclusion may not be exact since most of the specimens failed on one of the shear planes prior to failure on the other, it provides acceptable estimates of wall strength as shown in the succeeding section. The adjusted results are idealized with a three part linear curve to facilitate their use for analyzing composite Brick Walls. The idealization was selected to provide a lower bound of the test results. It is described by the following set of coordinates.

$$Pideal := \begin{bmatrix} 0 \\ 3.5 \\ 6.2 \\ 6.2 \end{bmatrix} \cdot kip \qquad \Delta ideal := \begin{bmatrix} 0 \\ .04 \\ .155 \\ .37 \end{bmatrix} \cdot in$$

The idealization of load capacity using the 10K fully grouted shear specimen results is appropriate if the vertical reinforcing bars are far enough apart to prevent their interaction. As indicated by figure 4.1, little interaction is expected if the bars are 1½ brick modules, a nominal distance of 15 inches, or more apart. Thus for specimens 1 and 2, the moment behavior may be predicted based on the behavior of the fully grouted shear specimen behavior as indicated above. However, for specimens 3 and 4, where the vertical bars are one brick module apart, flashing joint shear capacity will be less based on data shown in figure 4.1. Based on the evaluation comparing shear specimen results and center to center bar spacing as summarized in figure 4.2, the shear capacity of 10 inch spacing is approximately the same as was determined for the shear specimens using #4 reinforcing bar with 10K grout in reinforced cells only. Based in data summarized in table 4.1, the load deformation curve data for the dowels used in specimens 3 and 4 would be as follows based on shear specimens with 10K grout in the reinforced cells only.

$$Pideal10 := \begin{bmatrix} 0 \\ 3.5 \\ \frac{9.9}{2} \\ \frac{9.9}{2} \end{bmatrix} \cdot kip \qquad \Delta ideal10 := \begin{bmatrix} 0 \\ .04 \\ .102 \\ .15 \end{bmatrix} \cdot in$$

Figure 5.9 shows the idealized curves for the wall specimens and test results based on shear specimens fully grouted with 10K grout. Shear specimen results are adjusted by dividing applied loads by 2. The curves are shown in terms of deformations, rather than strains, because deformations provide a better measure of joint behavior than strain. Since axial deformation of the brick wall is small compared to joint deformations, the behavior of a group of reinforcing steel dowels may be modeled by using joint load deformation results for one dowel and multiplying by the total number of dowels resisting load to obtain the total joint load.

5.6.3 Idealization of Joint Mortar Behavior

As shown in figure 3.10, almost all of the strain observed in the brick wall is due to strain in the joints. This is consistent with observations during wall specimen testing that rotation and wall tension cracking were concentrated below the mid span joint in the top of the wall. Based on this observation and the fact that shear at the flashing joint is controlled by joint deformation, not strain, the parameters for determining compression forces are developed based on joint deformation, not strain. Joint deformations, Δjoint, are calculated as the corrected machine prism strains shown in figure 3.10 multiplied by the prism specimen gage length, g, and divided by the number of joints within the gage length, 3.

For making moment rotation calculations before the brick wall yields in compression, the stress deformation curve for a joint is modeled as a linear

relationship. The curve used, which was determined by inspection of the results, is shown in figure 5.10 along with the stress deformation curves for 10K fully grouted specimens #2 and #3. The linear curve is defined by:

$$\text{stress} := \begin{pmatrix} 0 \\ 4.5 \end{pmatrix} \cdot \text{ksi} \qquad \text{deformation} := \begin{pmatrix} 0 \\ .005 \end{pmatrix} \cdot \text{in}$$

To make calculations predicting ultimate moment and rotation, the variables for use in determining compression forces, and their location, due to bending in the brick wall are determined based on determining the area and centroid of the stress deformation curves. Parameters defining an equivalent rectangular stress block for use in ultimate strength calculations were determined as follows.

a) A joint strain for use in calculating maximum strains associated with the rectangular stress block was selected based on test results from specimens 2 and 3. As shown in figure 5.10, the stress deformation curves determined for specimens 2 and 3 intersect at approximately 0.0093 inch deformation and 85% of the average strength of specimens 2 and 3. This deformation of .0093 inch was selected based on this observation. Review of test results indicates that the joints will probably withstand deformations larger than .0093 inches before failure.

b) The area and first moment of area under the stress deformation curves for specimens 2 and 3 at deformations up to 0.0093 inch were determined by summing up the areas under the curves for each test data point.

c) The distance to the centroid of the areas from the "0" or neutral axis was estimated by dividing the first moment of area by the area under the test curves. The

width of an equivalent rectangular stress block is twice the distance from the outside of the curve at .0093 inch to the centroid of the curve. The equivalent stress block width factor, $\beta 1$, is twice the distance from the outside to the centroid of the curve.

d) The stress amplification factor, $\beta 3$, for use with the stress block was determined based on the magnitude of stress required for the area of the equivalent stress block to be approximately the same as the average area under the stress deformation curves established by testing of specimens 2 and 3.

Based on these analyses, the equivalent stress block factors are as follows:

$\beta 1 = .8$ $\beta 3 = .85$

The resulting stress block is shown in figure 5.10 along with the load deformation curves for specimens 2 and 3 and the curve used for linear bending analysis of the wall. The coordinates of the corners of the stress block are defined as follows.

$$\text{Load} := \begin{bmatrix} 0 \\ 3880 \\ 3880 \\ 0 \end{bmatrix} \cdot \text{ksi} \qquad \text{Deformation} := \begin{bmatrix} .0019 \\ .0019 \\ .0093 \\ .0093 \end{bmatrix}$$

5.6.4 Cracked Section Behavior For Linear Portions Of Joint Deformation Curve

The behavior of the cracked wall section for the lower portion of the joint deformation curve will be in the linear range for both the brick joint and the steel reinforcing bars resisting shear load at the flashing joint. This analysis is based on plane sections remaining plane and equilibrium of forces and moments at the wall section. The analysis is similar to that presented in Park and Paulay (1975) and

Winter et. al. (1964) for singularly reinforced rectangular elastic concrete beams except the deformations, instead of strains, are used in the calculations. The reason to use deformations in the calculation is because the shear dowels are not continuous and thus the use of strains, which imply a continuous stress and strain profile, are inappropriate. When using deformations, it must be realized that equal deformations will occur on both sides of the plane of symmetry at the section being analyzed. This means that joint deformations, if representative of total joint deformations as is the case in figure 5.10, must be split evenly between the two sides if the shear forces from one side of the plane of symmetry are being used.

The calculation for cracked section behavior for the first linear portion of the joint deformation curve for a wall specimen with two shear dowels on each side of the center line, for a total of four dowels, was performed as follows.

a) The stiffness ratio for the shear joint and mortar joint, n1, is calculated from the linear load deformation curves shown in figures 5.9 and 5.10. The area ratio, p1, is calculated based on the number of shear bars on each side of the centerline and the area of the brick wall assuming the wall is filled with grout. In order to adjust for the use of stress for the brick and load for the shear lugs, the load in the shear lugs is takes as applied over a unit area.

$b = 4.625\,in$ $d := 15 \cdot in$

$$n1 = \frac{\frac{3.5 \cdot ksi}{.04 \cdot in}}{\left[\frac{4.5 \cdot ksi}{\left(\frac{.005 \cdot in}{2}\right)}\right]} \qquad n1 = 0.049$$

$$p1 = \frac{2 \cdot in^2}{b \cdot d} \qquad p1 = 0.029$$

b) The section behavior is then calculated from these geometry ratios.

$$k1 = \sqrt{p1^2 + 2 \cdot p1 \cdot n1} - p1 \cdot n1 \qquad k1 = 0.059$$

$$j1 = 1 - \frac{k1}{3} \qquad j1 = 0.98$$

c) Section moment, M1, specimen load, P1, maximum brick stress, fb1, section rotation, $\phi 1$, and specimen deflection, $\Delta 1$, are calculated using the cracked section configuration. Since the section reaches yield prior to the shear in the shear joint reaching 7.4 kip per shear dowel, the section moment capacity in the linear range is controlled by brick joint stress. Since the shear joint with flashing deforms uniformly, rotations for the wall are concentrated at the point of maximum moment and deflections, $\Delta 1$, are calculated by summing uncracked deflections plus deflections due to wall rotations concentrated at the point of maximum moment.

$T1 := 2 \cdot 3.5 \cdot kip$ $\qquad M1 := T1 \cdot j1 \cdot d$ $\qquad M1 = 8.578 \cdot kip \cdot ft$

$$fbj1 := \frac{M1}{\frac{b \cdot d^2 \cdot k1 \cdot j1}{2}} \qquad fbj1 = 3.427 \cdot ksi$$

The section behavior is controlled by flashing joint shear, as assumed, because the stress in the brick joint, fbj1, is less than the mean joint strength of 4.6 ksi as shown in section 5.3.3.

$$P1 := \frac{4 \cdot M1}{L} \qquad P1 = 4.575 \cdot kip$$

$$\phi 1 = \frac{\dfrac{fbj1}{\left[\dfrac{4.5\ ksi}{\left(\dfrac{.005\ in}{2}\right)}\right]}}{k1 \cdot d} \qquad \phi 1 = 0.002$$

$$\Delta 1 := \Delta uncrack + \phi 1 \cdot \frac{L}{2} \qquad \Delta 1 = 0.121 \cdot in$$

As an alternative, deflections at a load of P1 were calculated using the average moment of inertia, as is used in ACI 318 (Building, 1989) for concrete beams as follows.

$$Icrack1 := \frac{b \cdot (k1 \cdot h)^3}{3} + 2 \cdot in^2 \cdot n1 \cdot ((1 - k1) \cdot h)^2 \qquad Icrack1 = 20.437 \cdot in^4$$

$$\Delta 1try := \frac{M1 \cdot L^2}{12 \cdot Ebrickwall \cdot \dfrac{Iuncrack + Icrack1}{2}} \qquad \Delta 1try = 0.085 \cdot in$$

Data shown in figure 5.12 indicates that specimen deformations at a load of 4.5 kips for specimens #1 and #2 were .0872 inches and .106 inches. Based on this comparison, it is apparent that using the ACI 318 method slightly under predicts displacements and assuming center rotation slightly over predicts displacements. Since the measured and estimated deflections at this low load level are so small, either method is considered acceptable. However, as discussed below, the

assumption of center rotation provides a better estimate at slightly higher loads and is thus considered more appropriate for use.

This calculation is then repeated for the second linear portion of the idealized shear joint load deformation curve as follows. Since load deformation behavior is linear, the additional deformations and loads are superimposed on the results from the first linear portion to obtain total load deformation information.

a) The stiffness ratio for the shear joint and mortar joint, n2, is calculated from the linear load deformation curves shown in figures 5.9 and 5.10. The area ratio, p1, is calculated based on the number of shear bars on each side of the centerline and the area of the brick wall assuming the wall is filled with grout.

$$n2 := \frac{\frac{(6.2 - 3.5)\cdot ksi}{(.155 - .04)\cdot in}}{\left[\frac{4.5\cdot ksi}{\left(\frac{.005\,in}{2}\right)}\right]} \qquad n2 = 0.013$$

$$p2 := \frac{2\cdot in^2}{b\cdot d} \qquad p2 = 0.029$$

b) The section behavior is then calculated from these geometry ratios.

$$k2 := \sqrt{p2^2 + 2\cdot p2\cdot n2} - p2\cdot n2 \qquad k2 = 0.039$$

$$j2 := 1 - \frac{k2}{3} \qquad j2 = 0.987$$

c) Change in section moment, $\delta M1$, is then calculated using the additional brick joint stress available before yield is reached in the joint

$\delta fbj2 := 4.6\,ksi - fbj1$ $\quad \delta fbj2 = 1.173\cdot ksi$

$\delta M2 := \delta fbj2 \cdot \frac{b \cdot d^2 \cdot k2 \cdot j2}{2}$ $\quad \delta M2 = 1.978\cdot kip\cdot ft$

$\delta T2 := \frac{\delta M2}{j2 \cdot d}$ $\quad \delta T2 = 1.603\cdot kip$

d) Section Moment, M2, maximum brick joint stress, fbj2, flashing joint shear, T2, specimen load, P2, section rotation, $\phi 2$, and specimen deflection, $\Delta 2$, are calculated.

$M2 := M1 + \delta M2$ $\quad M2 = 10.556\cdot kip\cdot ft$

$fbj2 := fbj1 + \delta fbj2$ $\quad fbj2 = 4.6\cdot ksi$

$T2 := T1 + \delta T2$ $\quad T2 = 8.603\cdot kip$

$P2 := \frac{4 \cdot M2}{L}$ $\quad P2 = 5.63\cdot kip$

$$\delta\phi 2 := \frac{\frac{\delta fbj2}{4.5\cdot ksi}}{\frac{\left(\frac{.005\cdot in}{2}\right)}{k2\cdot d}} \qquad \delta\phi 2 = 0.001$$

$\phi 2 := \phi 1 + \delta\phi 2$ $\quad \phi 2 = 0.003$

$\Delta 2 := \Delta uncrack + \phi 2 \cdot \frac{L}{2}$ $\quad \Delta 2 = 0.171\cdot in$

As an alternative, deflections at a load of P2 were calculated using the average moment of inertia, as is used in ACI 318 (Building, 1989) for concrete beams as follows.

$Icrack2 := \frac{b\cdot(k1\cdot h)^3}{3} + 2\cdot in^2\cdot n1\cdot((1 - k1)\cdot h)^2$ $\quad Icrack2 = 20.437\cdot in^4$

$$\Delta 2try := \frac{M2 \cdot L^2}{12 \cdot Ebrickwall \cdot \frac{Iuncrack + Icrack2}{2}} \qquad \Delta 2try = 0.105 \cdot in$$

Data shown in figure 5.12 indicates that specimen deformations at a load of 5.6 kips for specimens #1 and #2 were .143 inches and .175 inches. Based on this comparison, it is apparent that using the ACI 318 method under predicts displacements by 50% to 75% and assuming center rotation slightly predicts displacements within the range of the measured displacements. Based on this comparison, the assumption of center rotation provides a better estimate of deflections and will be used in subsequent calculations.

5.6.5 Estimate of Ultimate Strength of Section

The methodology for estimating wall behavior at ultimate strength is similar to the methodology used for concrete beams except that the compression stress block for the brick joint and the deformation properties of the shear joint with flashing are different. Compression forces in the brick joint are based on the equivalent rectangular stress block shown in figure 5.10 except that joint deformations are divided by two to account for symmetry. Forces in the shear joint are based on the idealized curves shown in figure 5.9 multiplied by the number of dowels on each side of the section being evaluated.

The estimate of ultimate strength for the wall specimen with two vertical reinforcing steel dowels on each side of the center line, for a total of four dowels in the specimen, is as follows:

a) The tensile force is determined based of the ultimate strength of the flashing shear joint idealized curve as shown in figure 5.9.

$Tult := 2 \cdot 6.2 \cdot kip$ $\quad Tult = 12.4 \cdot kip$

b) The size of the equivalent stress block, a, is determined by equilibrium for forces and the magnitude of the maximum stress, Fcbult, in the equivalent stress block. Using the value of $\beta 1$ and $\beta 3$ found for the equivalent stress block, the location of the neutral axis, c, is determined and the ultimate moment is estimated.

$\beta 1 := .85$ $\quad \beta 3 := .8$

$Fcbult := \beta 1 \cdot 4.57 \cdot ksi$ $\quad Fcbult = 3.885 \cdot ksi$

$$a := \frac{Tult}{b \cdot Fcbult} \qquad a = 0.69 \cdot in$$

$$c := \frac{a}{\beta 3} \qquad c = 0.863 \cdot in$$

$$Mult := Tult \cdot \left(d - \frac{ac}{2} \right) \qquad Mult = 15.143 \cdot kip \cdot ft$$

$$Pult := \frac{4 \cdot Mult}{L} \qquad Pult = 8.076 \cdot kip$$

c) Calculate section rotation at mid span based on maximum deformation of the brick joint, $\Delta jbmax$. Then check deformation of shear joint, $\Delta jsmax$, to verify that the shear dowels will resist load at maximum deformation. Calculate deflection due to center rotation, Δult, based on ultimate loads. Then calculate maximum

deflection, Δmax, based on summation of uncracked wall deflections and rotations at section of maximum moment due to ultimate strength bending.

$\Delta jbmax := .0093 \cdot in$ $\qquad \phi ult := \frac{\Delta jbmax}{c}$ $\qquad \phi ult = 0.011$

$\Delta jsult := \Delta jbmax \cdot \frac{d - c}{c}$ $\qquad \Delta jsult = 0.152 \cdot in$

$\Delta ult := \phi ult \cdot \frac{L}{2}$ $\qquad \Delta ult = 0.485 \cdot in$

$\Delta max := \Delta uncrack + \Delta ult$ $\qquad \Delta max = 0.495 \cdot in$

d) Calculate maximum deflection at mid span, Δjsmax, assuming that shear joint deformation controls maximum deflection, not compression strain in the joint. This is feasible due to the high degree of confinement provided to the joint mortar by the brick. Joint mortar spalling due to compressive strains may also have been prevented by the bearing plate and load at mid span.

$\Delta sjult := \frac{.32 \cdot in}{d - c} \cdot \frac{L}{2}$ $\qquad \Delta sjult = 1.019 \cdot in$

$\Delta sjmax := \Delta uncrack + \Delta sjult$ $\qquad \Delta sjmax = 1.029 \cdot in$

$\phi sjult := \frac{.32 \cdot in}{d - c}$ $\qquad \phi sjult = 0.023$

The estimate of ultimate strength for the wall specimen with four vertical reinforcing steel dowels on each side of the center line, for a total of eight dowels in the specimen, is as follows.

a) The tensile force is determined based of the ultimate strength of the flashing shear joint as shown in figure 5.9.

$Fult = \frac{9.9}{2} \cdot kip$ $\quad Tult2 := 4 \cdot Fult$ $\quad Tult2 = 19.8 \cdot kip$

b) The size of the equivalent stress block, ac, is determined by equilibrium for forces and the magnitude of the maximum stress, Fcbult, in the equivalent stress block. Using the value of a found for the equivalent stress block, the location of the neutral axis, c, is determined and the ultimate moment is estimated.

$\beta 1 = .85$ $\quad a := .8$ $\quad Fcbult := \beta 1 \cdot 4.57 \cdot ksi$ $\quad Fcbult = 3.885 \cdot ksi$

$ac2 = \frac{Tult2}{b \cdot Fcbult}$ $\quad ac2 = 1.102 \cdot in$

$c2 := \frac{ac2}{a}$ $\quad c2 = 1.378 \cdot in$

$Mult2 := Tult2 \cdot \left(d - \frac{ac2}{2} \right)$ $\quad Mult2 = 23.841 \cdot kip \cdot ft$

$Pult2 := \frac{4 \cdot Mult2}{L}$ $\quad Pult2 = 12.715 \cdot kip$

c) Calculate section rotation at mid span based on maximum deformation of the brick joint, $\Delta jbmax$. Then check deformation of shear joint, $\Delta jsmax$, to verify that the shear dowels will resist load at maximum deformation. Calculate deflection due to center rotation, Δult, based on ultimate loads. Then calculate maximum deflection, Δmax, based on summation of deflections due to plastic moment and linear elastic behavior.

$\Delta jbmax := .0093\,in \qquad \phi ult2 := \frac{\Delta jbmax}{c2} \qquad \phi ult2 = 0.007$

$\Delta jsult2 := \Delta jbmax \cdot \frac{d - c2}{c2} \qquad \Delta jsult2 = 0.092 \cdot in$

$\Delta ult2 := \phi ult2 \cdot \frac{L}{2} \qquad \Delta ult2 = 0.304 \cdot in$

$\Delta ult2 := \Delta uncrack + \Delta ult2 \qquad \Delta ult2 = 0.328 \cdot in$

d) Calculate maximum deflection at mid span, Δjsmax, assuming that shear joint deformation controls maximum deflection, not compression strain in the joint. This is feasible due to the high degree of confinement provided to the joint mortar by the brick.

$\Delta sjult2 := \frac{.1 \cdot in}{d - c2} \cdot \frac{L}{2} \qquad \Delta sjult2 = 0.33 \cdot in$

$\Delta sjmax2 := \Delta uncrack + \Delta sjult2 \qquad \Delta sjmax2 = 0.354 \cdot in$

$\phi sjult2 := \frac{.1 \cdot in}{d - c2} \qquad \phi sjult2 = 0.007$

5.6.6 Comparison Of Small Scale Test Wall Actual And Predicted Behavior

Actual test measurement and estimated wall behavior data are compared in figures 5.11 and 5.12. Inspection of these figures indicates that the model for the four dowel specimen predicts both displacements and rotations at the center of the brick wall versus test load well. Based on this comparison, the behavior of walls with vertical dowels spaced 20 inches or more apart can be predicted using the numerical model developed in this section.

The model for the eight dowel specimen predicts both ultimate moment and load well. Although it predicted rotations at the center of the wall reasonably well, there is a substantial difference between predicted displacements and measured displacements. The following were considered in evaluating this problem.

a) Measured and predicted rotations were similar. The differences observed indicate that displacements should also be similar since deflections and rotations both compared well for the four dowel specimens.

b) Shear deformations were estimated to be on the order of 0.009 inches for the wall specimen. Thus, shear deformations are too small to explain the differences.

c) Specimen 3 failed due to lateral tipping as the load was applied. The failure mode was breaking of the concrete beam at an end bearing resulting in instability. Since only specimen 3 failed by tipping it is expected that results for specimen 3 would be different from results for other specimens.

d) Specimen 4 was loaded and unloaded due to test error before deformation and load measurements were collected. This may have altered the magnitude of displacements observed during testing.

e) Vertical deflection measurements were made on only one side of the specimen since the instability problem which occurred was unexpected. Specimens 1 and 2 appeared stable during testing which implied that the use of a single LVDT to measure vertical displacement would be acceptable for the subsequent testing of specimens 3 and 4.

f) The numerical difference between predictions and measured value is approximately ¼ inch.

Based on these considerations, it is concluded that estimates based on the numerical model should be used.

5.7 Evaluation Of Results

The results obtained from the small scale wall tests and associated calculations, which are summarized in figures 5.11 and 5.12, demonstrate that reinforced brick walls and concrete beams supporting them can be built to resist in-plane bending loads using composite action even if they are separated by flashing. This implies that, with appropriate details, reinforced brick walls can mitigate damage due to unexpected foundation movements or loss of support. The principle construction provisions recommended to obtain optimum performance are as follows:

a) The first course of reinforced brick should use bond beam bricks with the broken away side facing downward for the cells on either side of a cell with a vertical reinforcing dowel in it.

b) The first two courses of brick must be grouted on either side of a cell with a vertical reinforcing dowel in it.

c) The minimum spacing of vertical reinforcing dowels is 20 inches. This provision is based on (1) data summarized in figure 4.1 and (2) the successful performance of the wall specimens with a total of four dowels as compared with the premature failure of the brick wall around the dowels in the wall with a total of eight dowels.

d) Based on the success of these tests and the problems indicated during shear joint testing where #6 reinforcing bars were used, a #4 is the maximum size of reinforcing

bar which should be used to develop composite action between a reinforced wall using Suprking bricks and its foundation.

e) Ultimate strength design methods predict the behavior of the wall.

f) Ultimate section rotations may be calculated based on flashing joint deformations in lieu of mortar joint compressive strains. This is acceptable because the joint mortar is confined by the bricks and prevented from catastrophic failure. As a result, the wall will develop a compressive hinge capable of adequate rotation to develop the dowels at the flashing joint. Similar large joint deformations have been in testing of concrete masonry when confining plates are provided to prevent masonry failure due to joint mortar deformation as described by Mayes and Clough (1975).

g) Vertical wall displacements may be predicted by assuming all rotation deformations are concentrated at the point of maximum moment since the wall cracking and deformation are concentrated at the point of maximum moment.

Calculations contained in this chapter may be used as a guide to estimate the impact less than favorable conditions. In addition, data presented in figure 4.1 may be used to alter behavior estimates if less than optimum conditions, such as less grouting or closer spacing than suggested, are provided.

These small scale wall tests demonstrate that use of a reinforced brick wall with a flashing joint between it and the building foundation provides significant resistance to in-plane bending moments associated with changes in foundation support conditions.

Chapter 6

Methodology For Design Of Wall Structures

6.1 General

6.1.1 Scope

This chapter provides recommendations for the use of reinforced Suprking brick walls to resist in-plane moments through the use of dowels to transfer shear through a flashing joint. These recommendations are considered special design provisions applicable to a particular configuration of wall and supplemental to applicable codes. Design of the wall should be in accordance with the legally adopted building code. The provisions recommended for strength design of the wall and flashing joints dowels are similar to those contained in ACI 318 (Building, 1989) for the design of reinforced concrete.

6.1.2 Applicable Code

Construction of reinforced brick walls should be in accordance with ACI 530 (Building, 1992). This code was written to cover the structural design and construction of masonry elements and is intended by be part of the general building code. The recommendations contained in this research for the use of reinforcing

bars as shear dowels for flashing joints in reinforced Suprking walls are considered to constitute a special system of design under the provisions of the ACI 530 (Building, 1992) code.

6.2 Materials

The following materials were used in this research and should be used for construction where this special system is used.

6.2.1 Hollow Brick

Hollow Clay masonry should consist of Suprking bricks as manufactured by the General Shale Company of Johnson City, Tennessee. Both regular and bond beam bricks with portions of their flanges removed are used in this system. The bricks should conform to ASTM C 652 (Standard, 1991).

6.2.2 Mortar

Type N mortar was used for this research. Types M and S mortar, which contain a smaller proportion of lime than Type N mortar, are also acceptable for construction using this special system.

6.2.3 Grout

Grout used in this research was Sonogrout 10K (Sonogrout, 1992). Either 10K grout or a grout with a 28 day compressive strength of 4300 psi or larger when tested in accordance with ASTM C1019-89a (Standard, 1989) should be used in the first two

courses of brick adjacent to a flashing joint. Other grouts which comply to the applicable code may be used elsewhere in the reinforced brick wall.

6.3.5 Flashing

Flashing used in this research was XXXX vinyl flashing. This flashing or an equivalent flashing should be used with this system. Copper sheet metal flashing may be used provided that shear joint dowel capacity is reduced.

6.3 Constructions Requirements

6.3.1 Steel Reinforcement

a) Steel reinforcement used as dowels to transfer shear at flashing joints should be #4 deformed bars meeting the requirements of ASTM A615, grade 60 (Standard, 1994). Other grades and types of reinforcing bars may be used if the capacity of the associated shear joints with flashing are determined.

b) The reinforcing steel should be embedded in grout or concrete on either side of the flashing joint for a distance required to develop the capacity of the #4 bar in tension.

c) The nominal minimum horizontal spacing of dowels should be 20 inches. This requirement is met if dowels are at least 18 inches center to center. Closer dowel spacing is acceptable if additional evaluation is provided. 6.3.2 Location Of Bond Beam Bricks

Bond beam bricks, with the break-out portion of their flanges removed, shall be used in the first course of brick adjacent to the flashing joint such that a continuous grouted cell may be formed next to the joint for one cell in both directions beyond the grouted cell with reinforcing. Bond beam bricks may be omitted provided additional evaluation is provided.

6.3.3 Grouting

a) Grout should be placed in all cells with reinforcing steel and in the cells on either side of the cells with reinforcing for a distance of at least two brick courses from the flashing joint.

b) In addition, grout in the first course of brick next to the joint should be continuous between the cell with reinforcing and the adjacent cells. This continuity should be assured by using bricks with at least one-half of their flanges removed and a grout consistency allowing free flow of grout between cells. Grout in adjacent cells may be omitted if additional evaluation is provided.

6.4 General Considerations

6.4.1 Design Methods

The design of reinforced brick walls for in-plane moments where shear joints with flashing are used for tension loads associated with bending should be based on strength design methods. This is due to (a) the local nature of deformations and (b) the relatively low stiffness of the shear dowels compared to the stiffness of the masonry making the classic assumptions of elastic beam theory inappropriate. In

order to provide compatibility with the elastic analysis provisions of the of the ACI 530 (Building, 1992) code, the allowable section forces should be one-fourth of the nominal strength.

6.4.2 Loading

Reinforced brick walls may be designed for in-plane moments associated with abnormal or unexpected events, such as subsidence, soil volume change, or loss of support due to erosion. For these loads, the nature of loading and the consequences of large deformations should be evaluated by the designer using nominal strength and estimates of ultimate deformations of the wall in lieu of allowable section forces.

6.4.3 Methods Of Analysis

Elastic methods of analysis may be used to determine in-plane moments for design of reinforced brick walls with flashing joint shear dowels. Nonlinear methods may be used if appropriate nonlinear behavior of the wall is considered.

6.4.4 Stiffness And Modulus Of Elasticity

For linear elastic section calculations, such as may be used to determine wall stiffness prior to tension cracking, the modulus of masonry, Em, should be 2,800,000 psi.

For deformation calculations, which are used to predict wall behavior when flashing joint shear resists wall bending tension, the idealized curves shown in figures 5.9 and 5.10 should be used to determine the relative stiffness of wall components.

6.4.5 Design Strength Of Masonry

The design strength of Suprking brick masonry should be 4500 psi.

6.4.6 Design Strength Of Flashing Joint Dowels

The optimal design strength of PVC flashing joint #4 reinforcing steel dowels is 6,200 lb. per a dowel in shear. If Copper sheet metal flashing is used, in lieu of PVC flashing, the optimal design strength of dowels should be reduced to 4,000 lb. per dowel in shear. Additional evaluations to assess the impact of less than optimum spacing of reinforcing steel, less grouting than recommended, the use of regular hollow brick units in the first course of the wall, and the use of grout other than 10K should be based on the data in figure 4.1.

6.4.7 Deflections

Deflections for reinforced brick walls subsequent to cracking should be based on concentrated section rotations associated with flashing joint shear deformations at the location of maximum moment. Deflections associated with uncracked wall behavior at other sections, although small compared to deflections due to cracked section behavior at the point of maximum moment, may be considered.

6.5 Design Procedures

6.5.1 Design Assumptions

Design of a reinforced Suprking brick wall using #4 reinforcing steel dowels at a flashing joint to resist tension loads associated with in-plane bending should be as follows.

a) Deformation in the brick masonry and the flashing joint should be assumed directly proportional to the distance from the neutral axis.

b) Maximum usable deformation of the flashing shear joint should be 0.37 inches.

c) Maximum compressive deformation of the brick joint at the point of maximum moment should be .0093 inches unless the top of the brick joint is confined. If the brick joint is confined, section rotations should be based on maximum deformation of the flashing joint.

d) Load in brick joints and flashing joint shear dowels should be based on section deformations and the relative stiffness of components.

e) Tensile strength of masonry should be neglected in determining the acceptability of section strength. Tensile strength of masonry may be considered in estimating wall deformations and interaction with other structures and materials.

f) The relationship of masonry compressive stress distribution and deformations may be assumed any shape consistent with stress deformation curves shown in figure 5.10. This requirement is satisfied by a rectangular stress block where $a=\beta_1 c$ and a uniform masonry stress of β_3 times the design strength of masonry is used.

g) The factor β_1 should be taken as 0.80.

h) The factor β_3 should be taken as 0.85.

6.5.2 Composite Behavior

The flashing joint with shear dowels will not provide composite behavior where horizontal strains may be assumed equal between structural components above and below the joint. The flashing joint should be assumed to transfer shear loads consistent with the stiffness of the dowels.

6.5.3 Distribution Of Dowels

Vertical steel reinforcing dowels at the flashing joint should be distributed such that the total joint shear due to moment at any section of the wall will be resisted by dowels between the section and the ends of the wall. This provision is intended to assure that horizontal shear in the flashing joint is resisted at all points during loading to prevent slip.

6.5.4 Combination Of Horizontal Wall Reinforcing And Flashing Joint Dowels

Tension loads resulting from in-plane bending should be resisted by either reinforcement placed within the reinforced brick wall or flashing joint shear dowels. The strength of these two elements should not be combined in determining nominal section strength.

Chapter 7

Design Examples

7.1 Summary

This chapter presents several design examples where reinforced brick walls are designed to resist in-plane bending using shear force at a flashing joint and #4 steel reinforcing bar dowels crossing the joint. The examples only address in-plane bending and determination of the location and number of #4 bars crossing the flashing joint. Other sources, such as ACI 530 (Building, 1992) and Schneider and Dickey (1994), provide methods and design examples for conditions not directly associated with shear transfer at the flashing joint.

7.2 Wall Design Program Using Mathcad

This section develops a personal computer program to automate the design of a reinforced brick wall attached to a concrete beam with a PVC flashing joint in between and reinforcing steel dowels to transfer shear from the wall to the foundation. The program Mathcad Plus 6.0 (Mathcad, 1995) is used because it generates calculations which may be directly included in official computations with little additional explanation. The program is as follows.

Shear Joint With Flashing And #4 Dowel Design Program.

The number of #4 reinforcing steel dowels required to cross the flashing joint between the point of maximum moment and the support of the wall is determined by this calculation. In addition, the moment curvature diagram for the wall and wall deflections are estimated for the number of dowels selected.

The designer must assure that the number of dowels between any point on the wall and the wall support is adequate to develop the flashing joint shear required by moments at the selected point on the wall. In addition, reinforcing around openings must be adequate to develop the shear forces in the flashing joint. The ultimate shear strength of #4 grade 60 reinforcing steel dowels crossing a PVC flashing joint is 6,200 lb.

The design steps to determine the number of #4 reinforcing steel dowels required are as follows.

1) Enter an estimate of the number of #4 reinforcing steel dowels between the point of maximum negative moment and the end support, Nestimate.

Nestimate :=

missing operand

2) Enter the nominal moment strength, Mnm, to be resisted by the brick wall.

Mnm := ▪ · lbf · ft

missing operand

3) Enter the height of the brick wall, h, from the flashing joint to the top of the top brick course constructed with the wall. The top course consists of grouted bond beam bricks.

h := ▪ · in

missing operand

4) Enter the distances, L1 and L2, from the point of maximum moment to either adjacent supports or points of inflection. These distances will be used to determine differential deflections assuming all section rotation after wall tensile cracking is concentrated at the point of maximum moment

L1 := ▪ · in

missing operand

L2 := ▪ · in

missing operand

5) The program will now perform the following calculations and provide results as shown.

a) Assign dimensional units to supplement Mathcad provided unit data

$kip := 1000\,lbf \qquad psi := \frac{lbf}{in^2} \qquad ksi := 1000\,psi$

b)Perform uncracked section analysis. The uncracked section analysis is based on classic beam theory assuming plane sections remain plane and that the tension stress in the brick does not exceed the splitting tension strength of the Suprking bricks. Tensile strength of the bricks, Tubrick, is estimated based on test value values. The

modulus of elasticity of the brick wall, Ebrickwall, is estimated based on test results for 10K grouted prisms specimens.

$Tubrick := 750 \cdot psi$ $Ebrickwall := 2800 \cdot ksi$

c) The height, h, and brick wall thickness, twallbrick, of the brick wall are then used to calculate the uncracked section moment of inertia, Iuncrack, and moment, Muncrack, when stress will reach the tensile strength of the brick wall. Section rotation at mid span of the specimen, ϕuncrack, is then calculated. This calculation assumes that the point of maximum moment does not occur at a grouted cell in the wall. If the wall is grouted at the point of maximum moment, the thickness, twallbrick, should be modified by not subtracting the width of the cell, 2.625 in.

$twallbrick := (4.625 - 2.625) \cdot in$ $Iuncrack := \frac{twallbrick \cdot h^3}{12}$

$Muncrack := \frac{Tubrick \cdot Iuncrack \cdot 2}{h}$ $Muncrack = \cdot kip \cdot ft$

$\phi uncrack := \frac{Tubrick \cdot 2 \cdot in}{Ebrickwall \cdot h}$ $\phi uncrack \cdot 10^6 =$

d) Deflection of the wall, Δuncrack, is calculated using the lengths, L1 and L2, as the distance between the supports and assuming that the specimen is simply supported with a concentrated load at the point of maximum moment. Deflections for other loading configurations may be determined by changing the formula for Δuncrack as appropriate. Since Δuncrack is small compared to other displacements, the use of the point load formula is generally acceptable.

$$\Delta uncrack := \frac{Muncrack \cdot L1 \cdot L2}{12 \cdot Ebrickwall \cdot Iuncrack} \qquad \Delta uncrack = \cdot in$$

e) Elastic cracked section analysis, first linear portion of the flashing joint deformation curve, is then used to calculate behavior up to a joint load of 3.5 kip per a dowel. The stiffness ratio for the shear joint and mortar joint, n1, and the area ratio, p1, is calculated based on the number of shear bars on each side of the centerline and the area of the brick wall assuming the wall is filled with grout. In order to adjust for the use of stress for the brick and load for the shear lugs, the load in the shear lugs is taken as applied over a unit area.

$b := 4.625\,in \qquad d := h$

$$n1 := \frac{\frac{3.5 \cdot ksi}{.04 \cdot in}}{\left[\frac{4.5 \cdot ksi}{\left(\frac{.005\,in}{2}\right)}\right]} \qquad n1 = 0.049$$

$$p1 := \frac{Nestimate \cdot in^2}{b \cdot d} \qquad p1 =$$

f) The section behavior is then calculated from these geometry ratios.

$$k1 := \sqrt{p1^2 + 2 \cdot p1 \cdot n1} - p1 \cdot n1 \qquad k1 =$$

$$j1 := 1 - \frac{k1}{3} \qquad j1 =$$

g) Section moment, M1, maximum brick stress, fb1, total section rotation, $\phi 1$, and specimen deflection, $\Delta 1$, are calculated using the cracked section configuration. The designer must verify that the section reaches yield stress of 4600 psi after the shear in

the flashing joint reaches 6.2 kip per shear dowel. This indicates that the section moment capacity in the linear range is controlled by brick joint stress. If the reverse is true, the calculations must be revised to be controlled by flashing joint stress. Due to the small value of the modular ratio n1, brick yielding usually controls cracked section behavior. The total section rotation, $\phi 1$, is calculated based on the total deformation determined for brick joints and should be used directly to determine total joint rotation. These calculations assume that the shear joint with flashing deforms uniformly, rotations for the wall are concentrated at the point of maximum moment, and that deflections, $\Delta 1$, are calculated by summing uncracked deflections plus deflections due to wall rotations concentrated at the point of maximum moment.

$T1 = Nestimate \cdot 3.5 \cdot kip$ $\quad M1a := T1 \cdot j1 \cdot d$ $\quad M1a = \cdot kip \cdot ft$

$$fbj1 = \frac{M1a}{\frac{b \cdot d^2 \cdot k1 \cdot j1}{2}} \qquad fbj1 = \cdot ksi \qquad \frac{fbj1}{4.6 \cdot ksi} =$$

$$\phi 1a := \frac{fbj1}{\left[\frac{4.5 \cdot ksi}{\left(\frac{.005 \cdot in}{2}\right)}\right]}{k1 \cdot d} \qquad \phi 1a =$$

$\phi 1 = if(\phi 1a \le \phi uncrack, \phi uncrack, \phi 1a)$

$M1 := if(M1a \le Muncrack, Muncrack, M1a)$

$$\Delta 1 := \Delta uncrack + \phi 1 \cdot \left(\frac{L1 + L2}{2}\right) \qquad \Delta 1 = \cdot in$$

h) The calculation for linear cracked section behavior is then repeated for the second linear portion of the idealized shear joint load deformation curve. Since load deformation behavior is linear, the additional deformations and loads are superimposed on the results from the first linear portion to obtain total load deformation information.

$$n2 := \frac{\frac{(6.2 - 3.5)\cdot ksi}{(.155 - .04)\cdot in}}{\left[\frac{4.5\cdot ksi}{\left(\frac{.005\,in}{2}\right)}\right]} \qquad n2 = 0.013$$

$$p2 := \frac{Nestimate\cdot in^2}{b\cdot d} \qquad p2 =$$

$$k2 := \sqrt{p2^2 + 2\cdot p2\cdot n2} - p2\cdot n2 \qquad k2 =$$

$$j2 := 1 - \frac{k2}{3} \qquad j2 =$$

$$\delta fbj2 := 4.6\,ksi - fbj1 \qquad \delta fbj2 = \cdot ksi$$

$$\delta M2 := \delta fbj2\cdot\frac{b\cdot d^2\cdot k2\cdot j2}{2} \qquad \delta M2 = \cdot kip\cdot ft$$

$$\delta T2 := \frac{\delta M2}{j2\cdot d} \qquad \delta T2 = \cdot kip$$

i) Section Moment, M2, maximum brick joint stress, fbj2, flashing joint shear, T2, section rotation, $\phi 2$, and specimen deflection, $\Delta 2$, are calculated as follows.

$$M2a := M1a + \delta M2 \qquad M2a = \cdot kip\cdot ft$$

$$fbj2 := fbj1 + \delta fbj2 \qquad fbj2 = \cdot ksi$$

$T2 := T1 + \delta T2$ $T2 = \cdot kip$

$$\delta\phi 2 := \frac{\frac{\delta fbj2}{4.5 \cdot ksi}}{\frac{\left(\frac{.005 \cdot in}{2}\right)}{k2 \cdot d}} \qquad \delta\phi 2 =$$

$\phi 2a := \phi 1a + \delta\phi 2$ $\phi 2a =$

$\phi 2 := if(\phi 2a \le \phi uncrack, \phi uncrack, \phi 2a)$

$M2 := if(M2a \le Muncrack, Muncrack, M2a)$

$$\Delta 2 := \Delta uncrack + \phi 2 \cdot \left(\frac{L1 + L2}{2}\right) \qquad \Delta 2 = \cdot in$$

j) Ultimate strength behavior is estimated using an idealized stress block for compression of the wall's top brick bond beam course.

$Fult := 6.2 \cdot kip$ $Tult := Nestimate \cdot Fult$ $Tult = \cdot kip$

k) The size of the equivalent stress block, a, is determined by equilibrium for forces and the magnitude of the maximum stress, Fcbult, in the equivalent stress block. Using the value of $\beta 1$ and $\beta 3$ found for the equivalent stress block, the location of the neutral axis, c, is determined and the ultimate moment is estimated.

$\beta 1 := .85$ $\beta 3 := .8$

$Fcbult := \beta 1 \cdot 4.57 \cdot ksi$ $Fcbult = \cdot ksi$

$$a := \frac{Tult}{b \cdot Fcbult} \qquad a = \cdot in$$

$$c := \frac{a}{\beta 3} \qquad c = \cdot in$$

$$Mnult := Tult \cdot \left(d - \frac{a}{2}\right) \qquad Mnult = \cdot kip \cdot ft$$

l) Calculate section rotation at mid span based on maximum deformation of the brick joint, Δjbmax. Then check deformation of shear joint, Δjsmax, to verify that the shear dowels will resist load at maximum deformation. Calculate deflection due to center rotation, Δult, based on ultimate loads. Then calculate maximum deflection, Δmax, based on summation of uncracked wall deflections and rotations at section of maximum moment due to ultimate strength bending.

$\Delta jbmax := .0093 in$

$$\phi ult := \frac{\Delta jbmax}{c} \qquad \phi ult =$$

$$\Delta jsult := \Delta jbmax \cdot \frac{d - c}{c} \qquad \Delta jsult = \cdot in$$

$$\Delta ult := \phi ult \cdot \frac{L1 + L2}{2} \qquad \Delta ult = \cdot in$$

$$\Delta max := \Delta uncrack + \Delta ult \qquad \Delta max = \cdot in$$

m) Calculate maximum deflection at mid span, Δjsmax, assuming that shear joint deformation controls maximum deflection, not compression strain in the joint. These deformations were observed in wall tests. They are probably due to the high degree of confinement provided to the joint mortar by the brick. In addition, joint mortar spalling due to compressive strains may also have been prevented during tests by the bearing plate and load at the point of maximum moment.

$$\Delta sjult := \frac{.32 \cdot in}{d - c} \cdot \frac{L1 + L2}{2} \qquad \Delta sjult = \cdot in$$

$$\Delta sjmax := \Delta uncrack + \Delta sjult \qquad \Delta sjmax = \cdot in$$

$$\phi sjult := \frac{.32 \cdot in}{d - c} \qquad \phi sjult =$$

n) Compare predicted ultimate moment, Mnult, with the required nominal moment strength, Mnm, to determine if number of dowels, Nestimate, is acceptable. The program should be iterated with different values of Nestimate until an acceptable design is determined.

$$Mnm = \cdot kip \cdot ft \qquad Mnult = \cdot kip \cdot ft \qquad \frac{Mnm}{Mnult} =$$

o) The moment rotation and moment displacement curves are generated by creating vectors summarizing results and plotting them as follows.

$$M := \begin{bmatrix} 0 \\ Muncrack \\ Muncrack \\ M1 \\ M2 \\ Mnult \\ Mnult \\ Mnult \end{bmatrix}$$

$$\phi := \begin{bmatrix} 0 \\ \phi uncrack \\ \phi 1 \cdot \dfrac{Muncrack}{M1} \\ \phi 1 \\ \phi 2 \\ \phi 2 + (Mnult - M2) \cdot \dfrac{\phi 2}{M2} \\ \phi ult \\ \phi sjult \end{bmatrix} \qquad \Delta := \begin{bmatrix} 0 \\ \Delta uncrack \\ \Delta uncrack + \phi_2 \cdot \left(\dfrac{L1 + L2}{2} \right) \\ \Delta 1 \\ \Delta 2 \\ \Delta uncrack + \phi_5 \cdot \left(\dfrac{L1 + L2}{2} \right) \\ \Delta max \\ \Delta sjmax \end{bmatrix}$$

The following sections demonstrate the use of this program in several example problems.

7.3 Wall Subjected To Mining Subsidence

Mining subsidence occurs as a result of the removal of minerals from the ground over a substantial area. As a result of the removal, the overlying rock mass subsides into the cavities created. As a result, the ground surface subsides a corresponding amount forming hollows and trenches, abrupt steps, cracks in the ground surface, and extensive subsidence troughs. The ground can sink vertically or move horizontally for as much as several yards depending on the extent of the minerals removed. Prediction of mining subsidence and determination of appropriate design provisions are discussed in references such as Kratzsch (1983).

Mining subsidence moves horizontally on the ground surface forming a wave shape as shown in figure 7.1. The wave may pass completely under the structure or stop while the structure is perched on the side of the slope in one of the three stages shown in figure 7.1. In any case, the wall structure should be designed considering the three stages. For convex curvature in stage 1, the top of the wall is in tension and the bottom of the wall is in compression. Steel reinforcing in a bond beam at the top of the wall could be designed using provisions contained in ACI 530 (Building, 1992) or other applicable document. Loads in the flashing joint shear dowels need not be considered in stage 1 due to due to low flashing joint stiffness relative to masonry compressive stiffness. The following example demonstrates that joint shear forces will be low due to relative joint stiffness effects.

a) Consider a compression stress block in the masonry immediately above the shear joint. Assume the maximum deformation in the masonry stress block is 0.0093 inches, as is assumed in figure 5.10, and the compressive force is 25 kips. The assumption of a 25 kip load is similar to the ultimate compressive load in the masonry found in this example for the case of concave curvature. The load in the shear joint will be determined for these conditions.

b) The shear joint, based on the design for the concave curvature case, requires four dowels between the point of maximum curvature and the end support. Based on this number of dowels and the stiffness of the shear joint dowels shown in figure 5.9, the force in each dowel, Fdowel, for a deformation is 0.0093 is as follows. The force

on the joint, Fjoint, is then calculated and compared with the masonry load of 25 kips.

$$Fdowel := 0.0093\frac{3.5}{.04}\cdot kip \qquad Fdowel = 0.814\cdot kip$$

$$Fjoint := 4\cdot Fdowel \qquad Fjoint = 3.255\cdot kip$$

$$Ratio := \frac{Fjoint}{25\cdot kip} \qquad Ratio = 0.13$$

As shown in this calculation, neglecting the joint forces will increase the conservatism of the design estimate of masonry compressive force for convex curvature by 15%. This improvement, which would not impact the design of the reinforcing steel in the bond beam at the top of the wall since the size of the ultimate strength compressive stress block is small compared to wall height, is considered unnecessary since joint design will be controlled by the concave curvature case. For nil curvature in stage 2, no special design provisions are required.

For concave curvature in stage 3, the bottom of the wall is in tension. The use of vertical steel reinforcing as dowels provides an economical method to resist the tension in the bottom of the wall resulting from concave earth curvature. To demonstrate the use of the research presented in this paper, consider a reinforced brick wall using Suprking bricks as shown in figure 6.2. Based on criteria for permanent damage described in Kratzsch (1983), the design of the brick wall flashing joint dowels should limit cracking to 0.2 inches. Using this criteria, the calculation is as follows.

7.3.1 Data For Use In Wall Analysis Program

The Dead Load, DL, and Long Term Live Load, LL, used for evaluation of wall behavior is due to subsidence is estimated based of the following assumptions.

(1) 12 foot wide strip of floor area contributes to the load on the wall

(2) a 6 inch wide by 2 foot deep concrete foundation with enough steel reinforcing to resist tension from wall shear dowels and earth movement is attached to the bottom of the wall

(3) the dead load from the floor and roof at the top and bottom of the wall, respectively, is 10 lb. per square foot

(4) the long term live load on the floor is 10 lb. per square foot

(5) there is no significant long term live load on the roof

These assumptions are then used for the following calculations.

$$DL := \left[(8 \cdot ft \cdot 4.625\,in + 2 \cdot ft \cdot 6 \cdot in) \cdot 150 \cdot \frac{lbf}{ft^3} \right] + (10 + 10) \cdot \frac{lbf}{ft^2} \cdot 12 \cdot ft \qquad DL = 852.5 \cdot \frac{lbf}{ft}$$

$$LL := 10 \cdot \frac{lbf}{ft^2} \cdot 12 \cdot ft \qquad LL = 120 \cdot \frac{lbf}{ft}$$

The estimated applied moment from DL, MDL, and LL, MLL, using the length of the wall, L, or 40 feet is determined for comparison with the strength of the wall.

$$L := 40 \cdot ft$$

$$MDL := \frac{DL \cdot L^2}{8} \qquad MDL = 170.5 \cdot kip \cdot ft$$

$$MLL := \frac{LL \cdot L^2}{8} \qquad MLL = 24 \cdot kip \cdot ft$$

In addition, acceptable angular rotation, faccept, is determined based on the criteria to prevent permanent damage.

$$\phi accept := \frac{.2 \cdot in}{8 \cdot ft} \qquad \phi accept = 0.002$$

7.3.2 Application of Shear Joint Design Program

The shear joint design program is used to determine the appropriate number of dowels on each side of the wall centerline as follows.

Shear Joint With Flashing And #4 Dowel Design Program.

The number of #4 reinforcing steel dowels required to cross the flashing joint between the point of maximum moment and the support of the wall is determined by this calculation. In addition, the moment curvature diagram for the wall and wall deflections are estimated for the number of dowels selected.

The designer must assure that the number of dowels between any point on the wall and the wall support is adequate to develop the flashing joint shear required by moments at the selected point on the wall. In addition, reinforcing around openings must be adequate to develop the shear forces in the flashing joint. The ultimate strength of #4 grade 60 reinforcing steel dowels to be developed by the wall opening design is 6,200 lb.

The design steps to determine the number of #4 reinforcing steel dowels required are as follows.

1) Enter an estimate of the number of #4 reinforcing steel dowels between the point of maximum negative moment and the end support, Nestimate.

Nestimate := 4

2) Enter the nominal moment strength, Mnm, to be resisted by the brick wall.

Mnm := MDL + MLL Mnm = 194.5·kip·ft

3) Enter the height of the brick wall, h, from the joint with flashing to the top brick course constructed with the wall. The top course consists of grouted bond beam bricks.

h := 8·ft

4) Enter the distances, L1 and L2, from the point of maximum moment to either adjacent supports or points of inflection. These distances will be used to determine differential deflections assuming all section rotation after wall tensile cracking is concentrated at the point of maximum moment

$L1 := \frac{L}{2}$ $L2 := \frac{L}{2}$

5) The program will now perform the following calculations and provide results as shown.

a) Assign dimensional units to supplement Mathcad provided unit data

kip = 1000 lbf $psi := \frac{lbf}{in^2}$ ksi := 1000 psi

b) Perform uncracked section analysis. The uncracked section analysis is based on classic beam theory assuming plane sections remain plane and that the tension stress in the brick does not exceed the splitting tension strength of the Suprking bricks. Tensile strength of the bricks, Tubrick, is estimated based on test value values. The modulus of elasticity of the brick wall, Ebrickwall, is estimated based on test results for 10K grouted prisms specimens.

$Tubrick := 750 \cdot psi$ $Ebrickwall := 2800 \cdot ksi$

c) The height, h, and brick wall thickness, twallbrick, of the brick wall are then used to calculate the uncracked section moment of inertia, Iuncrack, and moment, Muncrack, when stress will reach the tensile strength of the brick wall. Section rotation at mid span of the specimen, funcrack, is then calculated. This calculation assumes that the point of maximum moment does not occur at a grouted cell in the wall. If the wall is grouted at the point of maximum moment, the thickness, twallbrick, should be modified by not subtracting the width of the cell, 2.625 in.

$twallbrick := (4.625 - 2.625) \cdot in$

$$Iuncrack := \frac{twallbrick \cdot h^3}{12}$$

$$Muncrack := \frac{Tubrick \cdot Iuncrack \cdot 2}{h} \qquad Muncrack = 192 \cdot kip \cdot ft$$

$$\phi uncrack := \frac{Tubrick \cdot 2 \cdot in}{Ebrickwall \cdot h} \qquad \phi uncrack \cdot 10^6 = 5.58$$

d) Deflection of the wall, Δuncrack, is calculated using the lengths, L1 and L2, as the distance between the supports and assuming that the specimen is simply

supported with a concentrated load at the point of maximum moment. Deflections for other loading configurations may be determined by changing the formula for Duncrack as appropriate. Since Duncrack is small compared to other displacements, the use of the point load formula is generally acceptable.

$$\Delta uncrack := \frac{Muncrack \cdot L1 \cdot L2}{12 \cdot Ebrickwall \cdot Iuncrack} \qquad \Delta uncrack = 0.027 \cdot in$$

e) Elastic cracked section analysis, first linear portion of the flashing joint deformation curve, is then used to calculate behavior up to a joint load of 3.5 kip per a dowel. The stiffness ratio for the shear joint and mortar joint, n1, and the area ratio, p1, is calculated based on the number of shear bars on each side of the centerline and the area of the brick wall assuming the wall is filled with grout. In order to adjust for the use of stress for the brick and load for the shear lugs, the load in the shear lugs is taken as applied over a unit area.

$b = 4.625\,in \qquad d := h$

$$n1 := \frac{\frac{3.5 \cdot ksi}{.04 \cdot in}}{\left[\frac{4.5 \cdot ksi}{\left(\frac{.005\,in}{2}\right)}\right]} \qquad n1 = 0.049$$

$$p1 := \frac{Nestimate \cdot in^2}{b \cdot d} \qquad p1 = 0.009$$

f) The section behavior is then calculated from these geometry ratios.

$$k1 := \sqrt{p1^2 + 2 \cdot p1 \cdot n1} - p1 \cdot n1 \qquad k1 = 0.03$$

$$j1 := 1 - \frac{k1}{3} \qquad j1 = 0.99$$

g) Section moment, M1, maximum brick stress, fb1, total section rotation, $\phi 1$, and specimen deflection, $\Delta 1$, are calculated using the cracked section configuration. The designer must verify that the section reaches yield stress of 4600 psi after the shear in the flashing joint reaches 6.2 kip per shear dowel. This indicates that the section moment capacity in the linear range is controlled by brick joint stress. If the reverse is true, the calculations must be revised to be controlled by flashing joint stress. Due to the small value of the modular ratio n1, brick yielding usually controls cracked section behavior. The total section rotation, $\phi 1$, is calculated based on the total deformation determined for brick joints and should be used directly to determine total joint rotation. These calculations assume that the shear joint with flashing deforms uniformly, rotations for the wall are concentrated at the point of maximum moment, and that deflections, $\Delta 1$, are calculated by summing uncracked deflections plus deflections due to wall rotations concentrated at the point of maximum moment.

$T1 := Nestimate \cdot 3.5 \cdot kip$

$M1a := T1 \cdot j1 \cdot d \qquad M1a = 110.861 \cdot kip \cdot ft$

$$fbj1 := \frac{M1a}{\frac{b \cdot d^2 \cdot k1 \cdot j1}{2}} \qquad fbj1 = 2.068 \cdot ksi \qquad \frac{fbj1}{4.6 \cdot ksi} = 0.45$$

$$\phi 1a = \frac{fbj1}{\left[\frac{4.5 \cdot ksi}{\left(\frac{.005 \cdot in}{2}\right)}\right]} \cdot \frac{1}{k1 \cdot d} \qquad \phi 1a = 0$$

$$\phi 1 = if(\phi 1a \leq \phi uncrack, \phi uncrack, \phi 1a)$$

$$M1 = if(M1a \leq Muncrack, Muncrack, M1a)$$

$$\Delta 1 = \Delta uncrack + \phi 1 \cdot \left(\frac{L1 + L2}{2}\right) \qquad \Delta 1 = 0.121 \cdot in$$

h) The calculation for linear cracked section behavior is then repeated for the second linear portion of the idealized shear joint load deformation curve. Since load deformation behavior is linear, the additional deformations and loads are superimposed on the results from the first linear portion to obtain total load deformation information.

$$n2 = \frac{\frac{(6.2 - 3.5) \cdot ksi}{(.155 - .04) \cdot in}}{\left[\frac{4.5 \cdot ksi}{\left(\frac{.005 \cdot in}{2}\right)}\right]} \qquad n2 = 0.013$$

$$p2 = \frac{Nestimate \cdot in^2}{b \cdot d} \qquad p2 = 0.009$$

$$k2 = \sqrt{p2^2 + 2 \cdot p2 \cdot n2} - p2 \cdot n2 \qquad k2 = 0.018$$

$$j2 = 1 - \frac{k2}{3} \qquad j2 = 0.994$$

$$\delta fbj2 = 4.6 \cdot ksi - fbj1 \qquad \delta fbj2 = 2.532 \cdot ksi$$

$$\delta M2 := \delta fbj2 \cdot \frac{b \cdot d^2 \cdot k2 \cdot j2}{2} \qquad \delta M2 = 78.971 \cdot kip \cdot ft$$

$$\delta T2 := \frac{\delta M2}{j2 \cdot d} \qquad \delta T2 = 9.93 \cdot kip$$

i) Section Moment, M2, maximum brick joint stress, fbj2, flashing joint shear, T2, section rotation, $\phi 2$, and specimen deflection, $\Delta 2$, are calculated as follows.

$$M2a := M1a + \delta M2 \qquad M2a = 189.833 \cdot kip \cdot ft$$

$$fbj2 := fbj1 + \delta fbj2 \qquad fbj2 = 4.6 \cdot ksi$$

$$T2 := T1 + \delta T2 \qquad T2 = 23.93 \cdot kip$$

$$\delta\phi 2 := \frac{\frac{\delta fbj2}{4.5 \cdot ksi}}{\frac{\left(\frac{.005 \cdot in}{2}\right)}{k2 \cdot d}} \qquad \delta\phi 2 = 0.001$$

$$\phi 2a := \phi 1a + \delta\phi 2 \qquad \phi 2a = 0.001$$

$$\phi 2 := if(\phi 2a \le \phi uncrack, \phi uncrack, \phi 2a)$$

$$M2 := if(M2a \le Muncrack, Muncrack, M2a)$$

$$\Delta 2 := \Delta uncrack + \phi 2 \cdot \left(\frac{L1 + L2}{2}\right) \qquad \Delta 2 = 0.32 \cdot in$$

j) Ultimate strength behavior is estimated using an idealized stress block for compression of the wall's top brick bond beam course.

$$Fult := 6.2 \cdot kip \qquad Tult := Nestimate \cdot Fult \qquad Tult = 24.8 \cdot kip$$

k) The size of the equivalent stress block, a, is determined by equilibrium for forces and the magnitude of the maximum stress, Fcbult, in the equivalent stress block.

Using the value of β1 and β3 found for the equivalent stress block, the location of the neutral axis, c, is determined and the ultimate moment is estimated.

$\beta 1 := .85$ $\beta 3 := .8$ $Fcbult := \beta 1 \cdot 4.57 \cdot ksi$

$Fcbult = 3.885 \cdot ksi$ $a := \frac{Tult}{b \cdot Fcbult}$ $a = 1.38 \cdot in$

$c := \frac{a}{\beta 3}$ $c = 1.725 \cdot in$

$Mnult := Tult \cdot \left(d - \frac{a}{2}\right)$ $Mnult = 196.974 \cdot kip \cdot ft$

l) Calculate section rotation at mid span based on maximum deformation of the brick joint, Δjbmax. Then check deformation of shear joint, Δjsmax, to verify that the shear dowels will resist load at maximum deformation. Calculate deflection due to center rotation, Δult, based on ultimate loads. Then calculate maximum deflection, Δmax, based on summation of uncracked wall deflections and rotations at section of maximum moment due to ultimate strength bending.

$\Delta jbmax := .0093 in$ $\phi ult := \frac{\Delta jbmax}{c}$ $\phi ult = 0.005$

$\Delta jsult := \Delta jbmax \cdot \frac{d - c}{c}$ $\Delta jsult = 0.508 \cdot in$

$\Delta ult := \phi ult \cdot \frac{L1 + L2}{2}$ $\Delta ult = 1.294 \cdot in$

$\Delta max := \Delta uncrack + \Delta ult$ $\Delta max = 1.32 \cdot in$

m) Calculate maximum deflection at mid span, Δjsmax, assuming that shear joint deformation controls maximum deflection, not compression strain in the joint.

These deformations were observed in wall tests. They are probably due to the high degree of confinement provided to the joint mortar by the brick. In addition, joint mortar spalling due to compressive strains may also have been prevented during tests by the bearing plate and load at the point of maximum moment.

$$\Delta sjult := \frac{.32 \cdot in}{d - c} \cdot \frac{L1 + L2}{2} \qquad \Delta sjult = 0.815 \cdot in$$

$$\Delta sjmax := \Delta uncrack + \Delta sjult \qquad \Delta sjmax = 0.841 \cdot in$$

$$\phi sjult := \frac{.32 \cdot in}{d - c} \qquad \phi sjult = 0.003$$

n) Compare predicted ultimate moment, Mnult, with the required nominal moment strength, Mnm, to determine if number of dowels, Nestimate, is acceptable. The program should be iterated with different values of Nestimate until an acceptable design is determined.

$$Mnm = 194.5 \cdot kip \cdot ft \qquad Mnult = 196.974 \cdot kip \cdot ft \qquad \frac{Mnm}{Mnult} = 0.987$$

o) The moment rotation and moment displacement curves are generated by creating vectors summarizing results and plotting them as follows.

$$M = \begin{bmatrix} 0 \\ Muncrack \\ Muncrack \\ M1 \\ M2 \\ Mnult \\ Mnult \\ Mnult \end{bmatrix}$$

$$\phi = \begin{bmatrix} 0 \\ \phi uncrack \\ \phi 1 \cdot \frac{Muncrack}{M1} \\ \phi 1 \\ \phi 2 \\ \phi 2 + (Mnult - M2) \cdot \frac{\phi 2}{M2} \\ \phi ult \\ \phi sjult \end{bmatrix} \qquad \Delta := \begin{bmatrix} 0 \\ \Delta uncrack \\ \Delta uncrack + \phi_2 \cdot \left(\frac{L1 + L2}{2} \right) \\ \Delta 1 \\ \Delta 2 \\ \Delta uncrack + \phi_5 \cdot \left(\frac{L1 + L2}{2} \right) \\ \Delta max \\ \Delta sjmax \end{bmatrix}$$

As shown in the moment curvature diagram in figure 7.3, the design with four #4 reinforcing bar dowels on each side of the centerline of the wall is acceptable assuming that the basic requirement is that the estimated moment, Mnm, is less than the nominal strength, Mnult, and that crack size is less than 0.2 inches. Since the modular dimension of a Suprking brick is 10 inches, the vertical #4 reinforcing bars should be provided at 45 inches on center with bars in the corner cells. This amount of reinforcing is close to the minimum which would be provided in a reinforced brick wall. The cost of protecting this wall from subsidence effects is the cost of (a) grouting cells adjacent to vertical reinforcing for the first two courses next to the flashing joint and (b) using brick bond beam units in the first course next to the vertical reinforcing bars.

This marginal a design would generally not be acceptable for loads described in ACI 530 (Building, 1992). If the criteria suggested in chapter 5 were used, the moment

capacity would be increased by a factor of four resulting in vertical reinforcing at closer spacing than 20 inch minimum based on test results. It is considered acceptable for this example because (a) subsidence is considered an abnormal and unlikely event, (b) the possibility of the permanent condition after a subsidence event being concave curvature is small, and (c) the moments resisted by the wall would reduce as it deforms and the equivalent design span is reduced. Before deciding to install the additional bond beam bricks and grout required to assure appropriate shear capacity of the flashing joint, the designer should also consider that one #6 or 2 #4 reinforcing bars would be required at the top of the wall for the convex curvature condition associated with subsidence. In a location where subsidence is a possible event, the designer may also consider using bond beam bricks and placing a #6 steel reinforcing bar in the bottom course of the wall to improve wall performance.

7.4 Wall Subjected To Soil Expansion

Soil expansion occurs as a result of absorption of moisture in clays. The clay mineral "montmorillonite" is associated with most expansive soil problems as discussed by Chen (1975). The amount of expansion depends on the kind and amount of clay minerals present and their internal structure and characteristics. Significant variables associated with mitigation of damage due to soil expansion are control of moisture content and pressure applied to soils.

Chen (1975) also shows how expansion is caused by changes in moisture content and can be reduced by applying increased foundation pressures. Solutions to the expansive soil problem which he discusses as examples of control of changes in moisture content include use of piers extending below to a depth where moisture changes are small, removal of expansive soils to a depth where moisture is constant and back filling with non-expansive soils, and grouting soil to prevent the movement of moisture. Solutions to the expansive soil problem which he discusses, as examples of applying increased foundation pressures to control expansion, include stiff concrete slabs, box structures, and foundations with intermittent soil bearing to concentrate loads.

7.4.1 Example Of Solution To Distress Caused By Heaving Of Continuous Footings

A case study Chen (1975) discusses provides an excellent example of how a reinforced brick wall and a flashing joint with dowels could have avoided substantial expense. In this case, a soil heaving problem is solved by removing at least 4 inches of soil under a 10 foot long strip out of every 15 feet of foundation. Using the data from the example in section 7.3, the input data for the wall dowel design program is conservatively estimated as follows.

$$DL = 852 \frac{lbf}{ft} \qquad LL := 120 \frac{lbf}{ft} \qquad L := 10 ft$$

The shear joint program is then used to assess the behavior of this section. Only key answers from the program are shown in this example since the moments applied are

significantly less than the allowable moment and previous sections have shown how the program calculates behavior.

Shear Joint With Flashing And #4 Dowel Design Program.

1) Enter an estimate of the number of #4 reinforcing steel dowels between the point of maximum negative moment and the end support, Nestimate.

Nestimate := 2

2) Enter the nominal moment strength, Mnm, to be resisted by the brick wall. Enter the height of the brick wall, h, from the joint with flashing to the top brick course constructed with the wall. Enter the distances, L1 and L2, from the point of maximum moment to either adjacent supports or points of inflection.

$$Mnm := \frac{(DL + LL)\cdot L^2}{8} \qquad h := 8\cdot ft \qquad L1 := \frac{L}{2} \qquad L2 := \frac{L}{2}$$

3) Critical results calculated by the program were as follows.

$$Muncrack = 192\cdot kip\cdot ft \qquad \phi uncrack\cdot 10^6 = 5.58 \qquad \Delta uncrack = 0.002\cdot in$$

$$Mnm = 12.15\cdot kip\cdot ft \qquad Mnult = 98.843\cdot kip\cdot ft \qquad \frac{Mnm}{Mnult} = 0.123$$

This wall is acceptable with two dowels on each side of the center line of the 10 foot span since the nominal strength moment, Mnult, is approximately eight times the applied moment. Another interesting aspect of this design is that the nominal cracking moment is almost twice the nominal strength and 16 times the applied moment indicating that the wall would probably not have cracked if contact between the grade beam and the soil had been discontinuous when the structure was built.

7.5 Wall Subjected To Washout Between Pilings Or Piers

A common construction in coastal areas subject to hurricanes is to place structures on top of piles in order to protect against washout of foundations and to raise the bottom elevation of the building above the storm surge level. This type of construction has been successful as described by Greenwood (1996).

A common way to meet these type of construction requirements is to build a mound of sand to the elevation desired, drive piling through the sand, and construct the building using the sand for building support during construction. This results in a building which is resistant to hurricane damage and architecturally pleasing because it is connected to the ground. Reinforced concrete unit masonry construction, which does not require a flashing joint at the bottom of the wall, is well suited for creating composite behavior by using the wall and the pile cap tie beam together. This example shows that this construction scheme could also be implemented with minimal cost using reinforced Suprking bricks and a flashing joint with dowels.

7.5.1 Data For Use In Wall Analysis Program

The assumptions involved in this example are similar to the assumptions made in section 6.3.1 except that the dead load, DL, is increased to 75 lb. per square foot due to the use of concrete floors in this type of building and the span, L, should be reduced to 20 feet to be representative of typical pile spacing used in this type of structure. These assumptions are then used in the following calculations.

$$DL := (8 \cdot ft \cdot 4.625\,in + 2 \cdot ft \cdot 6 \cdot in) \cdot 150 \cdot \frac{lbf}{ft^3} + (75 + 10) \cdot \frac{lbf}{ft^2} \cdot 12 \cdot ft \qquad DL = 1632.5 \cdot \frac{lbf}{ft}$$

$$LL := 120 \cdot \frac{lbf}{ft} \qquad L := 20 \cdot ft$$

$$MDLLL := \frac{(DL + LL) \cdot L^2}{8} \qquad MDLLL = 87.625 \cdot kip \cdot ft$$

The joint program will now perform the calculations to determine the appropriate number of dowels.

Shear Joint With Flashing And #4 Dowel Design Program.

The number of #4 reinforcing steel dowels required to cross the flashing joint between the point of maximum moment and the support of the wall is determined by this calculation. In addition, the moment curvature diagram for the wall and wall deflections are estimated for the number of dowels selected.

The designer must assure that the number of dowels between any point on the wall and the wall support is adequate to develop the flashing joint shear required by moments at the selected point on the wall. In addition, reinforcing around openings must be adequate to develop the shear forces in the flashing joint. The ultimate strength of #4 grade 60 reinforcing steel dowels to be developed by the wall opening design is 6,200 lb.

The design steps to determine the number of #4 reinforcing steel dowels required are as follows.

1) Enter an estimate of the number of #4 reinforcing steel dowels between the point of maximum negative moment and the end support, Nestimate.

Nestimate := 6

2) Enter the nominal moment strength, Mnm, to be resisted by the brick wall. This is determined by adjusting the design moment, MDLLL, by the appropriate factor considering the provisions of the methodology described in section 6.4.1 and the one-third stress increase permitted by ACI 530 (Building, 1992) for wind load associated load combinations. This load condition is considered associated with wind load because the wash out of the supporting soil is a result of storm action.

$$Mnm := MDLLL \cdot \frac{4}{1.33}$$

3) Enter the height of the brick wall, h, from the joint with flashing to the top brick course constructed with the wall. The top course consists of grouted bond beam bricks.

$h := 8 \cdot ft$

4) Enter the distances, L1 and L2, from the point of maximum moment to either adjacent supports or points of inflection. These distances will be used to determine differential deflections assuming all section rotation after wall tensile cracking is concentrated at the point of maximum moment

$$L1 := \frac{L}{2} \qquad L2 := \frac{L}{2}$$

5) The program will now perform the following calculations and provide results as shown.

a) Assign dimensional units to supplement Mathcad provided unit data

$kip := 1000\,lbf \qquad psi := \frac{lbf}{in^2} \qquad ksi := 1000\,psi$

b)Perform uncracked section analysis. The uncracked section analysis is based on classic beam theory assuming plane sections remain plane and that the tension stress in the brick does not exceed the splitting tension strength of the Suprking bricks. Tensile strength of the bricks, Tubrick, is estimated based on test value values. The modulus of elasticity of the brick wall, Ebrickwall, is estimated based on test results for 10K grouted prisms specimens.

$Tubrick := 750\,psi \qquad Ebrickwall := 2800\,ksi$

c) The height, h, and brick wall thickness, twallbrick, of the brick wall are then used to calculate the uncracked section moment of inertia, Iuncrack, and moment, Muncrack, when stress will reach the tensile strength of the brick wall. Section rotation at mid span of the specimen, ϕuncrack, is then calculated. This calculation assumes that the point of maximum moment does not occur at a grouted cell in the wall. If the wall is grouted at the point of maximum moment, the thickness, twallbrick, should be modified by not subtracting the width of the cell, 2.625 in.

$twallbrick := (4.625 - 2.625)\cdot in \qquad Iuncrack := \frac{twallbrick\cdot h^3}{12}$

$Muncrack := \frac{Tubrick\cdot Iuncrack\cdot 2}{h} \qquad Muncrack = 192\cdot kip\cdot ft$

$\phi uncrack := \frac{Tubrick\cdot 2\cdot in}{Ebrickwall\cdot h} \qquad \phi uncrack\cdot 10^6 = 5.58$

d) Deflection of the wall, Δuncrack, is calculated using the lengths, L1 and L2, as the distance between the supports and assuming that the specimen is simply supported with a concentrated load at the point of maximum moment. Deflections for other loading configurations may be determined by changing the formula for Δuncrack as appropriate. Since Δuncrack is small compared to other displacements, the use of the point load formula is generally acceptable.

$$\Delta uncrack := \frac{Muncrack \cdot L1 \cdot L2}{12 \cdot Ebrickwall \cdot Iuncrack} \qquad \Delta uncrack = 0.007 \cdot in$$

e) Elastic cracked section analysis, first linear portion of the flashing joint deformation curve, is then used to calculate behavior up to a joint load of 3.5 kip per a dowel. The stiffness ratio for the shear joint and mortar joint, n1, and the area ratio, p1, is calculated based on the number of shear bars on each side of the centerline and the area of the brick wall assuming the wall is filled with grout. In order to adjust for the use of stress for the brick and load for the shear lugs, the load in the shear lugs is taken as applied over a unit area.

$b := 4.625\,in \qquad d := h$

$$n1 := \frac{\frac{3.5 \cdot ksi}{.04 \cdot in}}{\left[\frac{4.5 \cdot ksi}{\left(\frac{.005\,in}{2}\right)}\right]} \qquad n1 = 0.049$$

$$p1 := \frac{Nestimate \cdot in^2}{b \cdot d} \qquad p1 = 0.014$$

f) The section behavior is then calculated from these geometry ratios.

$$k1 := \sqrt{p1^2 + 2 \cdot p1 \cdot n1} - p1 \cdot n1 \qquad k1 = 0.038$$

$$j1 := 1 - \frac{k1}{3} \qquad j1 = 0.987$$

g) Section moment, M1, maximum brick stress, fb1, total section rotation, $\phi 1$, and specimen deflection, $\Delta 1$, are calculated using the cracked section configuration. The designer must verify that the section reaches yield stress of 4600 psi after the shear in the flashing joint reaches 6.2 kip per shear dowel. This indicates that the section moment capacity in the linear range is controlled by brick joint stress. If the reverse is true, the calculations must be revised to be controlled by flashing joint stress. Due to the small value of the modular ratio n1, brick yielding usually controls cracked section behavior. The total section rotation, $\phi 1$, is calculated based on the total deformation determined for brick joints and should be used directly to determine total joint rotation. These calculations assume that the shear joint with flashing deforms uniformly, rotations for the wall are concentrated at the point of maximum moment, and that deflections, $\Delta 1$, are calculated by summing uncracked deflections plus deflections due to wall rotations concentrated at the point of maximum moment.

$$T1 := Nestimate \cdot 3.5 \cdot kip \qquad M1a := T1 \cdot j1 \cdot d \qquad M1a = 165.87 \cdot kip \cdot ft$$

$$fbj1 := \frac{M1a}{\frac{b \cdot d^2 \cdot k1 \cdot j1}{2}} \qquad fbj1 = 2.488 \cdot ksi \qquad \frac{fbj1}{4.6 \cdot ksi} = 0.541$$

$$\phi 1a := \frac{fbj1}{\left[\frac{4.5 \cdot ksi}{\left(\frac{.005 \cdot in}{2}\right)}\right]} \cdot \frac{1}{k1 \cdot d} \qquad \phi 1a = 0$$

$$\phi 1 := if(\phi 1a \le \phi uncrack, \phi uncrack, \phi 1a)$$

$$M1 := if(M1a \le Muncrack, Muncrack, M1a)$$

$$\Delta 1 := \Delta uncrack + \phi 1 \cdot \left(\frac{L1 + L2}{2}\right) \qquad \Delta 1 = 0.052 \cdot in$$

h) The calculation for linear cracked section behavior is then repeated for the second linear portion of the idealized shear joint load deformation curve. Since load deformation behavior is linear, the additional deformations and loads are superimposed on the results from the first linear portion to obtain total load deformation information.

$$n2 := \frac{\frac{(6.2 - 3.5) \cdot ksi}{(.155 - .04) \cdot in}}{\left[\frac{4.5 \cdot ksi}{\left(\frac{.005 \cdot in}{2}\right)}\right]} \qquad n2 = 0.013$$

$$p2 := \frac{Nestimate \cdot in^2}{b \cdot d} \qquad p2 = 0.014$$

$$k2 := \sqrt{p2^2 + 2 \cdot p2 \cdot n2} - p2 \cdot n2 \qquad k2 = 0.023$$

$$j2 := 1 - \frac{k2}{3} \qquad j2 = 0.992$$

$$\delta fbj2 := 4.6 \cdot ksi - fbj1 \qquad \delta fbj2 = 2.112 \cdot ksi$$

$$\delta M2 := \delta fbj2 \cdot \frac{b \cdot d^2 \cdot k2 \cdot j2}{2} \qquad \delta M2 = 85.467 \cdot kip \cdot ft$$

$$\delta T2 := \frac{\delta M2}{j2 \cdot d} \qquad \delta T2 = 10.766 \cdot kip$$

i) Section Moment, M2, maximum brick joint stress, fbj2, flashing joint shear, T2, section rotation, $\phi 2$, and specimen deflection, $\Delta 2$, are calculated as follows.

$$M2a := M1a + \delta M2 \qquad M2a = 251.338 \cdot kip \cdot ft$$

$$fbj2 := fbj1 + \delta fbj2 \qquad fbj2 = 4.6 \cdot ksi$$

$$T2 := T1 + \delta T2 \qquad T2 = 31.766 \cdot kip$$

$$\delta\phi 2 := \frac{\frac{\delta fbj2}{4.5 \cdot ksi}}{\frac{\left(\frac{.005 \cdot in}{2}\right)}{k2 \cdot d}} \qquad \delta\phi 2 = 0.001$$

$$\phi 2a := \phi 1a + \delta\phi 2 \qquad \phi 2a = 0.001$$

$$\phi 2 := if(\phi 2a \le \phi uncrack, \phi uncrack, \phi 2a)$$

$$M2 := if(M2a \le Muncrack, Muncrack, M2a)$$

$$\Delta 2 := \Delta uncrack + \phi 2 \cdot \left(\frac{L1 + L2}{2}\right) \qquad \Delta 2 = 0.116 \cdot in$$

j) Ultimate strength behavior is estimated using an idealized stress block for compression of the wall's top brick bond beam course.

$$Fult := 6.2 \cdot kip \qquad Tult := Nestimate \cdot Fult \qquad Tult = 37.2 \cdot kip$$

k) The size of the equivalent stress block, a, is determined by equilibrium for forces and the magnitude of the maximum stress, Fcbult, in the equivalent stress block.

Using the value of β1 and β3 found for the equivalent stress block, the location of the neutral axis, c, is determined and the ultimate moment is estimated.

$\beta 1 := .85$ $\beta 3 := .8$

$Fcbult := \beta 1 \cdot 4.57 \cdot ksi$ $Fcbult = 3.885 \cdot ksi$

$a := \frac{Tult}{b \cdot Fcbult}$ $a = 2.071 \cdot in$

$c = \frac{a}{\beta 3}$ $c = 2.588 \cdot in$

$Mnult := Tult \cdot \left(d - \frac{a}{2} \right)$ $Mnult = 294.391 \cdot kip \cdot ft$

l) Calculate section rotation at mid span based on maximum deformation of the brick joint, Δjbmax. Then check deformation of shear joint, Δjsmax, to verify that the shear dowels will resist load at maximum deformation. Calculate deflection due to center rotation, Δult, based on ultimate loads. Then calculate maximum deflection, Δmax, based on summation of uncracked wall deflections and rotations at section of maximum moment due to ultimate strength bending.

$\Delta jbmax := .0093 in$ $\phi ult := \frac{\Delta jbmax}{c}$ $\phi ult = 0.004$

$\Delta jsult := \Delta jbmax \cdot \frac{d - c}{c}$ $\Delta jsult = 0.336 \cdot in$

$\Delta ult := \phi ult \cdot \frac{L1 + L2}{2}$ $\Delta ult = 0.431 \cdot in$

$\Delta max := \Delta uncrack + \Delta ult$ $\Delta max = 0.438 \cdot in$

m) Calculate maximum deflection at mid span, Δjsmax, assuming that shear joint deformation controls maximum deflection, not compression strain in the joint. These deformations were observed in wall tests. They are probably due to the high degree of confinement provided to the joint mortar by the brick. In addition, joint mortar spalling due to compressive strains may also have been prevented during tests by the bearing plate and load at the point of maximum moment.

$$\Delta sjult := \frac{.32 \cdot in}{d - c} \cdot \frac{L1 + L2}{2} \qquad \Delta sjult = 0.411 \cdot in$$

$$\Delta sjmax := \Delta uncrack + \Delta sjult \qquad \Delta sjmax = 0.418 \cdot in$$

$$\phi sjult := \frac{.32 \cdot in}{d - c} \qquad \phi sjult = 0.003$$

n) Compare predicted ultimate moment, Mnult, with the required nominal moment strength, Mnm, to determine if number of dowels, Nestimate, is acceptable. The program should be iterated with different values of Nestimate until an acceptable design is determined.

$$Mnm = 263.534 \cdot kip \cdot ft \qquad Mnult = 294.391 \cdot kip \cdot ft \qquad \frac{Mnm}{Mnult} = 0.895$$

Based on this calculation, the use of six reinforcing bar dowels on each side of the centerline of the wall is required to resist the moments which will result from washout of material between the piles. This number of dowels would require a spacing of 20 inches in a 10 foot span length which is the lower spacing limit required by section 6.3.1 b) of the methodology. The provisions of section 6.5.3

need to be used to assure that the shear capacity of the flashing joint with dowels is acceptable at all sections. The calculation to perform this check for the moment just beyond the dowel at 40 inches from the centerline was done with the wall design program as follows. For this calculation, the explanations and most of the step by step calculations included in the program have been omitted.

$$MLLDD40 := \frac{(DL + LL)\cdot\left(\frac{L}{2} + 40\cdot in\right)\cdot\left(\frac{L}{2} - 40\cdot in\right)}{2} \qquad Nestimate := 4$$

$$Mnm := MLLDD40\cdot\frac{4}{1.33} \qquad Mnm = 234.252\cdot kip\cdot ft$$

$$Mnult = 196.974\cdot kip\cdot ft \qquad \frac{Mnm}{Mnult} = 1.189$$

This calculation was also performed at 20, 60, and 80 inches from the span centerline. The results for the first four dowels were as follows.

Distance from Centerline	$\frac{Mnm}{Mnult}$
0	.895
20 inches	1.042
40 inches	1.189
60 inches	1.003
80 inches	.596

Based on these results, the shear dowels are not acceptable just outside of the second dowel, at 40 inches, and some other solution would be required since the dowels are already spaced at the minimum distance for optimal performance. In this case, the

design can be accepted because the estimate of moment neglected continuity in the wall which, provided reinforcing is provided at the top of the wall, could be considered. Alternatively, the data summarized in figure 4.1 could be used to justify dowel spacing at 15 inches for the area of high shear transfer. Assuming a propped cantilever, the shear dowels spacing of 20 inches would be acceptable based on the following calculation.

$$Mnmcorrected := 234 \cdot \frac{\frac{9}{128}}{\left(\frac{1}{8}\right)} \cdot kip \cdot ft \qquad Mnmcorrected = 131.625 \cdot kip \cdot ft$$

$$Mnult := 197 \cdot kip \cdot ft \qquad \frac{Mnmcorrected}{Mnult} = 0.668$$

This example demonstrates another use of the design methods developed in this thesis as well as the care which must be exercised to assure that the performance of the joint with flashing is capable of resisting the applied loads at all points along the joint.

Chapter 8

Recommendations For Additional Research

8.1 General

This research has demonstrated the viability of using #4 steel reinforcing bars to transfer shear across hollow brick flashing joints. As summarized in section 1.2, several preferred construction details were identified to maximize shear transfer and ductility of the flashing joint. In addition, data to evaluate flashing shear joint behavior if preferred construction details are not implemented is provided. Numerical models were developed based on test results and were used to establish a design methodology for flashing shear joints. The methodology was then used with several examples to demonstrate its use.

As concluded in section 1.3, the availability of this methodology enables the designer to use the inherent strength of a system consisting of a hollow brick wall and a foundation separated by a flashing joint to resist moments resulting from in-plane forces. Additional research to facilitate the wider use of this methodology and reduce factors of safety associated with the use of flashing joint shear dowels is recommended based on the scope and results of this research. In addition to the

general need to perform system qualification testing using substantially more samples, the following are identified as areas where additional research could provide a better understanding of flashing joint and brick wall behavior.

8.2 Recommendations For Parametric Studies

Several parametric studies were identified during the research which would assist in verifying and quantifying the parameters used for analysis of flashing joint dowels. These studies would include assessing the variability of the following:

a) A mortar joint deformation limit of 0.0093 inch was developed and used to assess the ultimate strength behavior of brick joints. Prism tests using the 3/8 inch nominal joint as well as other joints could be used to more precisely define the value of the limit and the effect of joint thickness on the limit. These tests could also be used to obtain additional data supporting assumptions related to the equivalent stress block used in strength calculations.

b) Wall specimen reinforcing steel dowel spacing of ten and twenty inches were used for this research. Evaluations indicate that the behavior of walls with fifteen inch dowel spacing would be the same as for walls with 20 inch dowel spacing. Additional wall bending tests could be used verify this conclusion or identify additional factors affecting dowel behavior as a function of dowel spacing.

c) PVC flashing was used for this research. Tests using copper flashing could be used to verify the effect of copper flashing on joint behavior.

d) Based on this testing, which used #4 and #6 reinforcing bars, #4 reinforcing bars are acceptable and #6 bars are not. Testing using #5 reinforcing bars could be used to determine if they are acceptable.

e) The reinforcing bar embedment used in this testing was adequate to develop bar strength but was slightly less than ACI 530 (Building, 1992) requirements. Additional testing using greater bar embedment could be used to determine if additional embedment, perhaps even more than required by the ACI 530 (Building, 1992), is beneficial to flashing joint shear capacity.

8.3 Recommendations Related To Masonry Behavior

Several areas where additional research related to overall masonry behavior would be beneficial were also identified as part of the research. These additional areas are related to the use of concrete masonry units (cmu) in lieu of hollow brick, energy dissipation associated with oscillating loads, and confinement of mortar joints in hollow brick walls as compared to cmu walls. These studies could include the following:

a) Concrete unit masonry is generally substantially weaker than hollow brick due to the difference in basic materials and manufacturing methods. As a result, the pull-out failure mode for the reinforcing bar dowels may be substantially different than observed for hollow brick. The specific concern is that the face shells of the cmu will be unable to resist the tension loads associated with the pull-out failure cone. Tests performed as part of this research demonstrate that the Suprking hollow brick can resist these forces for #4 bars. Pull-out

tests using cmu should be performed prior to their use in resisting flashing joint shear forces. Alternatively, thicker cmu units, such as 16 inch wall thickness units, could be used based on existing tests for cmu as reflected in ACI 530 (Building, 1992) requirements.

b) The tests performed as part of this research used monotonically increasing loads up to and beyond the ultimate strength of the specimens. Unloading and loading of specimens after failure indicated that a flashing joint with reinforcing steel dowels may display substantial energy dissipation associated with hysteretic behavior. Additional tests could verify and quantify this behavior and support the use of flashing joints to dissipate the effects of oscillating loads such as those due to earthquakes.

c) Concrete unit masonry wall bending tests reported by Mayes and Clough (1975) indicate brittle failure of cmu in compression and recommend the use of metal plates to increase ductility. This research indicates that Suprking hollow bricks provide sufficient confinement of joint mortar in compression to assure ductility and eliminate the need for joint confining plates. Wall in-plane bending tests could be used to verify this observation and identify possible additional benefits inherent in using hollow brick in lieu of cmu for walls subject of large in-plane moments. Wall out-of-plane bending tests could also be used to verify this observation. In addition, they could demonstrate the viability of using hollow brick walls where large ductility in response to out-of-plane loads, such as loads resulting from missile or blast effects, is desired.

REFERENCES

References

Building Code Requirements For Masonry Structures (1992). ACI 530-92/ASCE 5-92/TMS 402-92, The Masonry Society, Boulder, Colorado.

Building Code Requirements For Reinforced Concrete (1989). ACI 318-89, The American Concrete Institute, Detroit, Michigan.

Chen, Ju Hua (1975). Foundations On Expansive Soils, Elsevier Scientific Publishing Company, New York, NY.

"Concrete Manual, A Manual For The Control Of Concrete Construction, 7th Edition." (1963). United States Department Of The Interior Bureau Of Reclamation, Denver, Colo.

Columber, Christopher Eugene (1994). "Structural Clay Tile Component Behavior," M. S. thesis, University of Tennessee, Knoxville, TN.

Greenwood, David J., and Hatheway, Darryl J. (1996). "Assessing Opal's Impact," Civil Engineering, ASCE 66 (1), 40-43.

Kratzsch, Helmut (1983). Mining Subsidence Engineering, Translated by R.F.S. Fleming, Springer-Verlag, Berlin Heidelberg, Germany.

"Manual of Steel Construction, Load & Resistance Factor Design, 1st Ed." (1986). AISC, Chicago, IL.

Mathcad PLUS 6.0. (1995). Users Guide, Mathsoft Inc., Cambridge, Massachusetts.

Mayes, Ronald L. and Ray W. Clough (1975). A Literature Survey - Compressive, Tensile, Bond and Shear Strength of Masonry. Report No. EERC 75-15, Earthquake Engineering Research Center, College of Engineering, University of California. Berkeley, California.

McGinley, W. M., and J. G. Borchelt (1989). "Friction Between Brick And Its Support," Proceedings 5th Canadian Masonry Symposium, Department of Civil Engineering, University of British Columbia, Vancouver, B. C., Canada, 713-722.

Park, R. and T. Paulay (1975). Reinforced Concrete Structures, John Wiley & Sons, Inc., New York, NY.

Paulay, T., and M. J. N. Priestley (1992). Seismic Design of Reinforced Concrete and Masonry Buildings, John Wiley & Sons, Inc., New York, NY.

Priestley, M. J. N. and D. M. Elder (1983). "Stress-Strain Curves for Unconfined and Confined Concrete Masonry." Journal of the American Concrete Institute, No. 3, Vol.80, ACI, Detroit, MI.

Salmon, Charles G., and John E. Johnson (1990). Steel Structures: Design and Behavior, Emphasizing Load and Resistance Factor Design, 3rd Edition, Harper Collins Publishers Inc., New York, NY.

Schneider, Robert R., and Walter L. Dickey (1994). Reinforced Masonry Design, 3rd Edition, Prentice-Hall, Inc., Englewood Cliffs, New Jersey.

"Sonogrout 10K (Formerly Sonogrout G. P.) High - Strength Nonshrink Nonmetalic Grout." (1992). Sonneborn Building Products, ChemRex Inc., Minneapolis, MN.

"Specifications for Masonry Structures." (1992). ACI 530.1-92/ASCE 6-92/TMS 602-92, The Masonry Society, Boulder, Colorado.

"Standard Specification for Deformed And Plain Billet-Steel Bars for Concrete Reinforcement." (1994). A 615 - 94, ASTM, Philadelphia, Pa.

"Standard Test Method For Compressive Strength of Cylindrical concrete Specimens." (1994). C 39 - 94, ASTM, Philadelphia, Pa.

"Standard Test Methods of Sampling and Testing Brick and Structural Clay Tile." (1991). C 67 - 91, ASTM, Philadelphia, Pa.

"Standard Test Method for Compressive Strength of Hydraulic Cement Mortars (Using 2 - in. or 50 - mm Cube Specimens)." (1990). C 109 - 90, ASTM, Philadelphia, Pa.

"Standard Specification for Facing Brick (Solid Masonry Units Made from Clay or Shale)." (1991). C 218 - 91c, ASTM, Philadelphia, Pa.

"Standard Specification for Mortar for Unit Masonry." (1991). C 270 - 91a, ASTM, Philadelphia, Pa.

"Standard Test Method for Splitting Tensile Strength of Cylindrical Concrete Specimens." (1990). C - 496 - 90, ASTM, Philadelphia, Pa.

"Standard Specification for Hollow Brick (Hollow Masonry Units Made From Clay of Shale)." (1991). C 652 - 91c, ASTM, Philadelphia, Pa.

"Standard Test Method for Splitting Tensile Strength of Masonry Units." (1984). C 1006 - 84, ASTM, Philadelphia, Pa.

"Standard Method of Sampling and Testing Grout." (1989). C 1019 - 89a, ASTM, Philadelphia, Pa.

"Standard Test Methods for Compressive Strength of Masonry Prisms." (1991). E 447 - 84 (Reapproved 1991), ASTM, Philadelphia, Pa.

Subasic, Christine A. and J. Greg Borchelt (1993). "Clay and Shale Brick Material Properties A Statistical Report," Proceedings The 6th North American Masonry Conference, Vol. 1, Department of Civil and Architectural Engineering, Drexel, Philadelphia, PA, 283-294.

Tawresey, John G. (1993). "Strength Design Stress Factors Determined From The Masonry Stress-Strain Relationship," Proceedings The 6th North American Masonry Conference, Vol. 1, Department of Civil and Architectural Engineering, Drexel, Philadelphia, PA, 261-270.

Winter, George and L. C. Urquhart, C. E. O'Rourke, Arthur H. Nilson (1964). Design Of Concrete Structures, 7th Edition. McGraw-Hill Book Company, New York, NY.

APPENDIX

TABLES AND FIGURES

Table 2.1

Coefficient Of Friction Of Joint At Bottom Of Brick Wall

Normal Load On Joint Due To Weight Of Wall

Flashing Type	Load Direction	Estimated Normal Stress	Average Static Coefficient of Friction	Average Kinetic Coefficient of Friction
PVC	In-Plane	8.3 psi	.521	.471
PVC	Out of Plane	8.3 psi	.695	.650
Copper	In-Plane	8.3 psi	.430	.397
Copper	Out of Plane	8.3 psi	.454	.428
None (Bond broken before friction testing)	Out of Plane	8.3 psi	.861	.830

Notes on Coefficient Of Friction Testing Results

1. Data presented in this table summarize tests and results reported in McGinley and Borchelt (1989).
2. The tests were conducted using small solid brick wall specimens on concrete beams with gravity and small applied loads. No reinforcing or other connection between the wall and the supporting concrete beam was provided

Table 3.1

System Noise Measurements

(1) Test Description	10K Grout Prism Test #2	10K Grout Prism Test #3	10K Full Grout Shear Test #3	Wall Test, 4 Reinforcing Bars Test #2	Wall Test, 4 Reinforcing Bars Test #2
(2) Data Type	LVDT on specimen (inches)	Load Cell in Machine (kips)	LVDT in specimen (inches)	LVDT cen-ter vertical (inches)	Load Cell on ram (kips)
(3) Max. Data, No Load	.392	12.2	.366	1.348	.125
(4) Min. Data No Load	.392	9.4	.366	1.347	.116
(5) Max. Data With Load	.374	109.1	-.17	-.759	9.26
(6) Error in %	.01 %	2.9 %	.04 %	.05 %	.1 %

Table 4.1

Summary Of Shear Specimen Results

Type of Specimen	Reference Section	Mean Ultimate Specimen Load	Coefficient Of Friction
#4 Reinforcing Bar, 10K Grout In Reinforced Cells Only	4.4	9.9 kip	.356
#4 Reinforcing Bar, Mortar Grout In Reinforced Cells Only	4.5	8.2 kip	.293
#4 Reinforcing Bar, 10K Grout In All Cells	4.6	15.2 kip	.544
#6 Reinforcing Bar, 10K Grout In Reinforced Cells Only	4.7	12.9 kip	.183
#6 Reinforcing Bar, 10K Grout In All Cells	4.7	20.9 kip	.297

kip = 1000 pounds force

Table 5.1

Description Of LVDT Measurements On Wall Specimen

Channel	Location Description	Purpose of Measurement
0	Floor to Concrete Beam at center of specimen	Determine vertical deflections at center of specimen
1	Concrete Beam to Concrete Beam	Determine axial deformation of beam at center of specimen
2	End of Concrete Beam to End of Brick Wall	Determine joint movement
3	Floor to Concrete Beam	Determine vertical deflections
4	Concrete Beam to Brick Wall	Determine joint deformation
5	Top of Brick Wall to Top of Brick Wall	Determine horizontal wall deformation
6	Floor to Concrete Beam	Determine vertical deflections
7	End of Concrete Beam to End of Brick Wall	Determine joint movement at end of wall

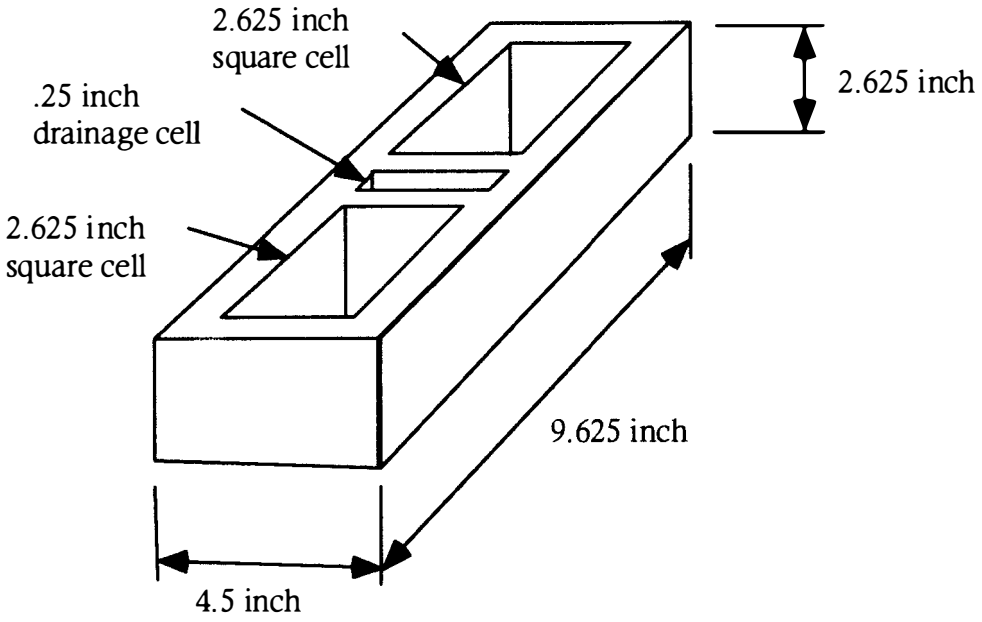
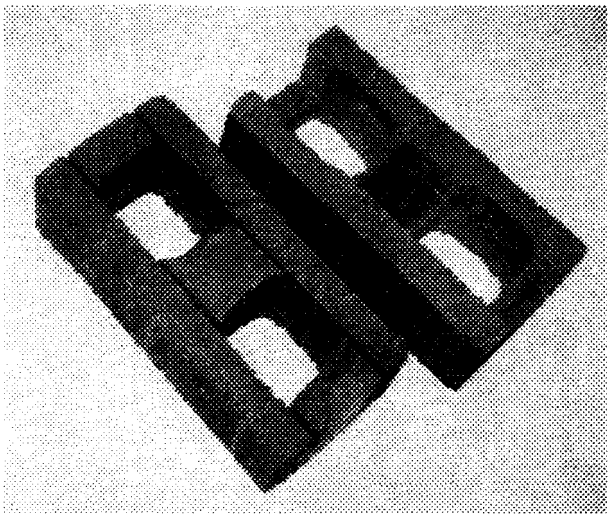


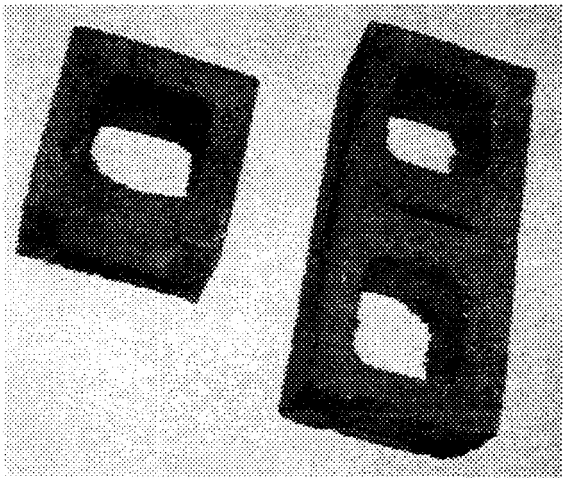
Figure 1.1

Schematic Sketch Of Suprking Brick



Photograph Of Suprking Brick Bond Beam Units

Before Breaking Out Flanges (Left) And After Breaking Out Flanges



Photograph Of Suprking Brick (Right) and Split Suprking Brick

Figure 1.2

Photographs Of Suprking Brick Units

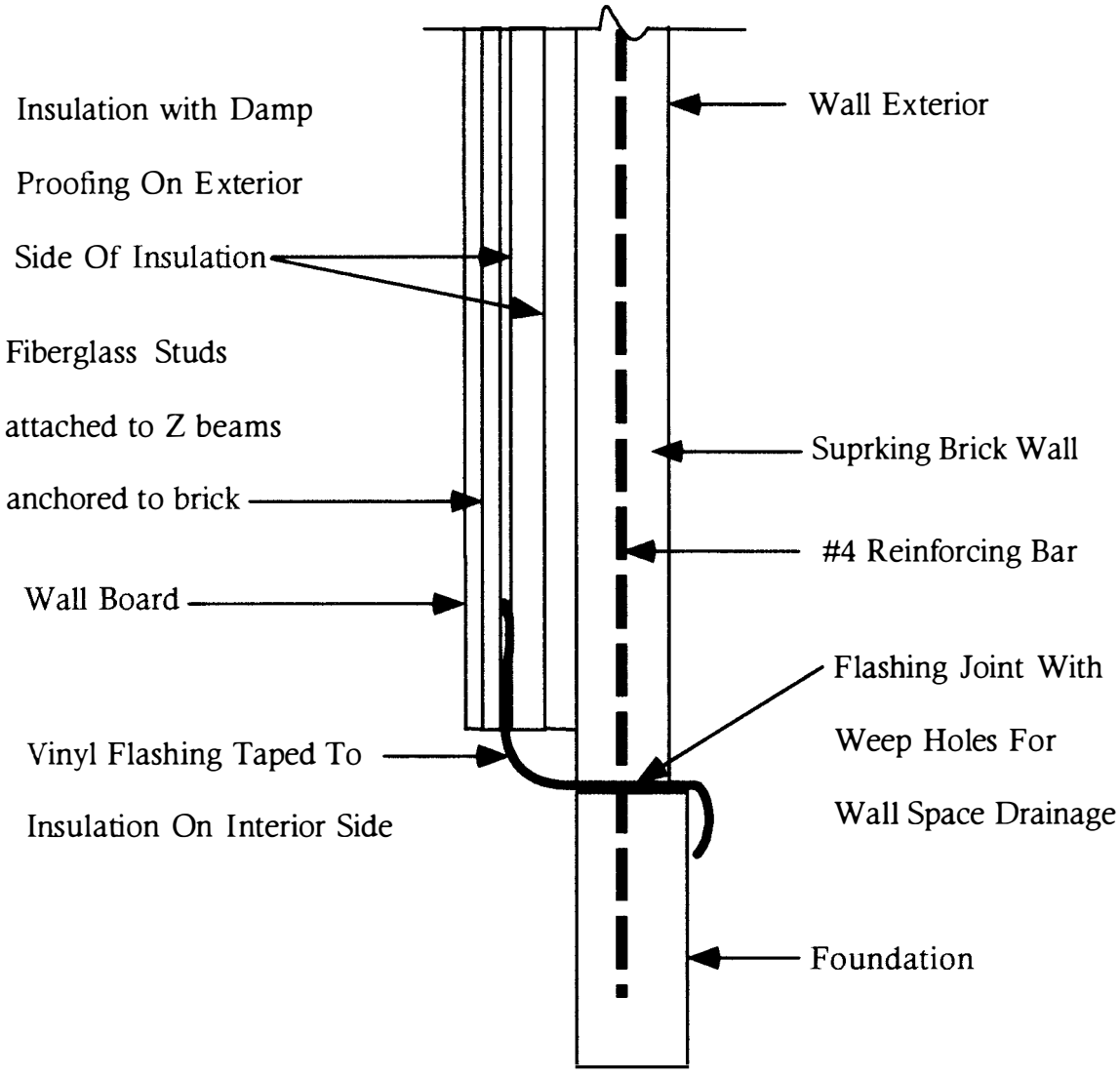


Figure 2.1

Schematic Sketch Of Suprking Brick Wall System

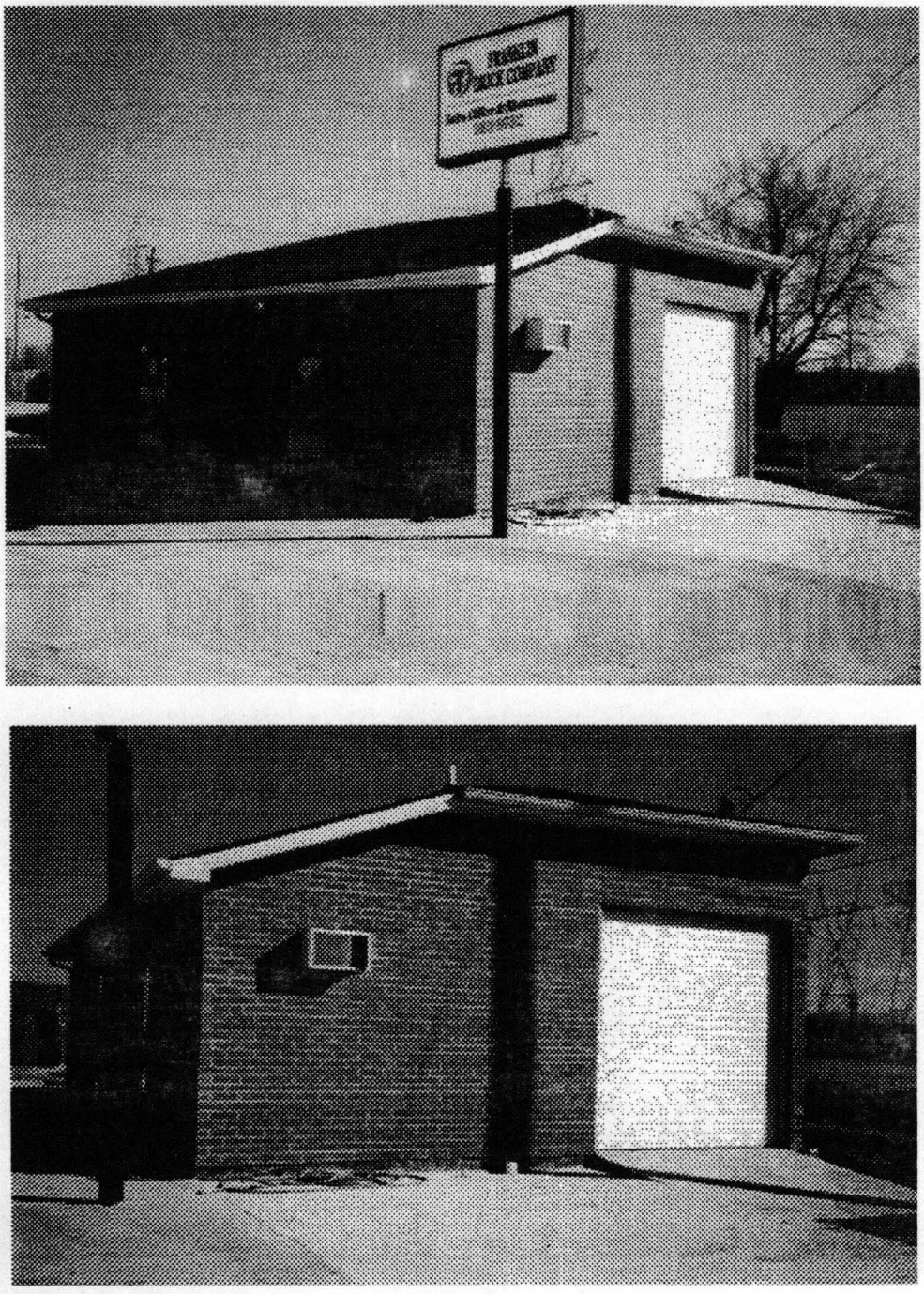
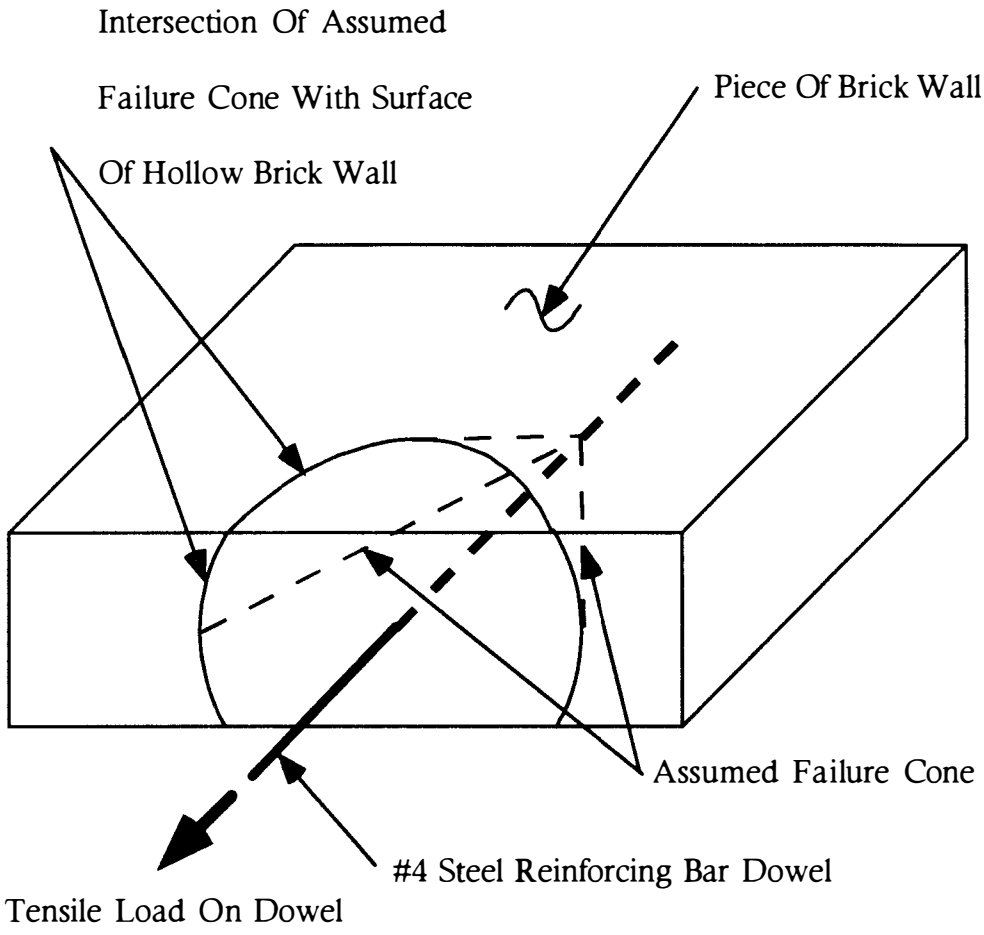


Figure 2.2

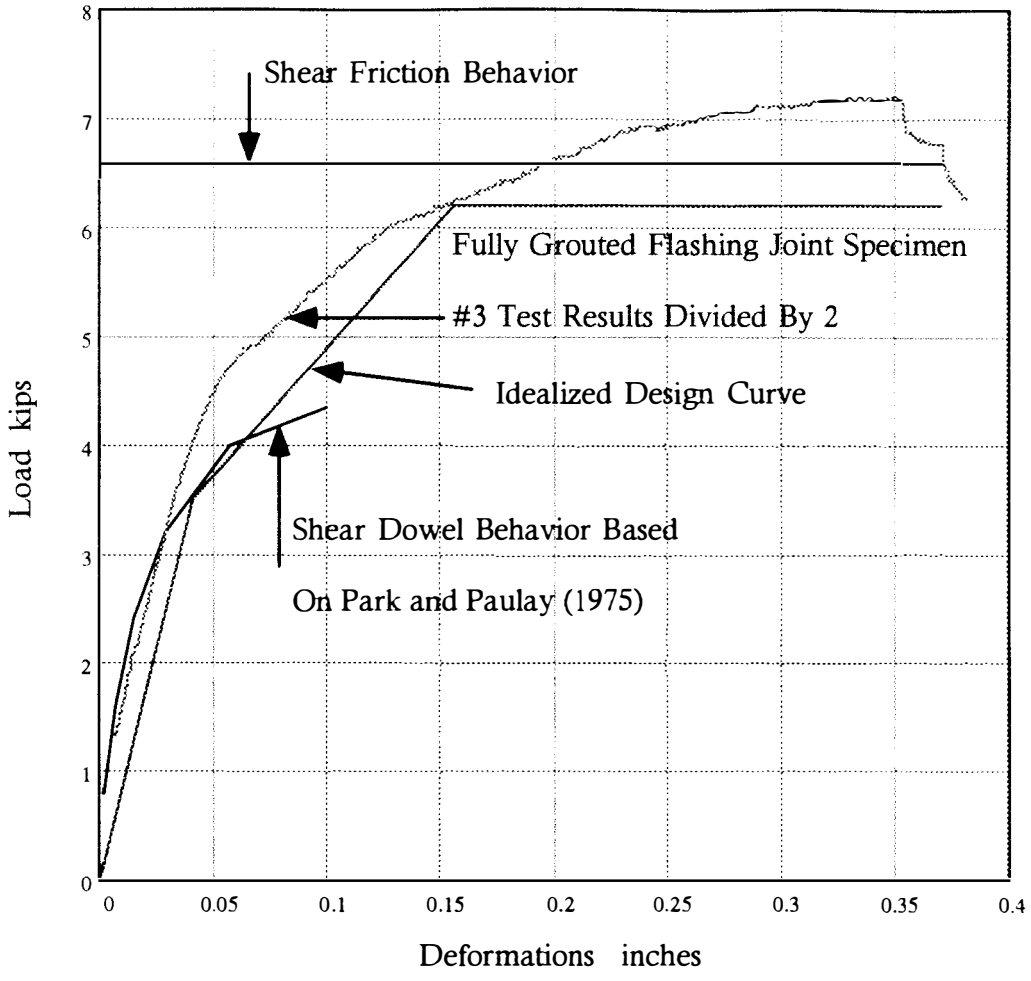
Small Industrial Building Constructed With Suprking Brick System



Idealized Pull-Out Failure Cone

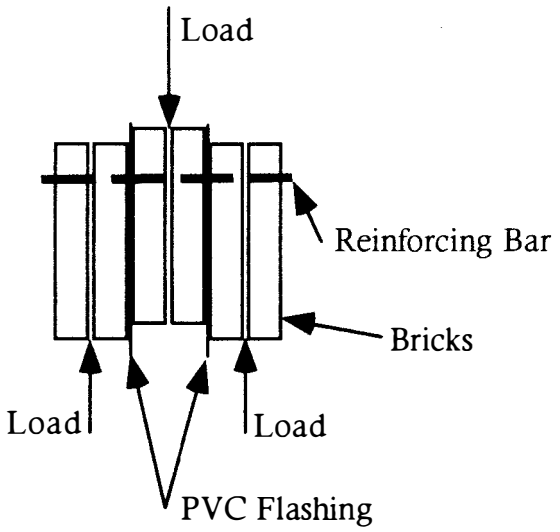
For Dowel In Hollow Brick Wall Flashing Joint

Figure 2.3

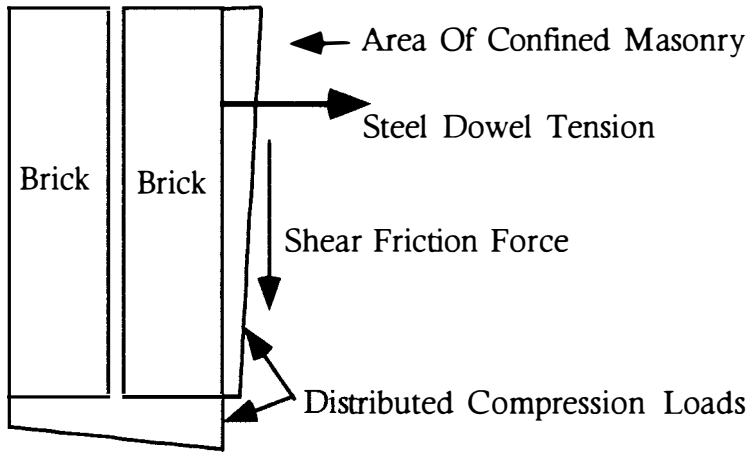


Comparison Of Shear Friction, Dowel, #4 Fully Grouted Shear Specimen, And Idealized Flashing Joint Behavior

Figure 2.4



Shear Specimen



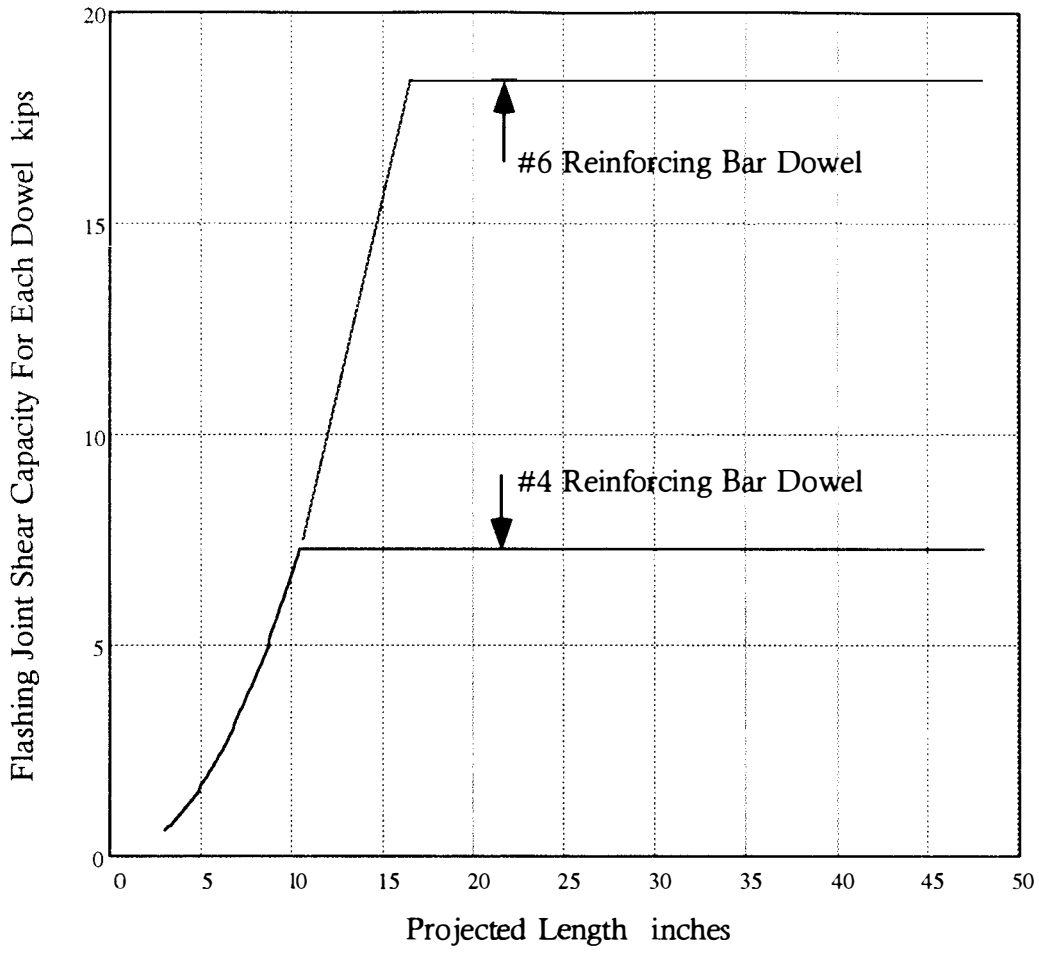
Free Body Diagram

Left Side Of Shear Specimen

Shear Specimen And

Free Body Diagram Of Left Side Of Shear Specimen

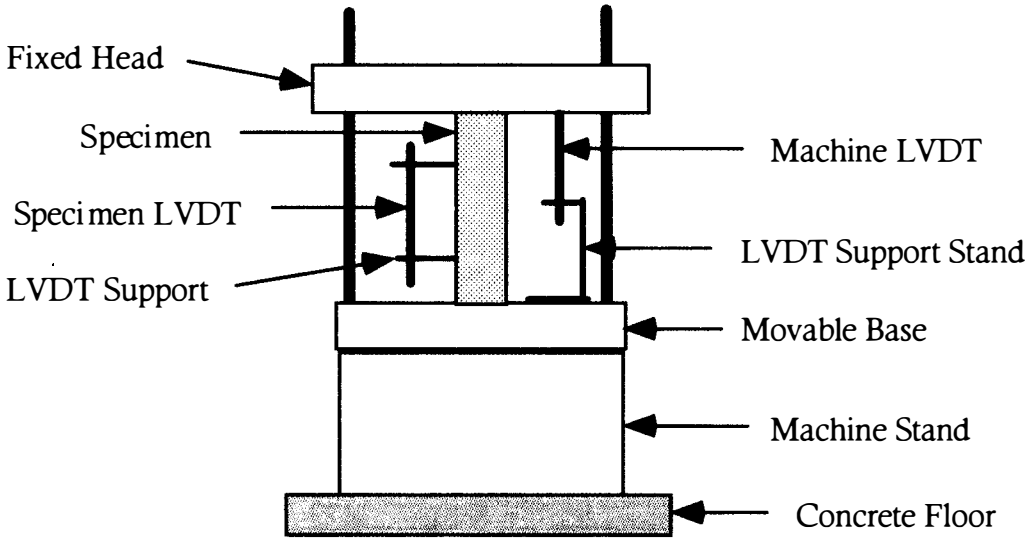
Figure 2.5



Note: Projected length is the length of the Suprking hollow brick wall contributing to the tensile pull out strength of the reinforcing bar dowels.

Flashing Joint Shear Capacity For Each Dowel Versus Projected Length Estimated From ACI 530 Equations (Building, 1992)

Figure 2.6



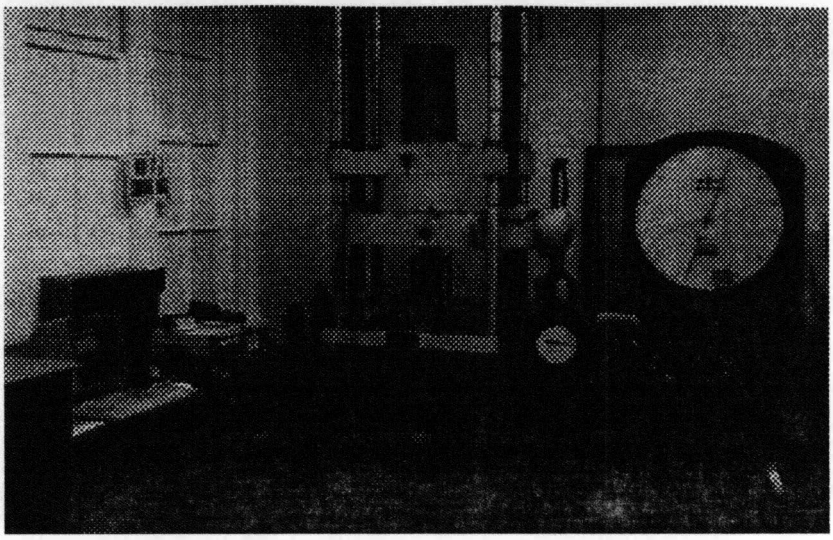
Tinius Olsen Universal Test Machine

Model # 1950; 120,000 pound capacity

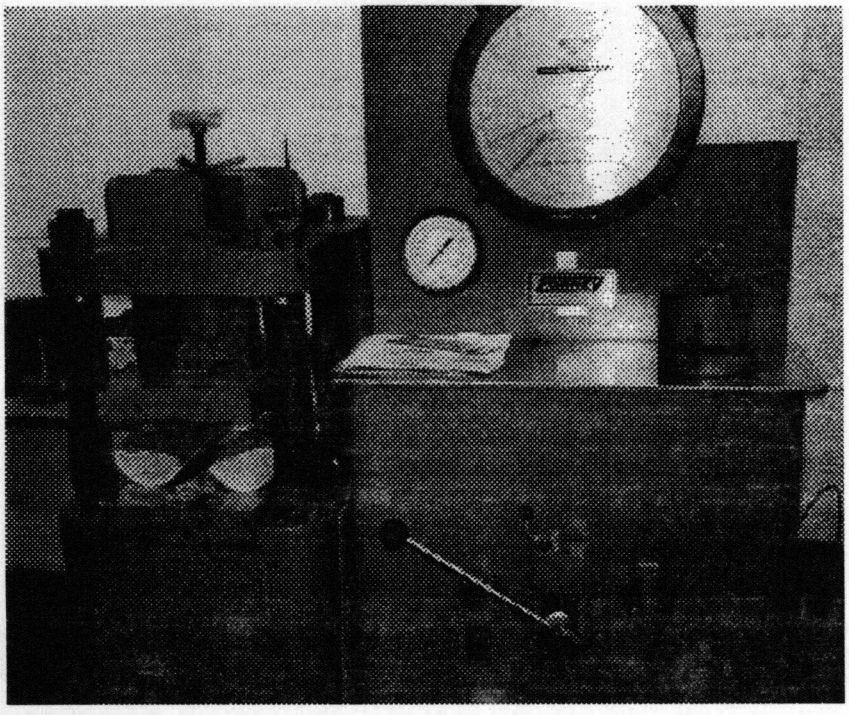
Set-up to apply compressive load in figure

Component Testing Equipment Arrangement

Figure 3.1



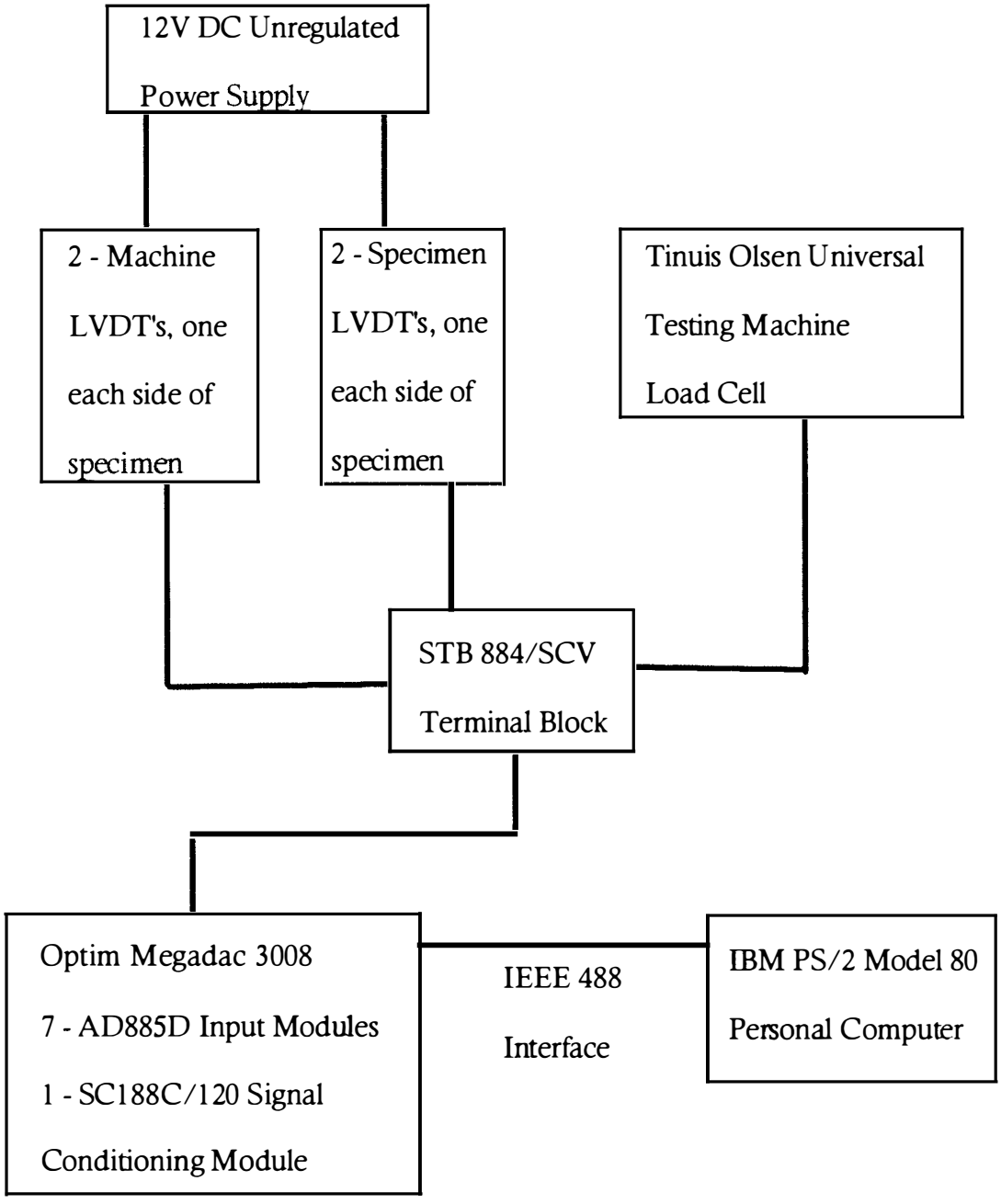
Tinius Olsen Test Machine and Data Collection Equipment (On Left)



Forney Test Machine Set Up To Split Concrete Cylinders

Figure 3.2

Test Equipment



Component Test Instrumentation Arrangement

Figure 3.3

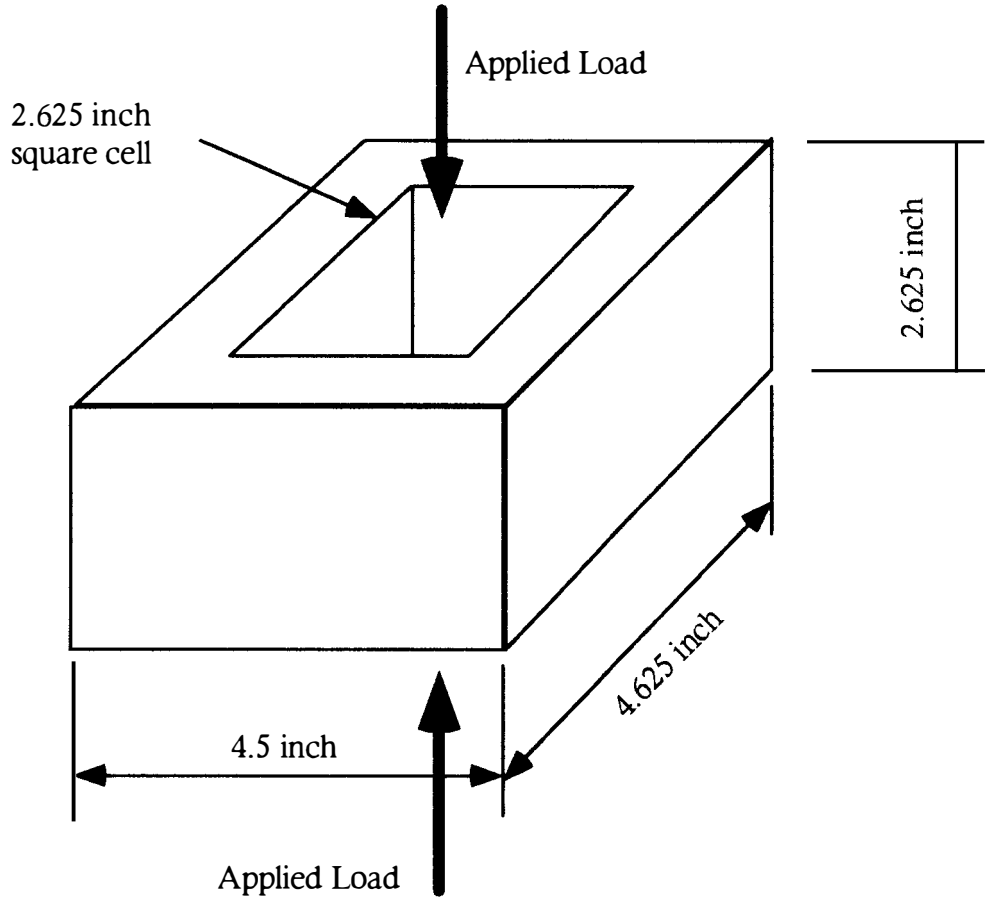


Figure 3.4

Half Brick Compressive Strength Specimen

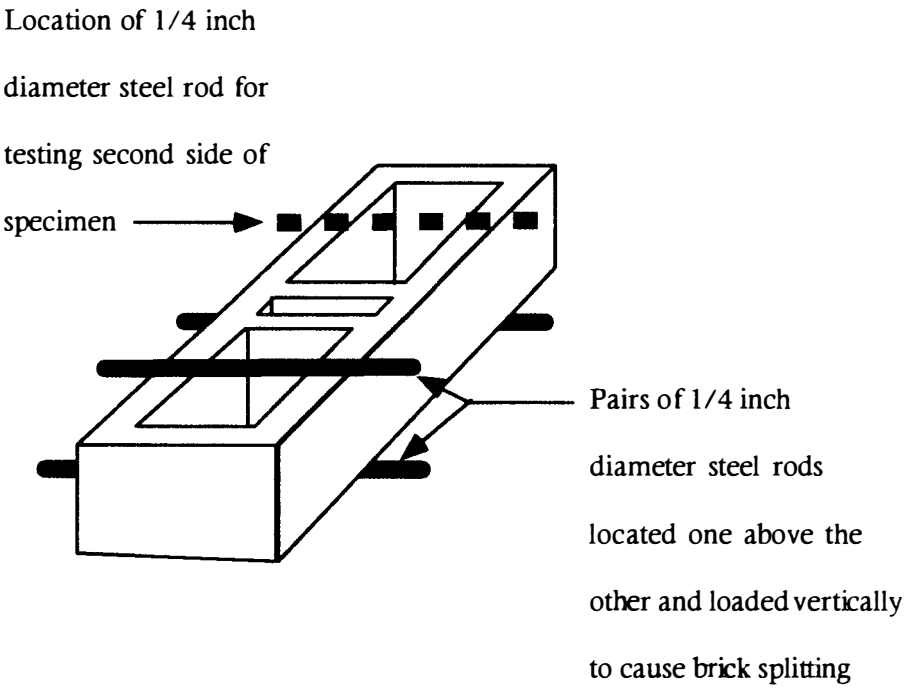
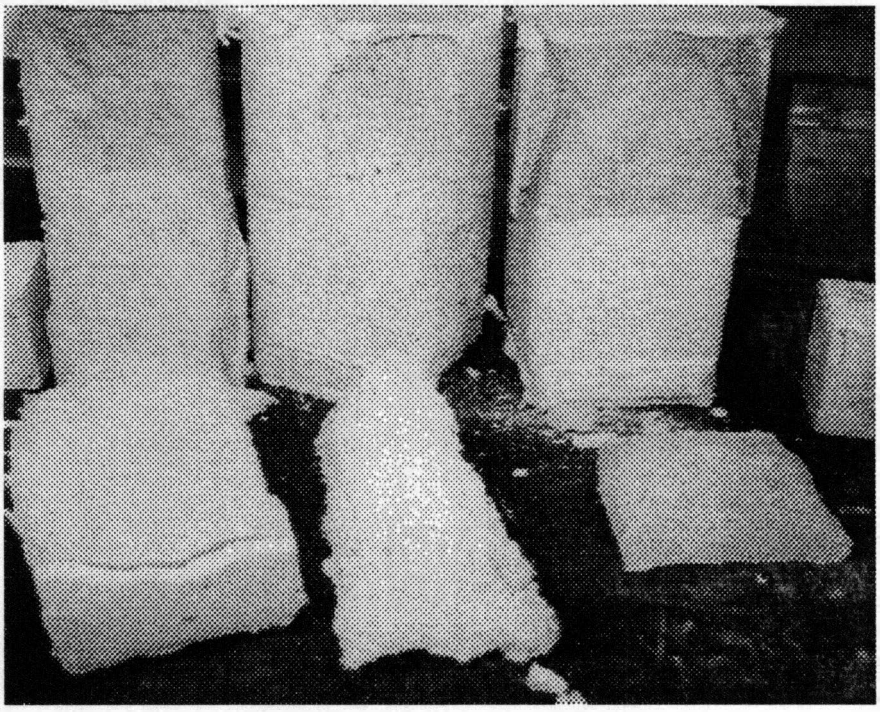


Figure 3.5

Splitting Tensile Strength Test Arrangement

Suprking Brick



Three grout specimens are shown in this figure. The specimens on the left and right sides were made using 10K grout. The specimen in the center was made by thinning Type N mortar. As can be observed from this photograph, the failure mode of all three specimens was similar.

Figure 3.6

Photograph Of Grout Specimens After Failure

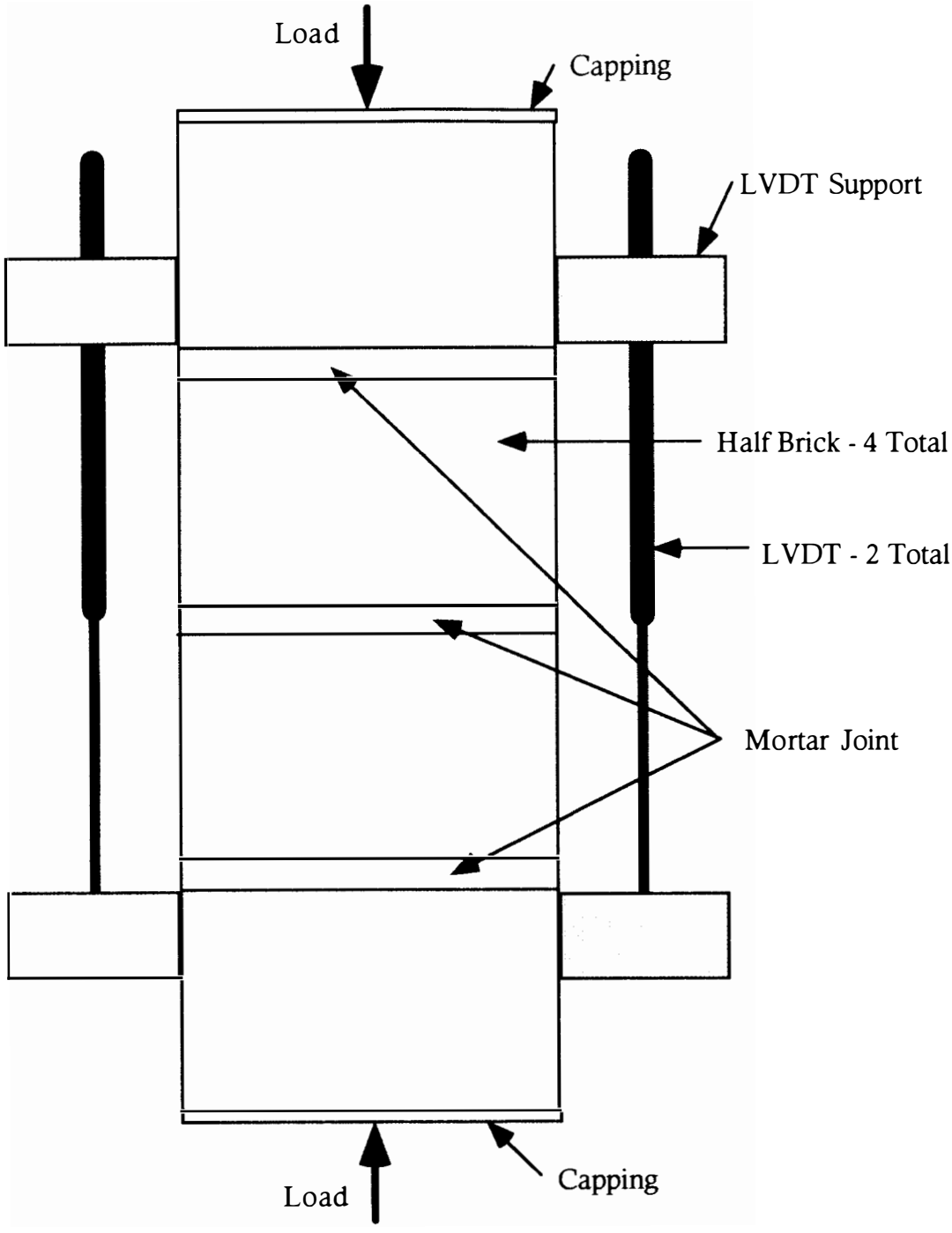
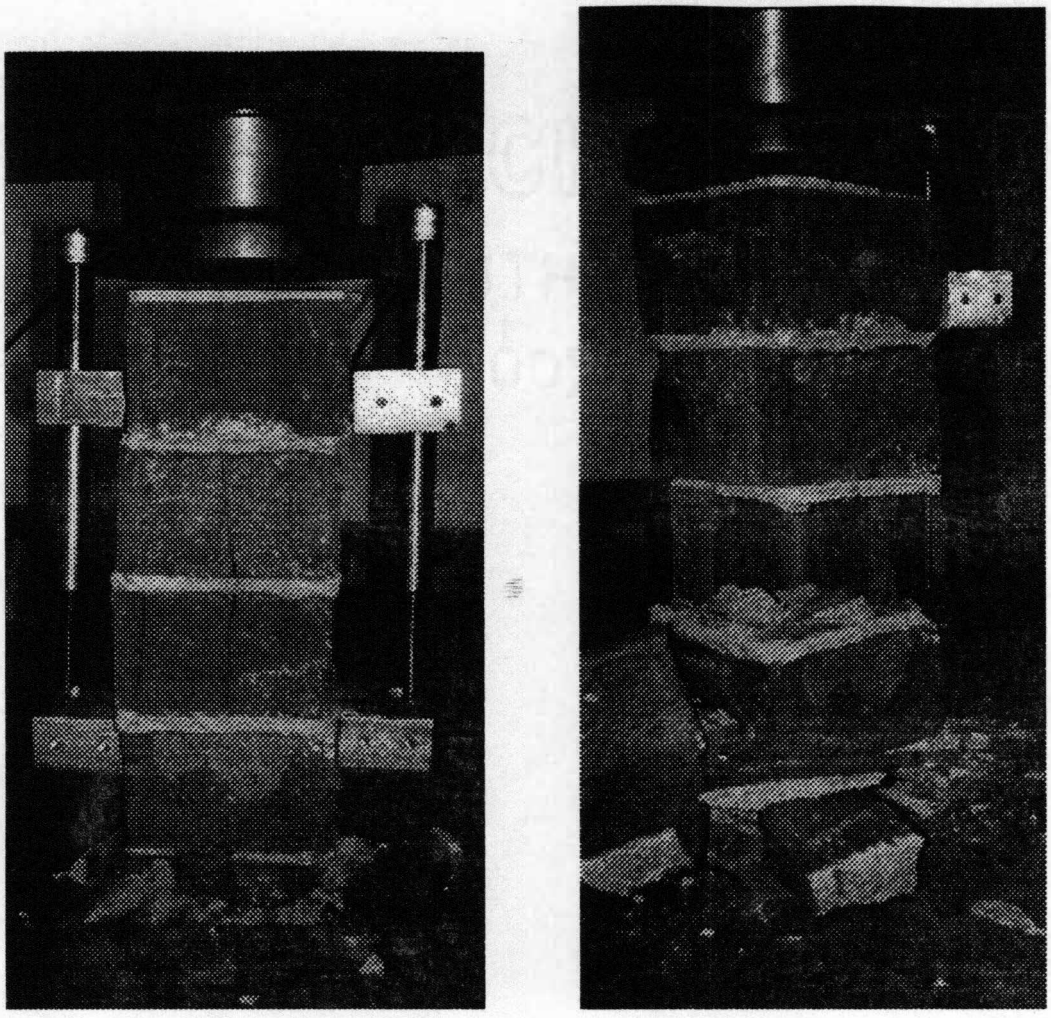


Figure 3.7

Brick Prism Specimen for Compression Testing



These are photographs of two ungrouted Suprking brick prisms immediately after failure. The specimen at the left has vertical cracks in the face shell in the middle two ½ bricks. The specimen at the right has lost a substantial portion of the ½ brick in the second course after splitting of the face shell.

Figure 3.8

Photograph Of Ungrouted Brick Prism Specimens

In Test Machine After Specimen Failure

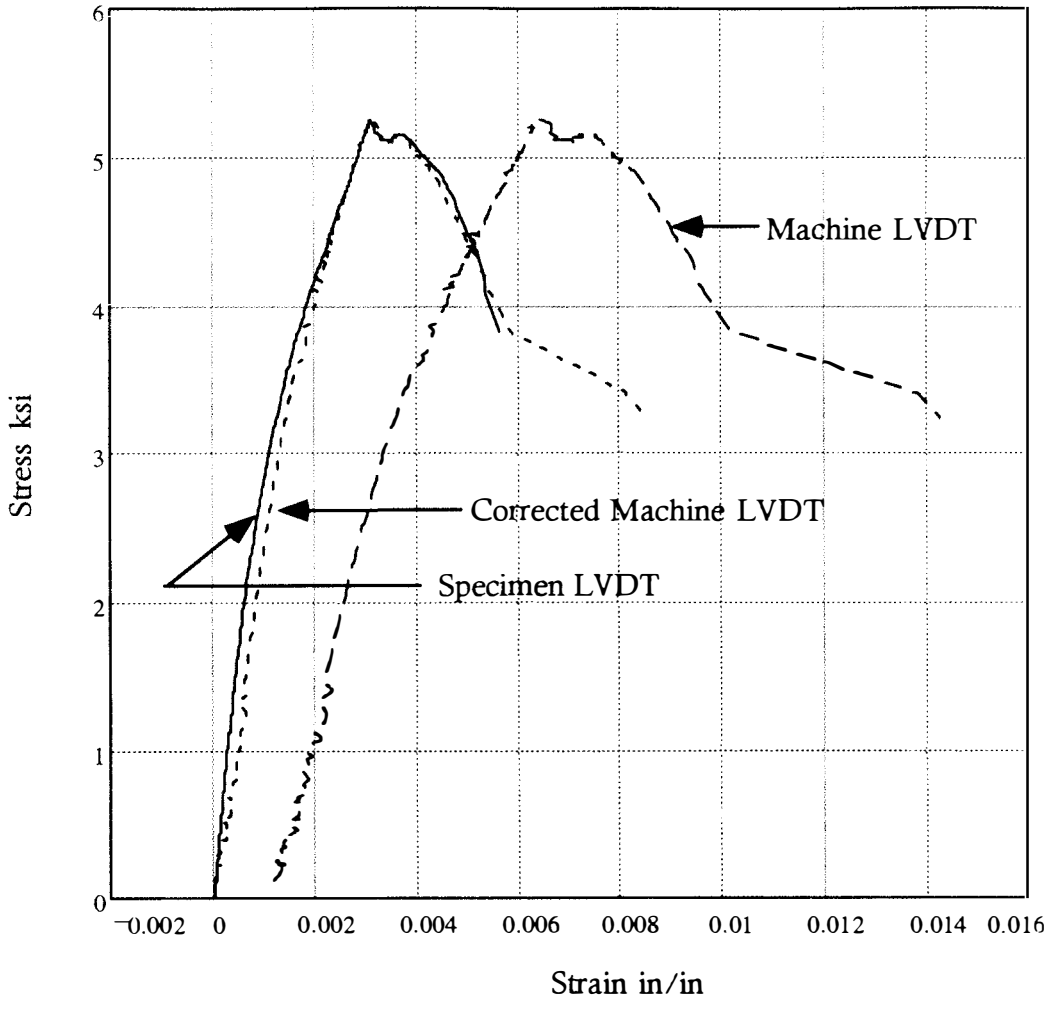


Figure 3.9

Ungrouted Brick Prism #2 Stress Strain Curves

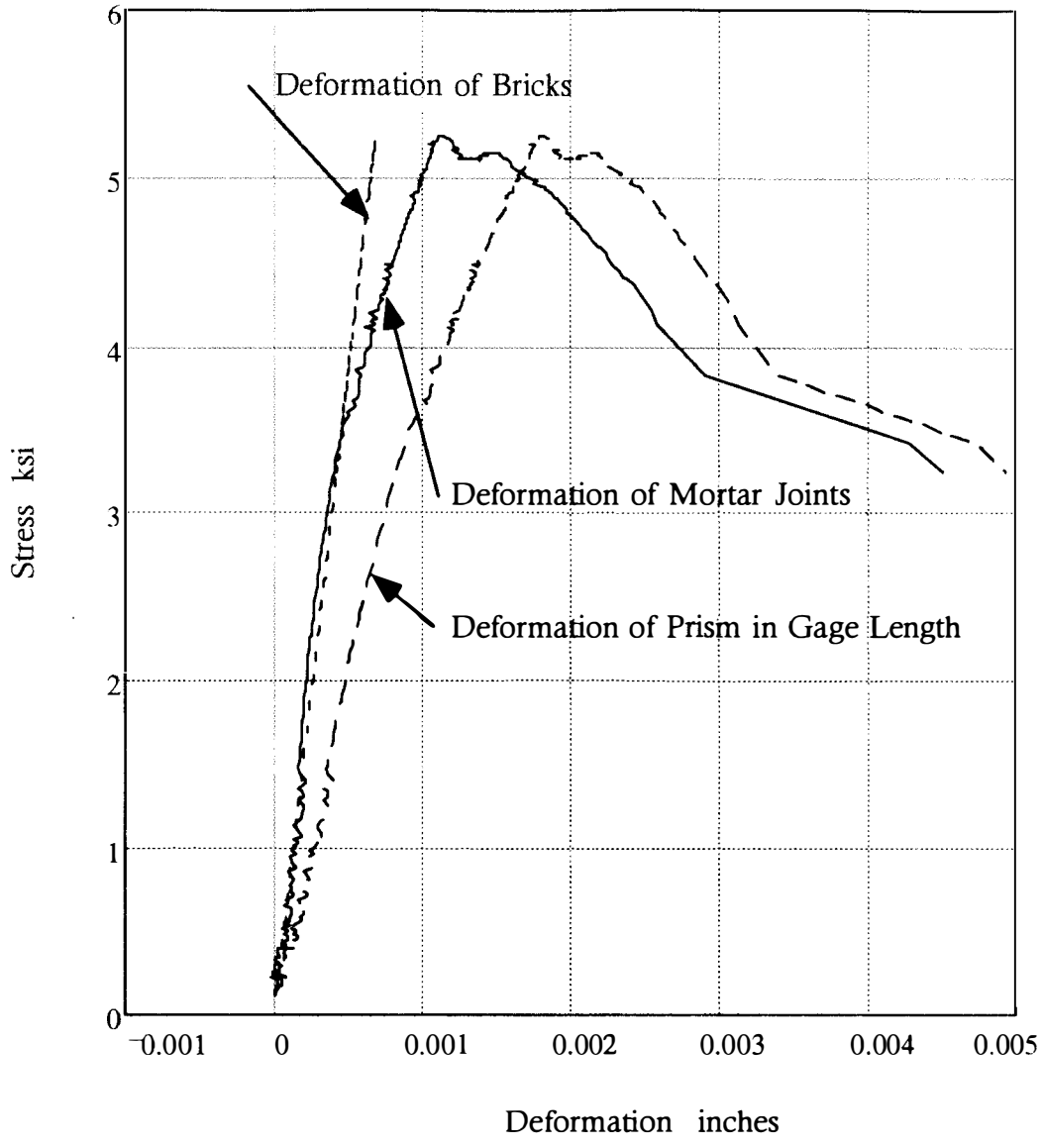


Figure 3.10

Ungrouted Prism Specimen #2 Deformation Of Components

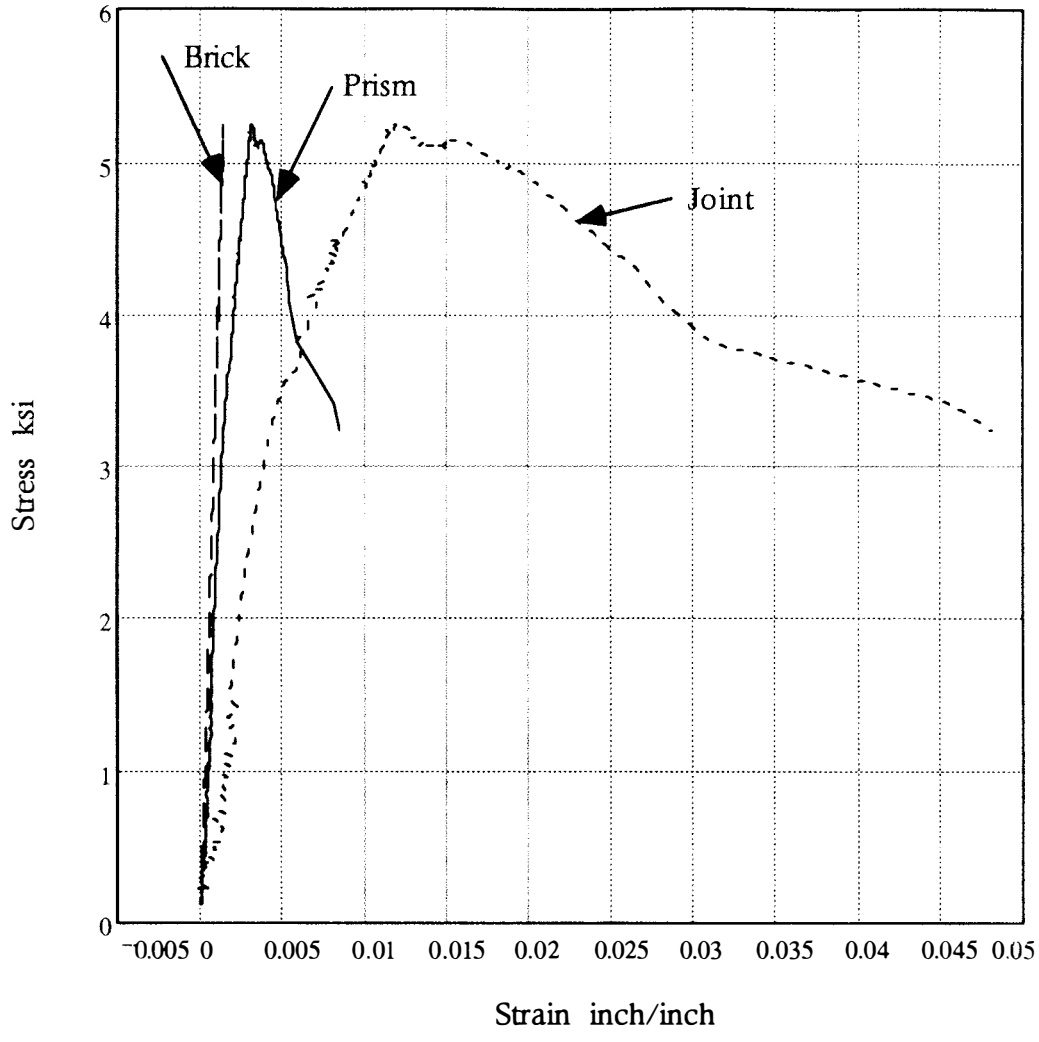


Figure 3.11

Ungrouted Prism Specimen #2 Stress Versus Strain Of Components

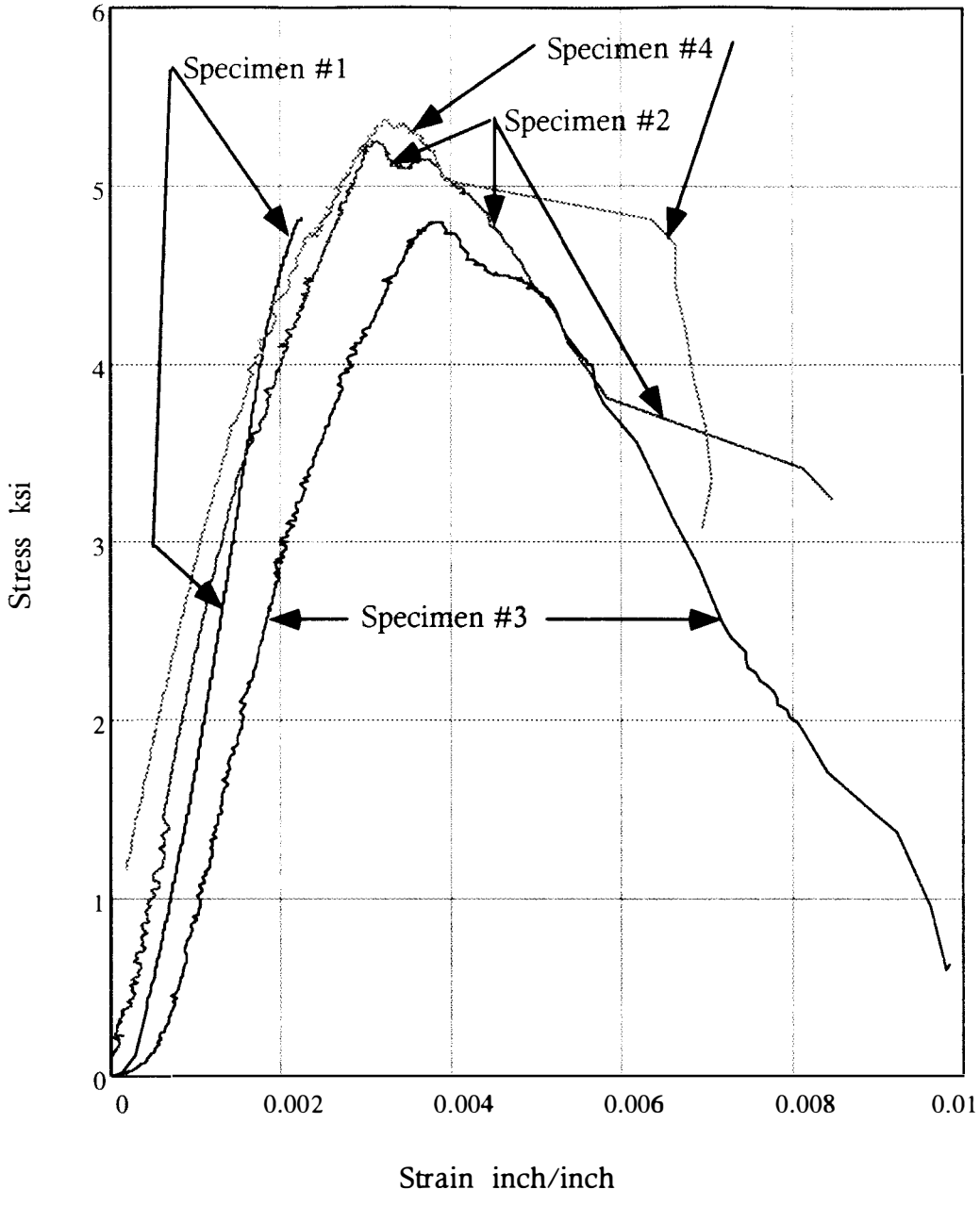
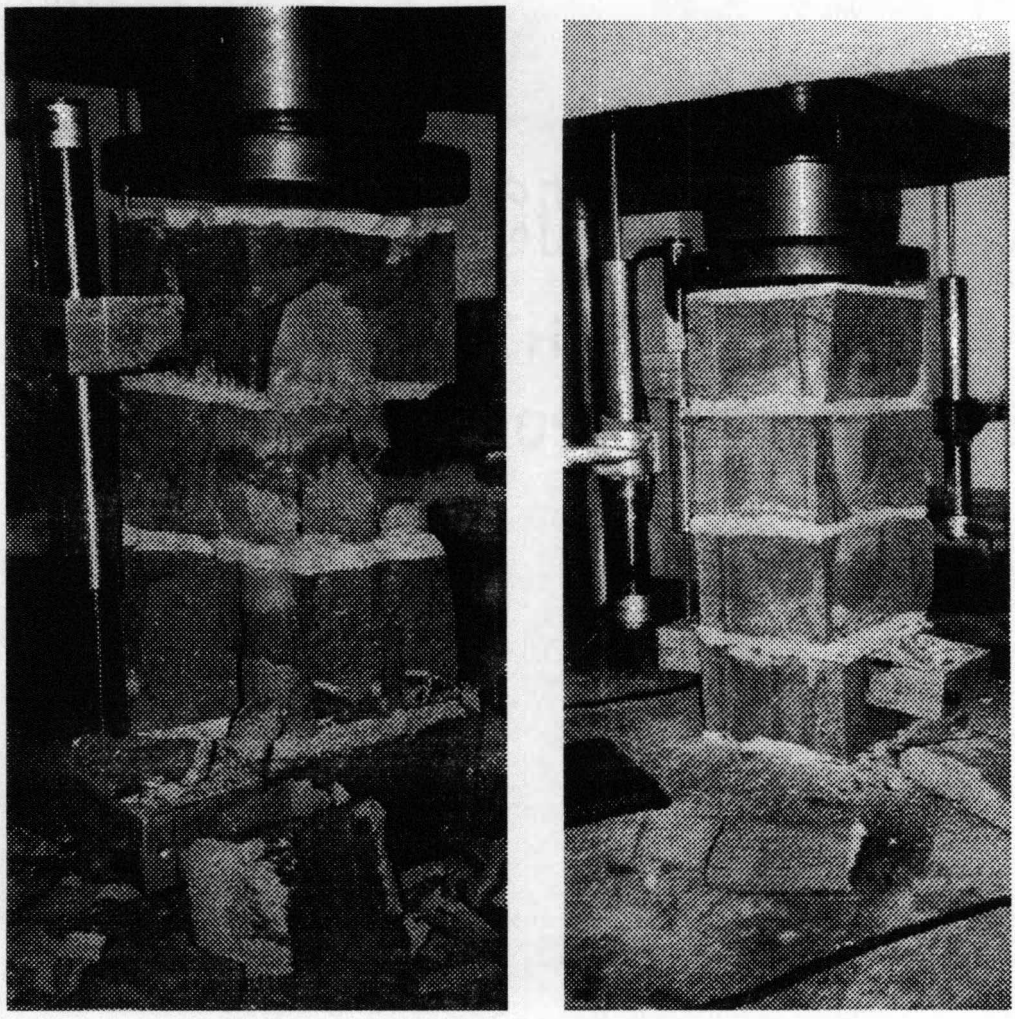


Figure 3.12

Ungrouted Prism Stress Strain Curves



These photographs are of two different Suprking brick prisms grouted with 10K grout in the test machine immediately after failure. The grout core can be seen in both pictures where the face shell has fallen off the specimens. Note that an LVDT for measuring specimen deformations is shown in the left hand picture. LVDTs for measuring machine movement are shown in the right hand picture.

Figure 3.13

Photograph Of 10K Grouted Brick Prism Specimens

In Test Machine After Specimen Failure

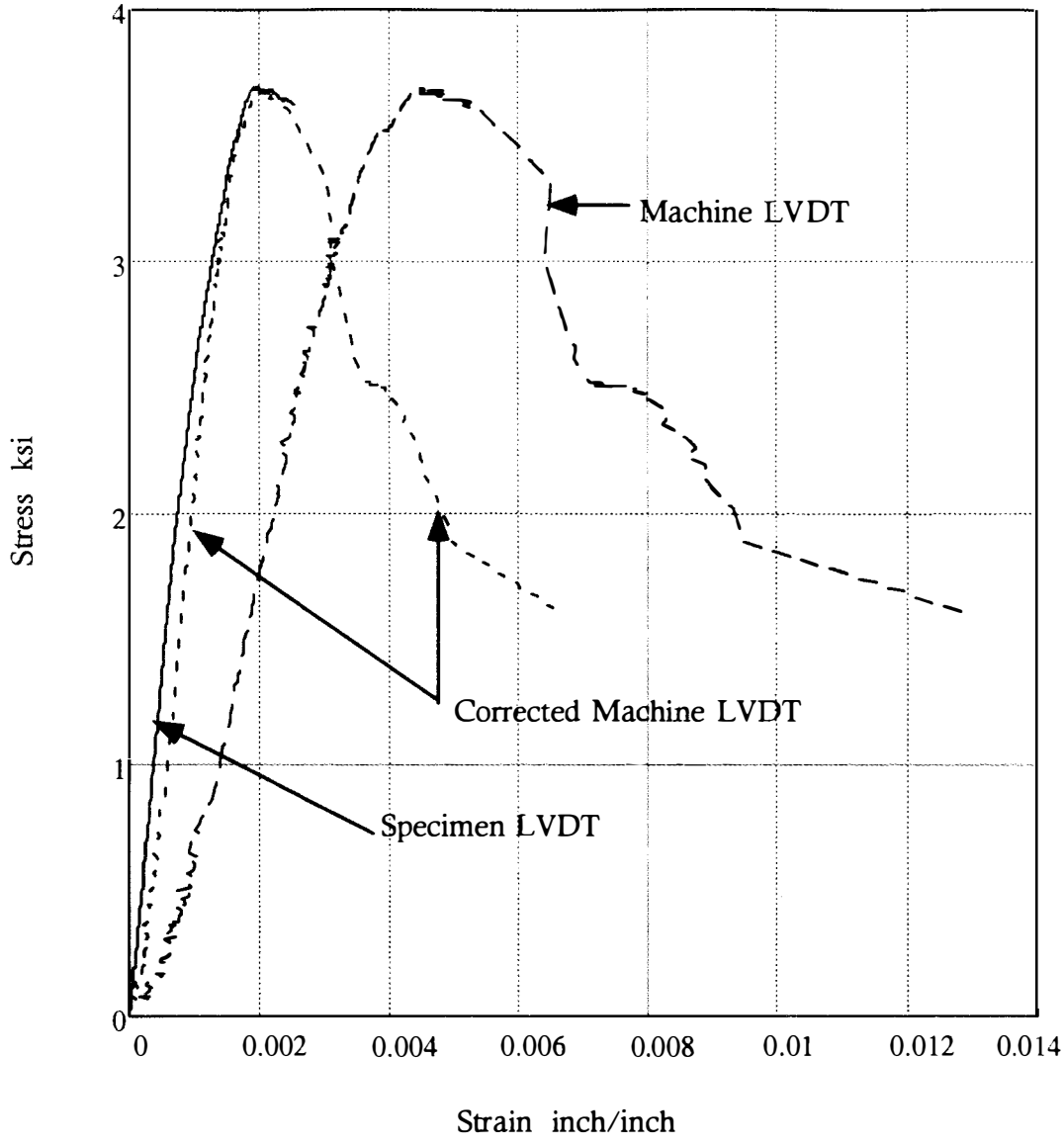


Figure 3.14

10K Grouted Brick Prism #1 Stress Strain Curves

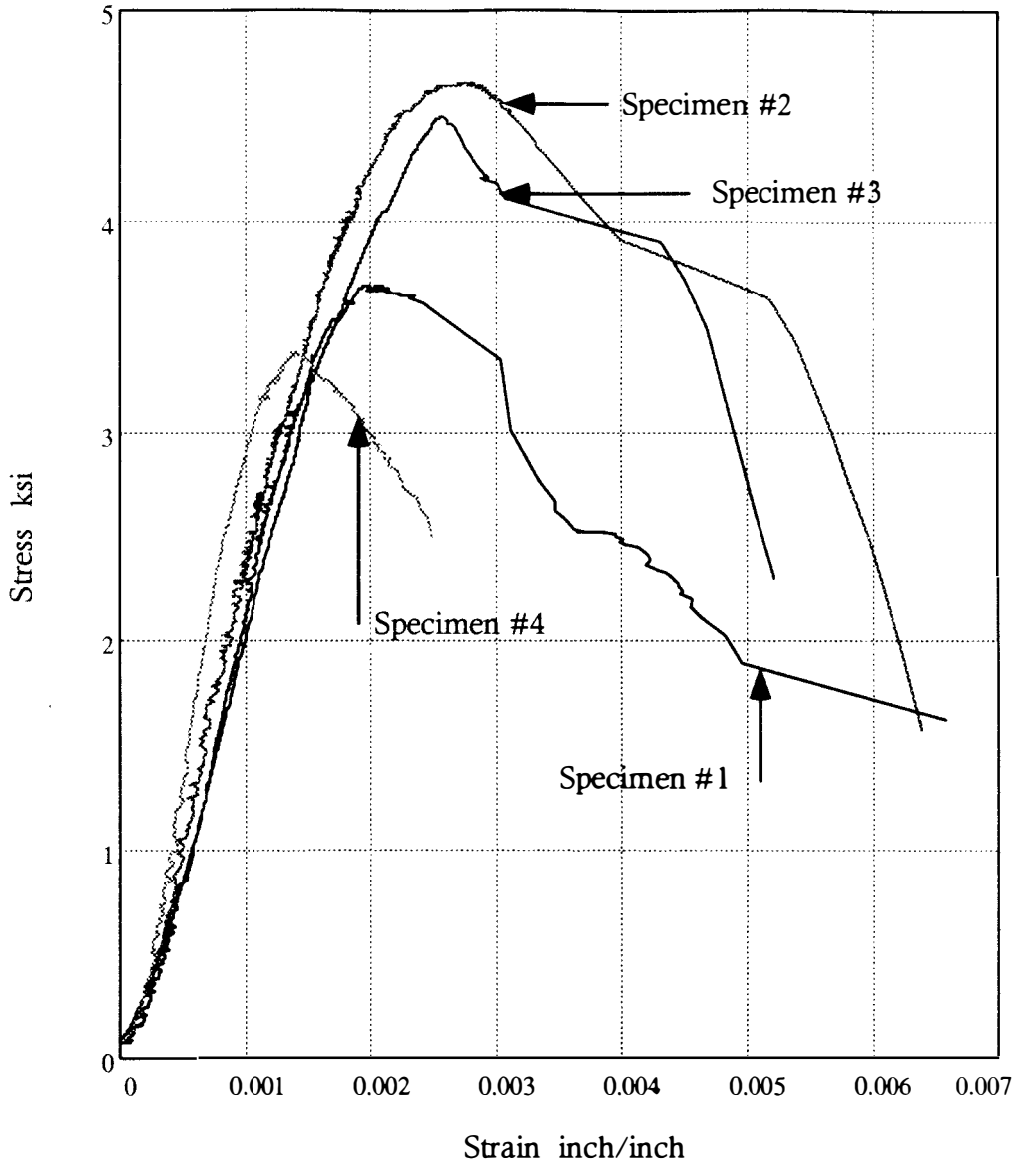


Figure 3.15

10K Grouted Prism Stress Strain Curves

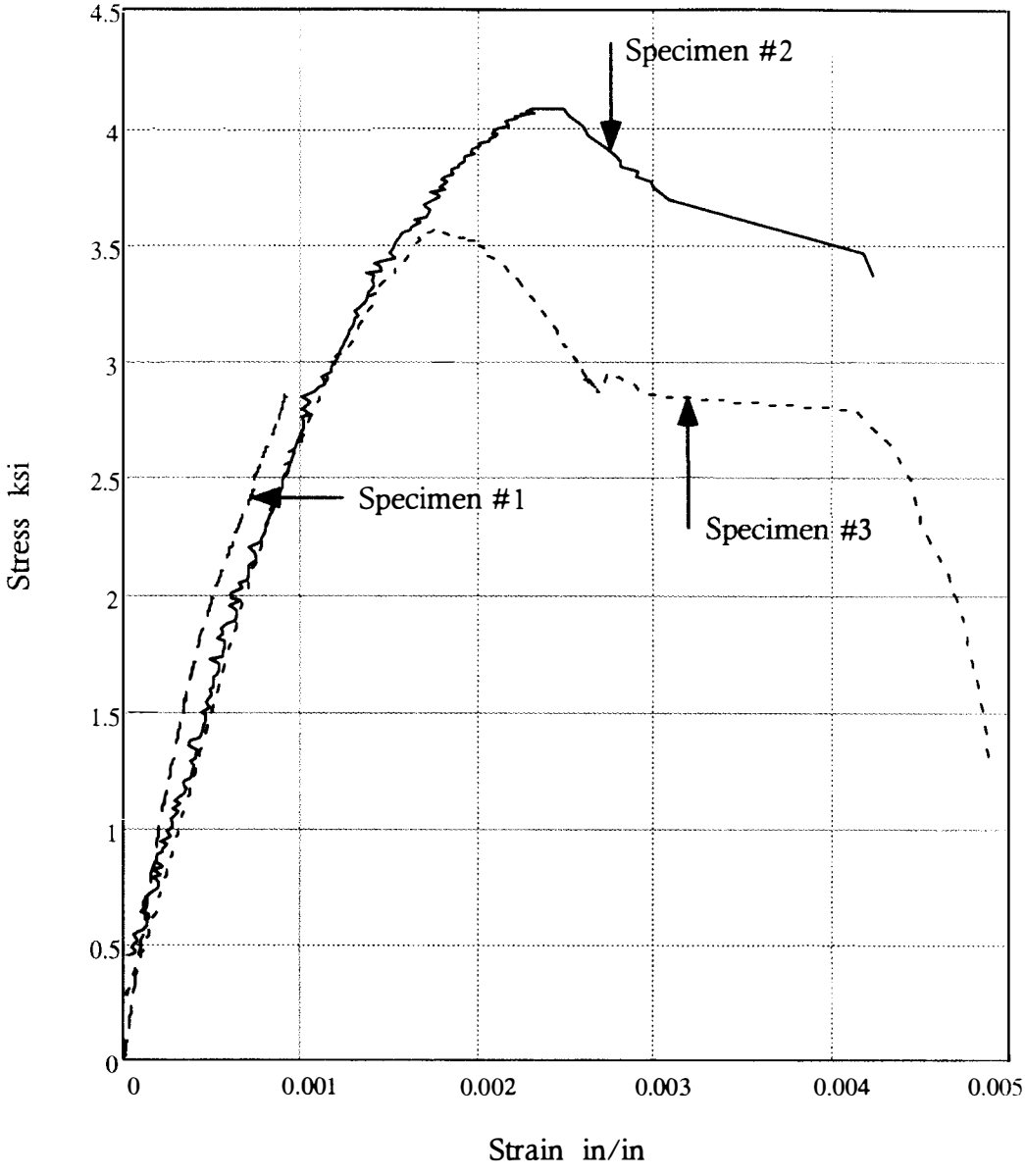
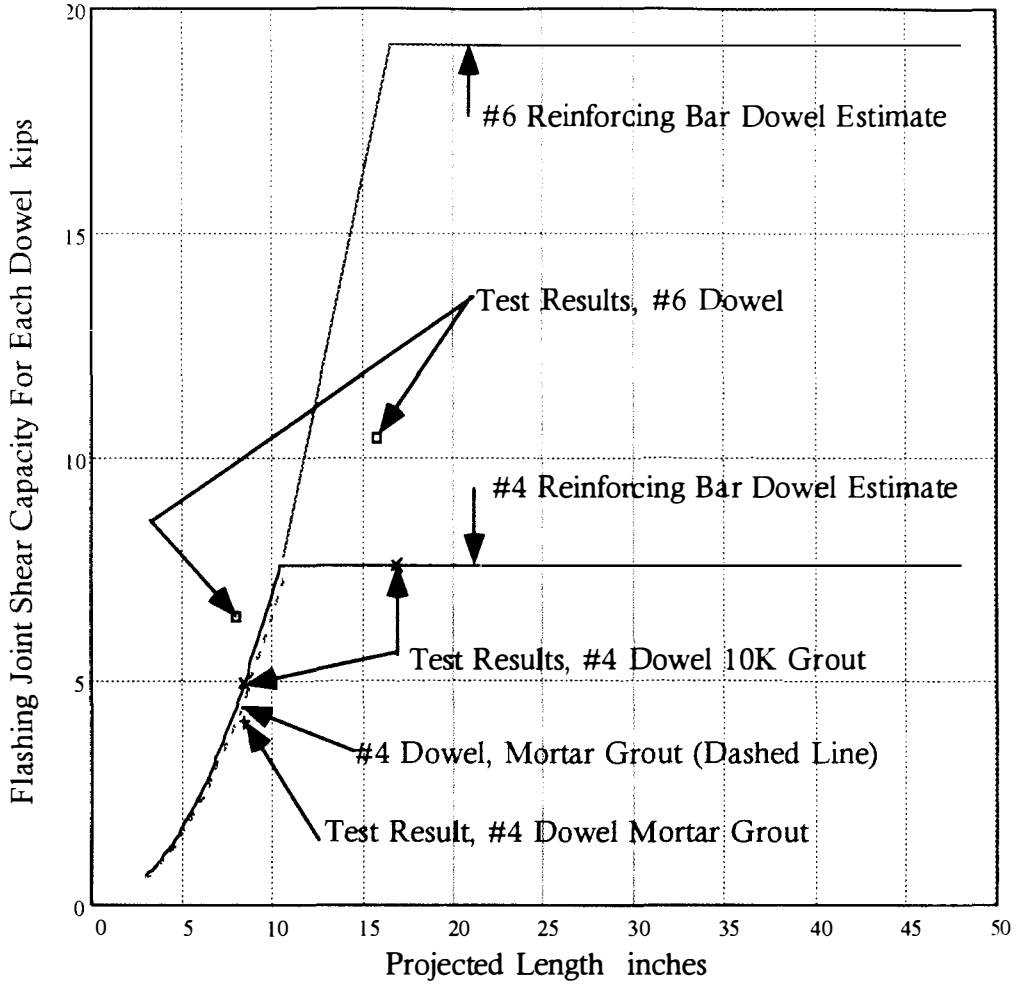


Figure 3.16

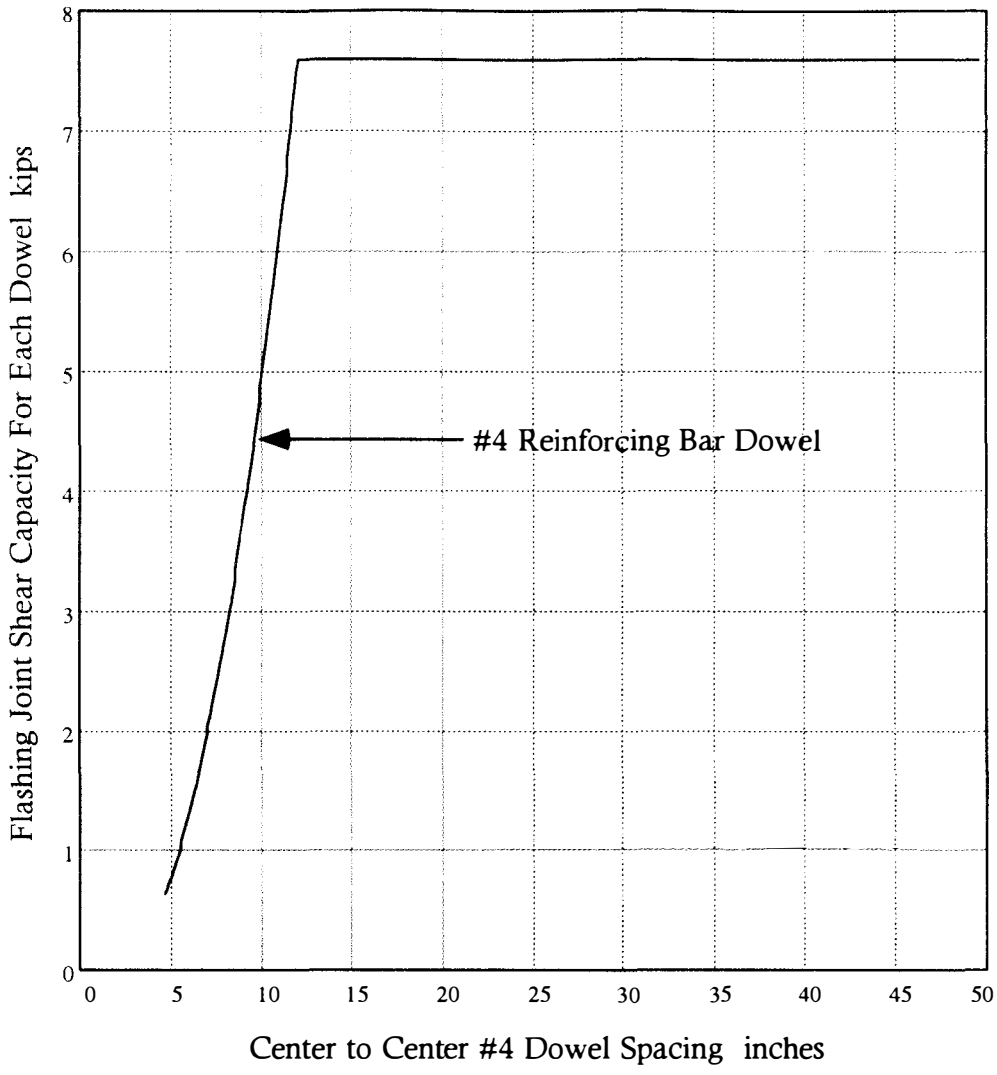
Type N Mortar Grouted Prism Stress Strain Curves



Note: Projected length is the length of the Suprking hollow brick wall contributing to the tensile pull out strength of the reinforcing bar dowels.

Plot Of Shear Specimen Test Results On Curves For Flashing Joint Shear Capacity For Each Dowel Versus Projected Length

Figure 4.1



Note: Flashing joint shear capacity for each dowel shown in this figure is based on the coefficient of friction 0.544 as determined from tests using PVC flashing, #4 reinforcing bar, and 10K grout in all cells.

Flashing Joint Shear Capacity For #4 Dowel Versus Dowel Spacing

Figure 4.2

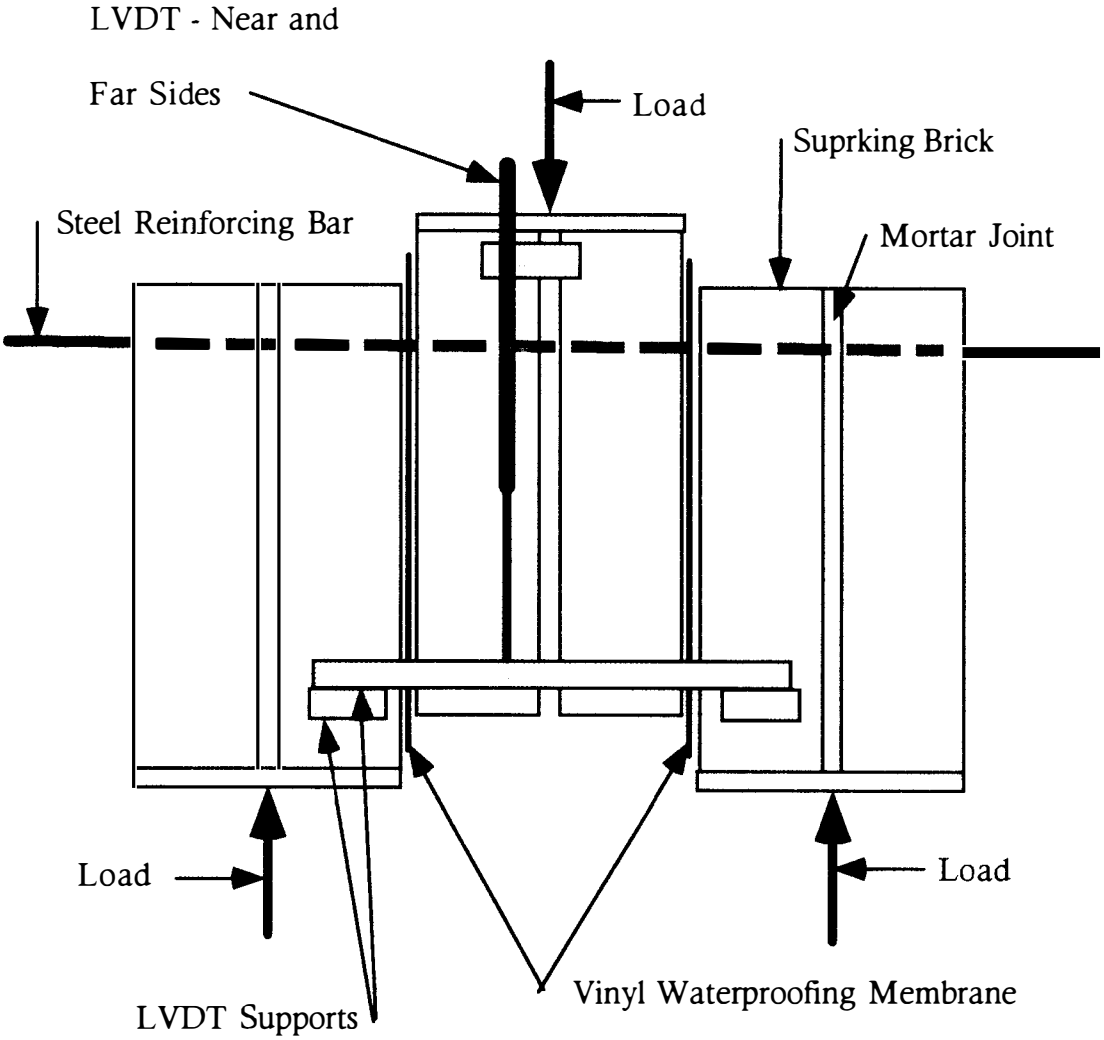


Figure 4.3

Shear Joint Specimen

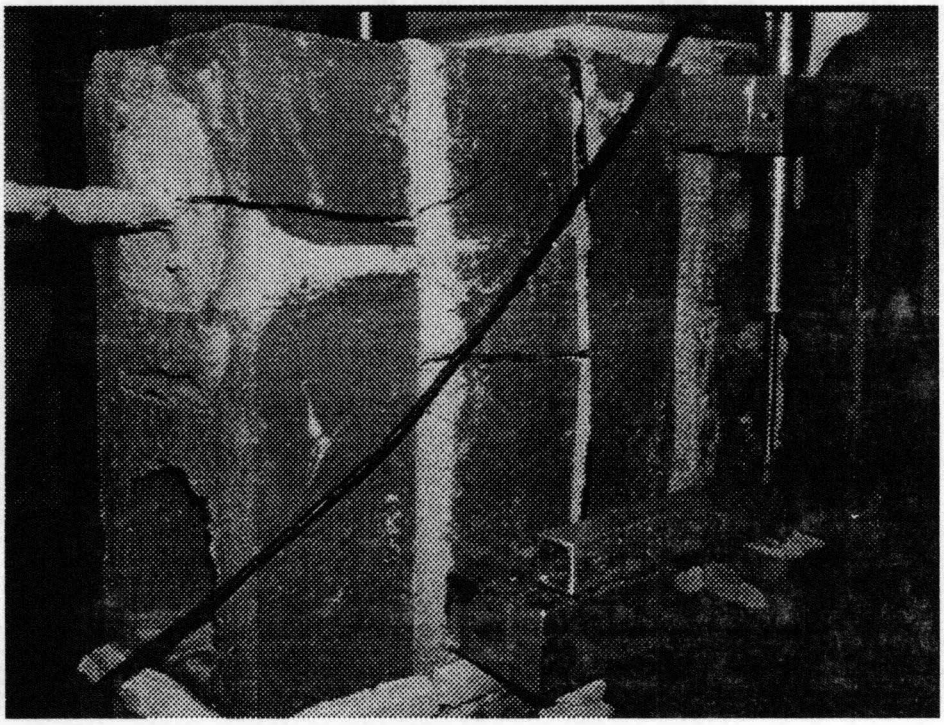


Figure 4.4

Failed Shear Specimen With 10K Grout In Reinforced Cells

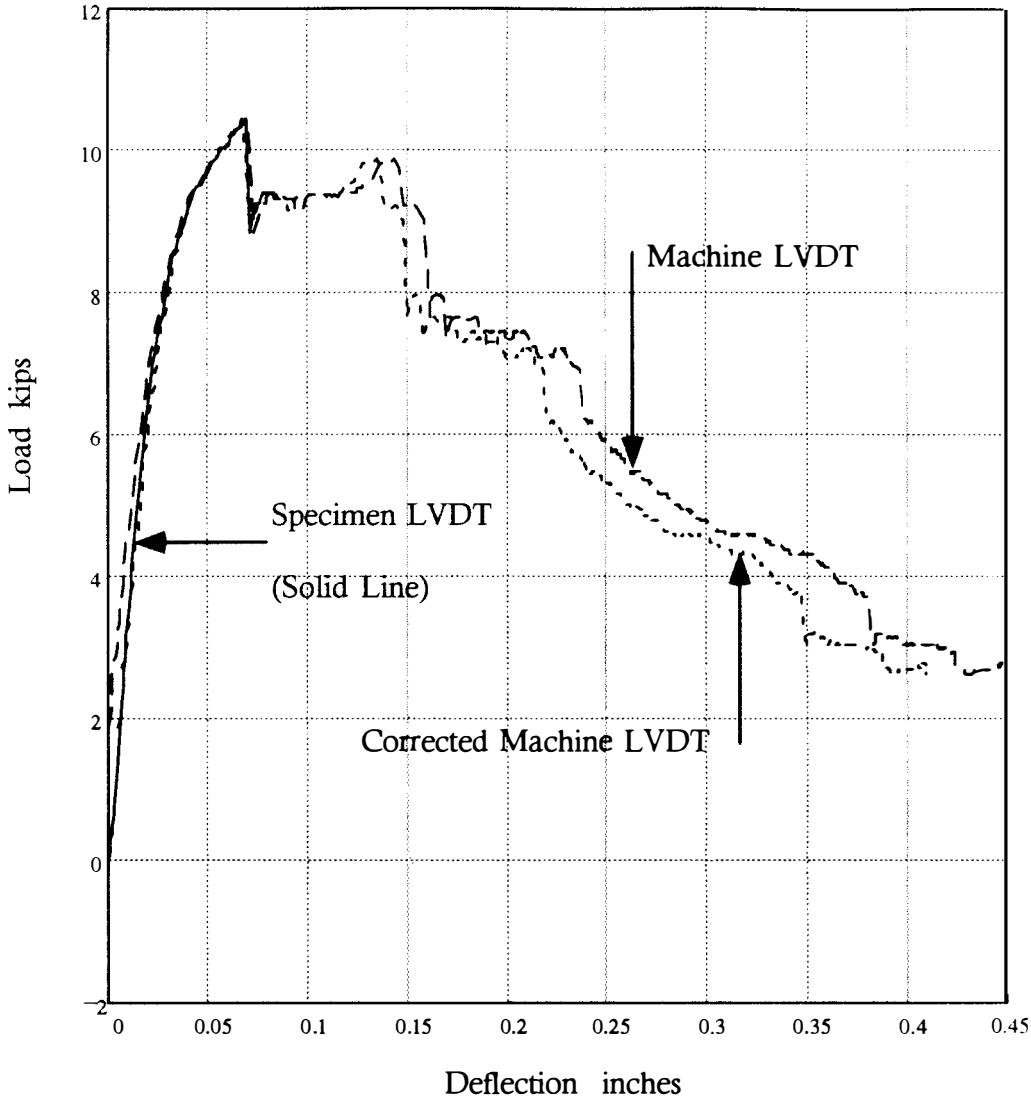


Figure 4.5

Shear Test Of Joints With Vinyl Flashing, #4 Reinforcing Bar, 10K Grout In Reinforced Cells

Specimen #3 Load Deformation Curves

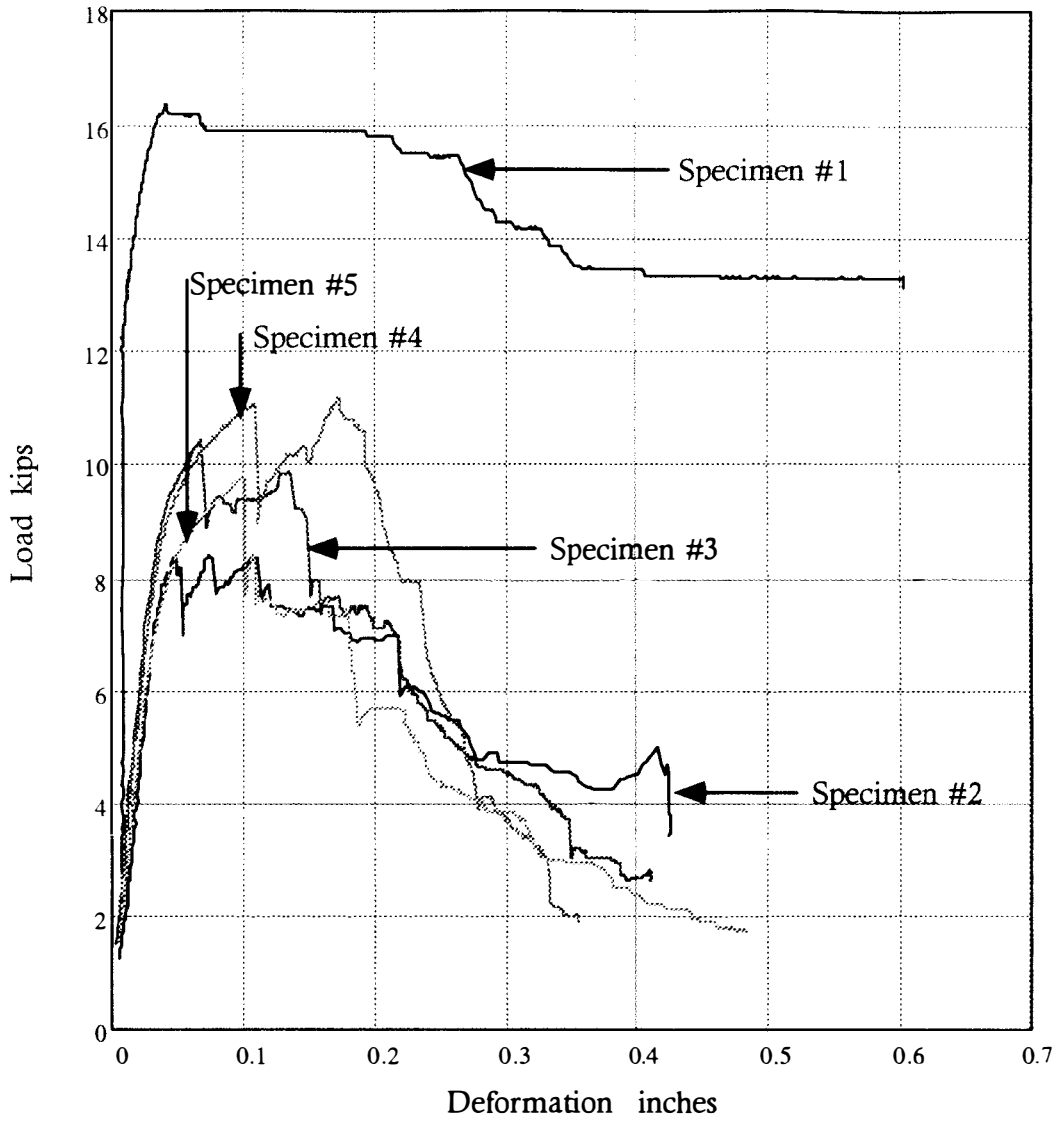


Figure 4.6

Shear Test Of Joints With Vinyl Flashing, #4 Reinforcing Bar, 10K Grout In Reinforced Cells

Load Deformation Curves

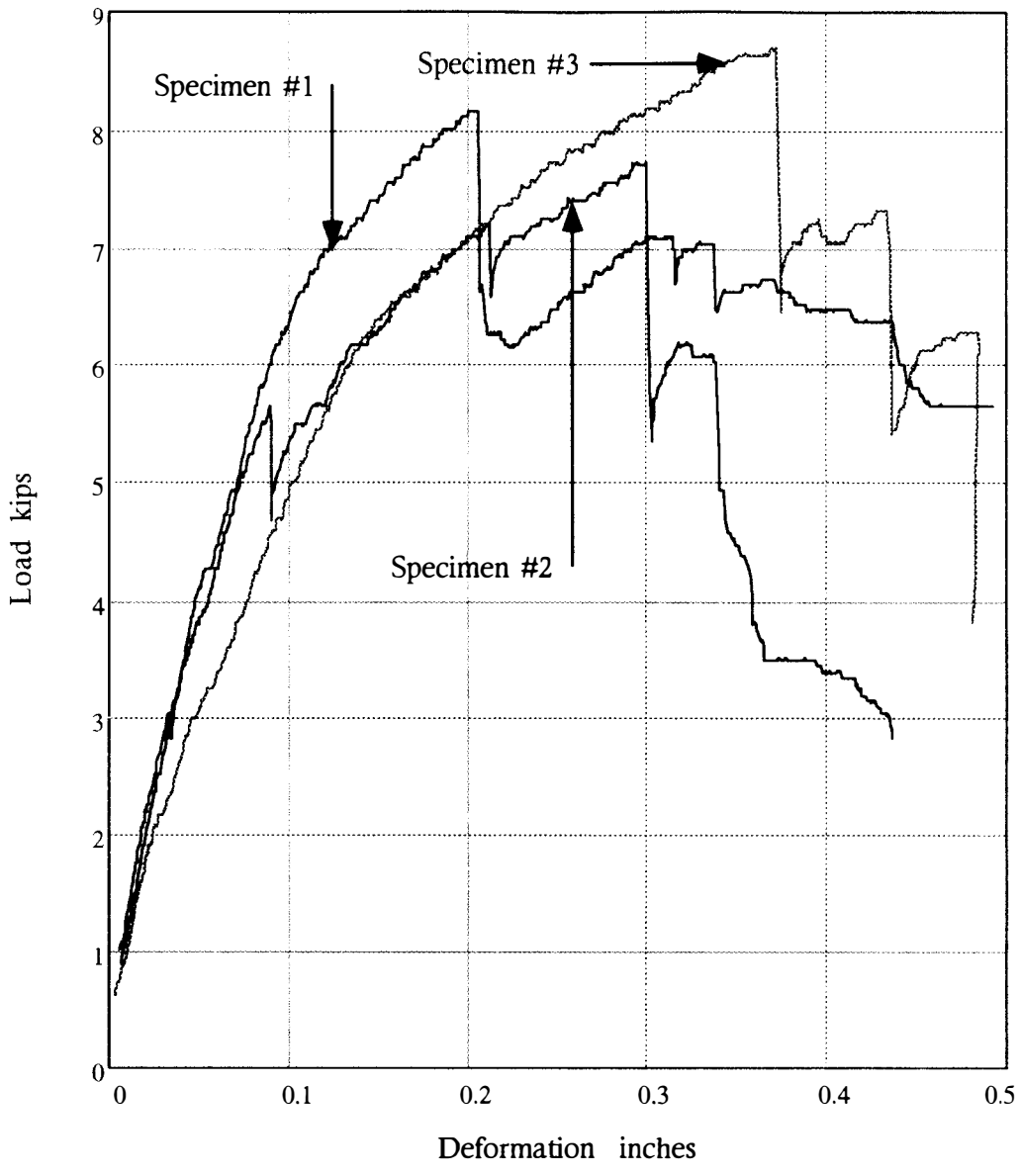
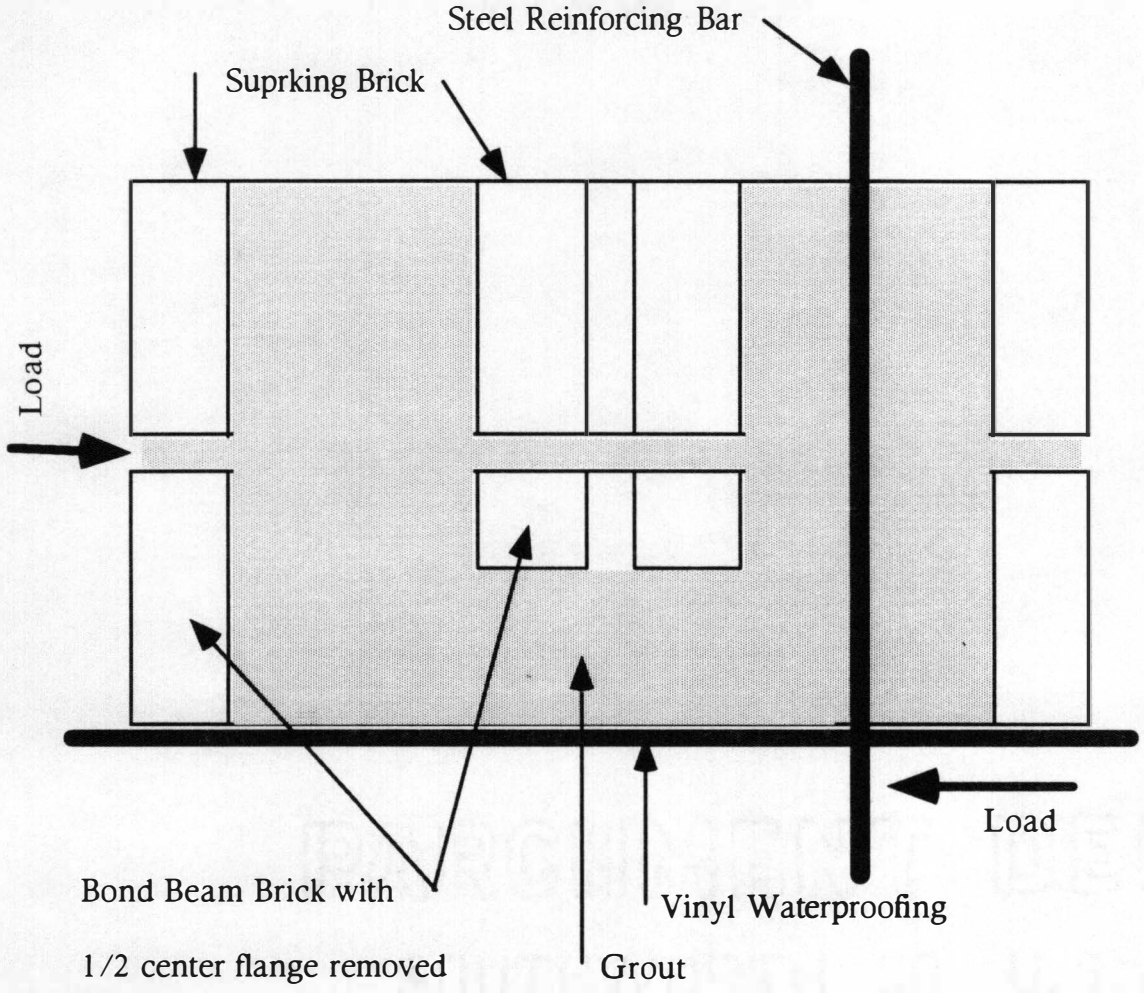


Figure 4.7

Shear Test Of Joints With Vinyl Flashing, #4 Reinforcing Bar, Mortar Grout In Reinforced Cells - Load Deformation Curves



Note: This figure shows the flashing joint in a horizontal orientation as it exists at the flashing joint in a wall. For the shear test specimens, the joint and load are orientated vertically.

Figure 4.8

Section Of Grouted Bond Beam Brick Next To Vinyl Flashing

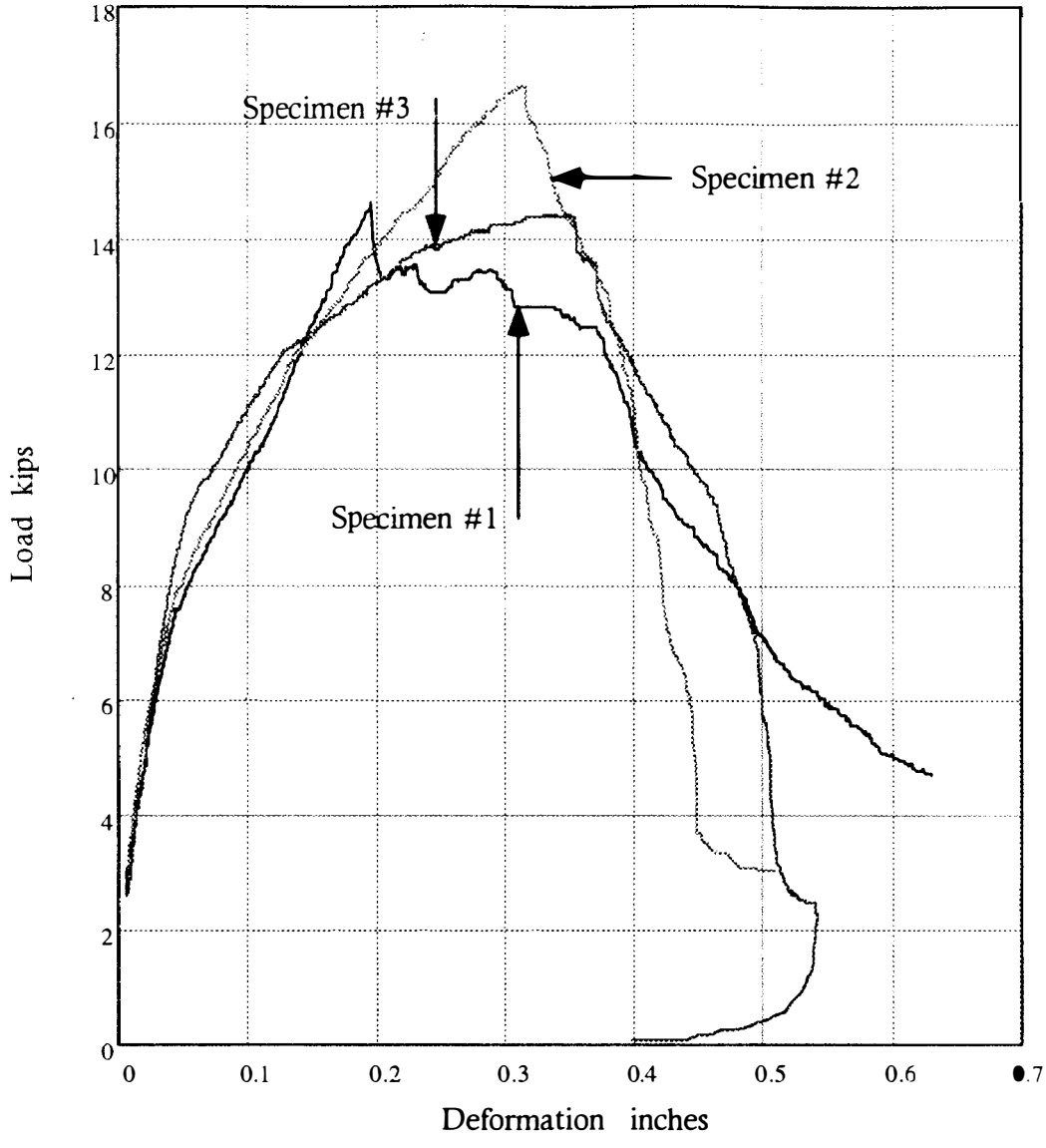


Figure 4.9

Shear Test Of Joints With Vinyl Flashing, #4 Reinforcing Bar, 10K Grout In All Cells

Load Deformation Curves

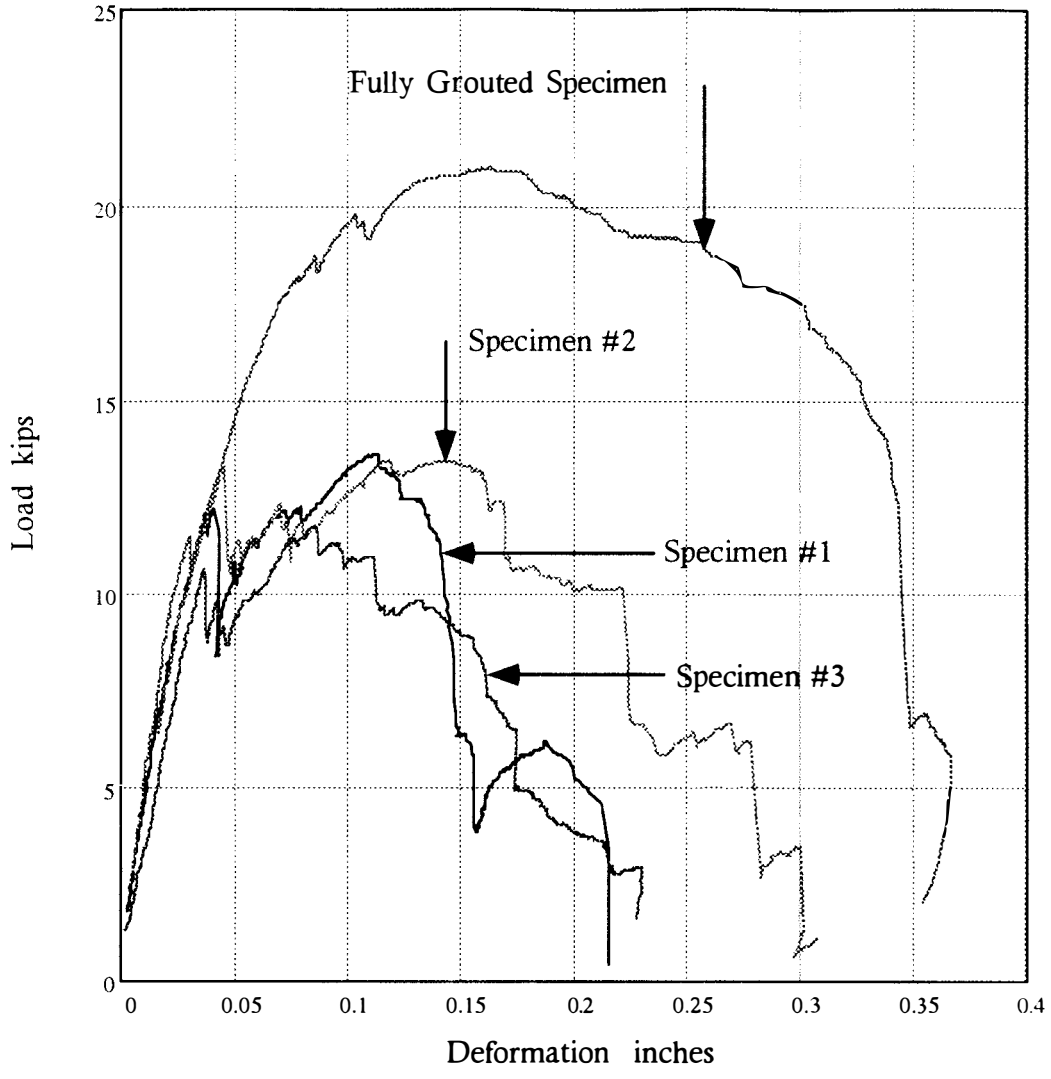
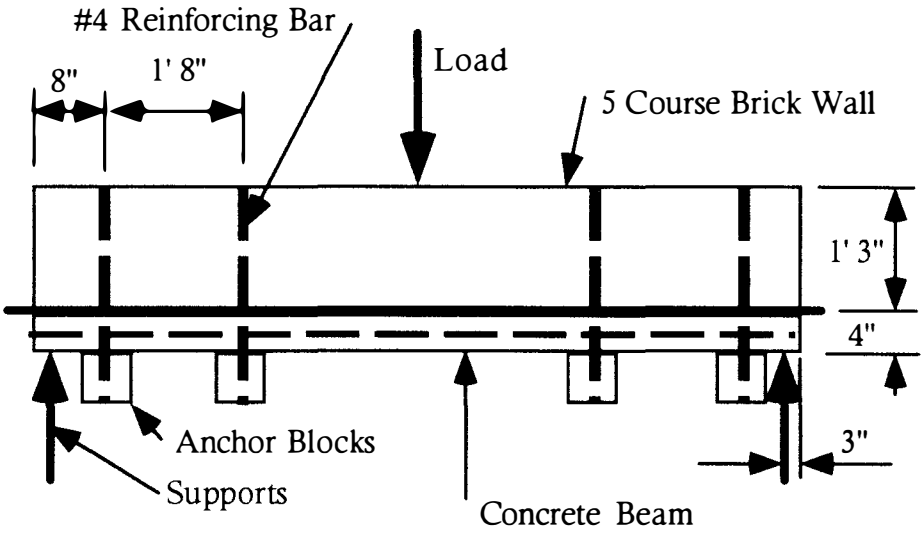


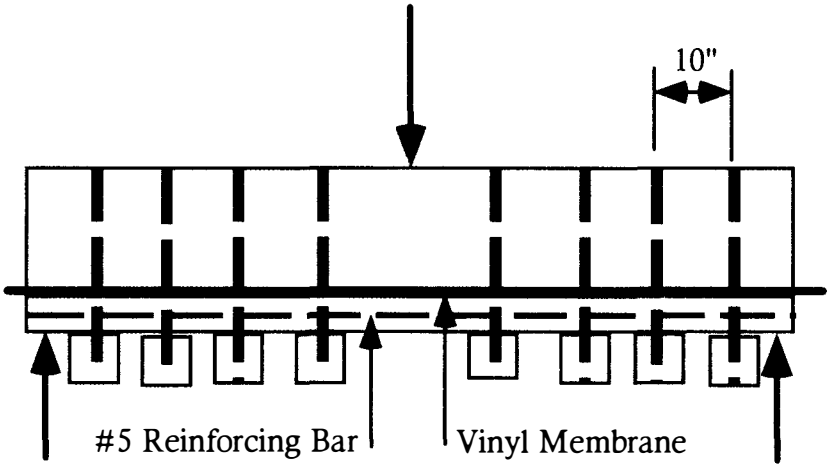
Figure 4.10

Shear Test Of Joints With Vinyl Flashing, #6 Reinforcing Bar, 10K Grout In Reinforced Cells Or All Cells

Load Deformation Curves



Wall Specimen with 4 Vertical #4 Dowels



Wall Specimen with 8 Vertical #4 Dowels

Figure 5.1

Sketch of Wall Specimen Elevations

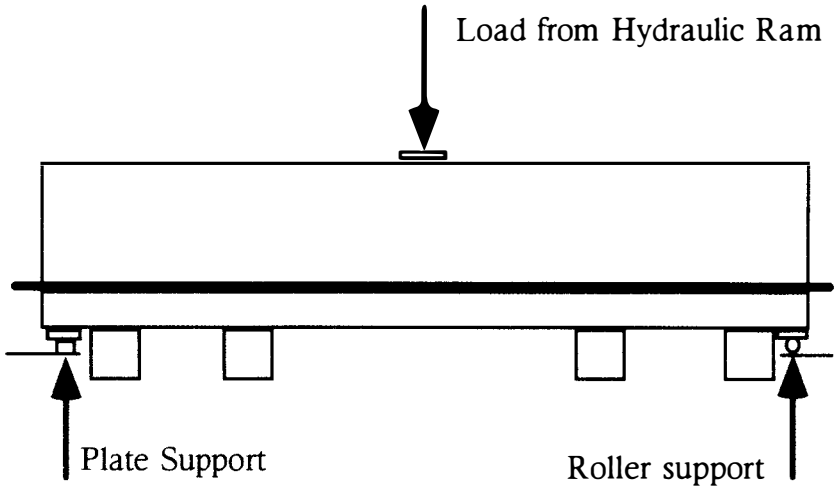
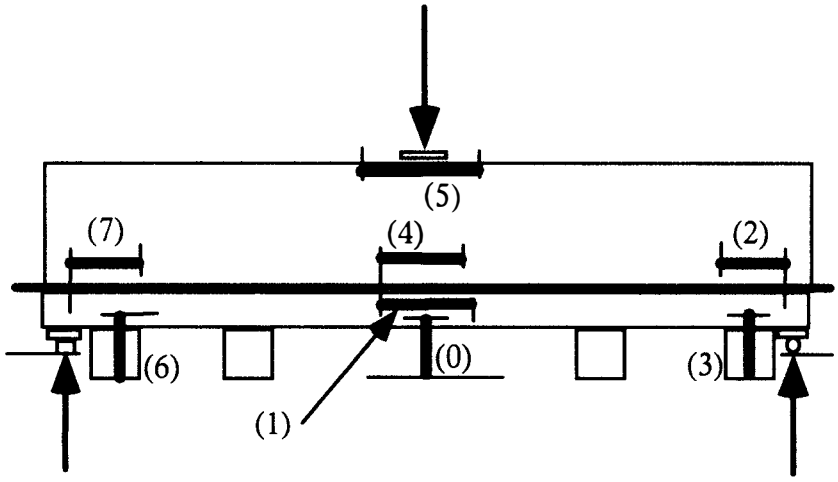


Figure 5.2

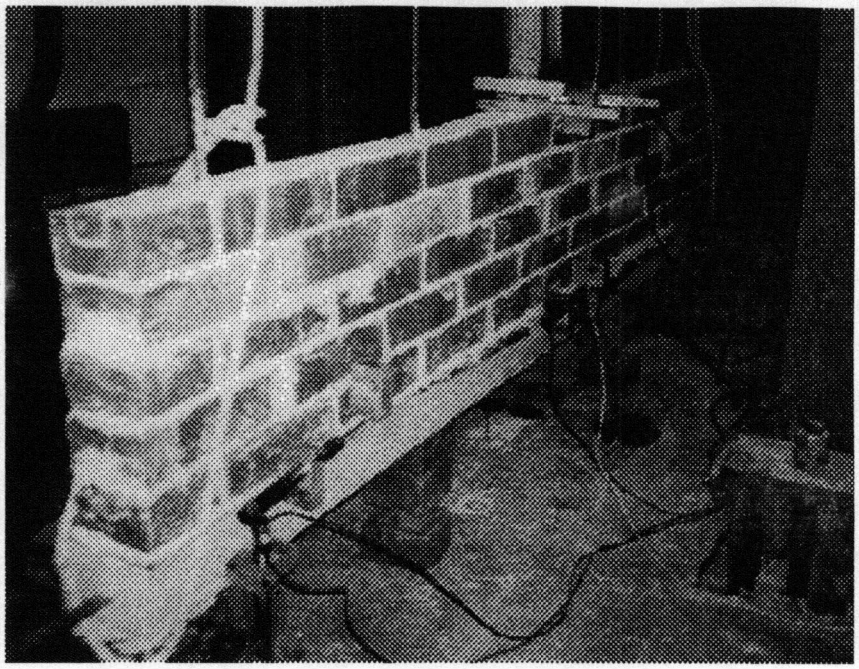
Specimen Support And Loading Configuration



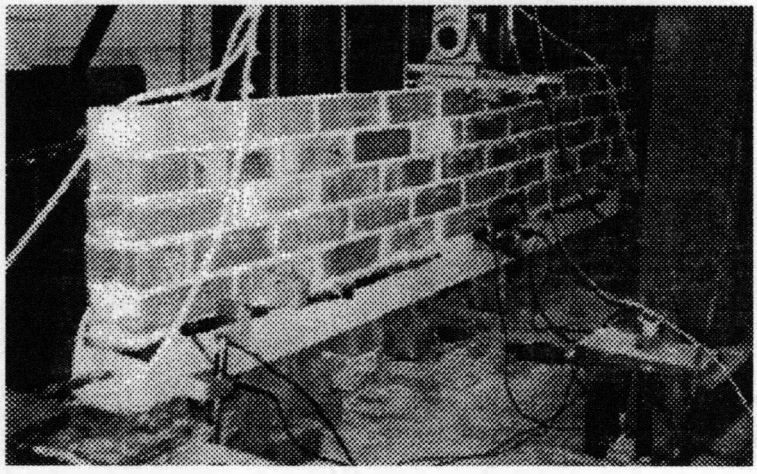
(x) indicates channel number

Figure 5.3

LVDT Locations On Wall Specimen



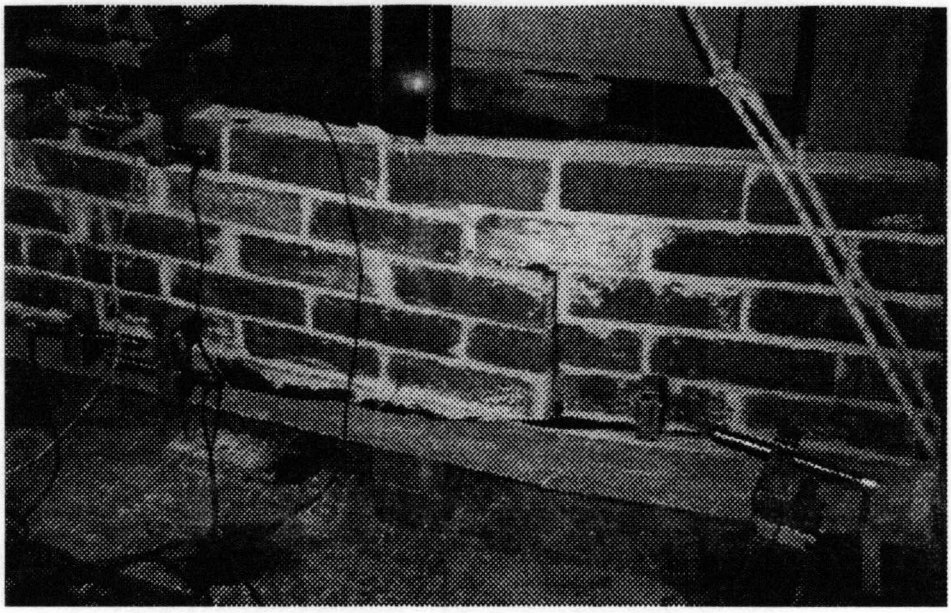
Wall Specimen With Four Vertical #4 Dowels



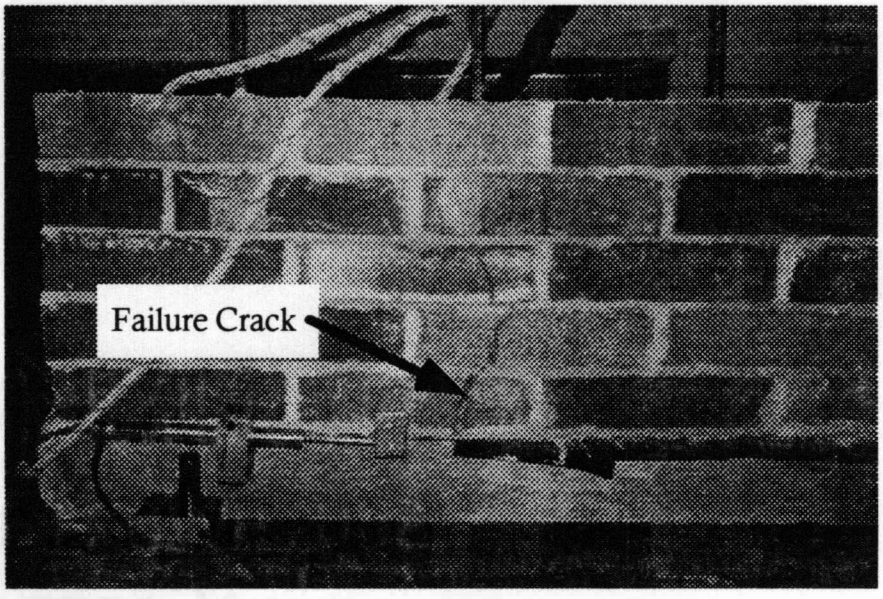
Wall Specimen With Eight Vertical #4 Dowels

Figure 5.4

Photographs Of Wall Specimens



Specimen #2, Failure Between Two Of The #4 Dowels



Specimen #3, Failure At 2nd Dowel From End

Figure 5.5

Photographs Of Specimen #2 and #3 Failures

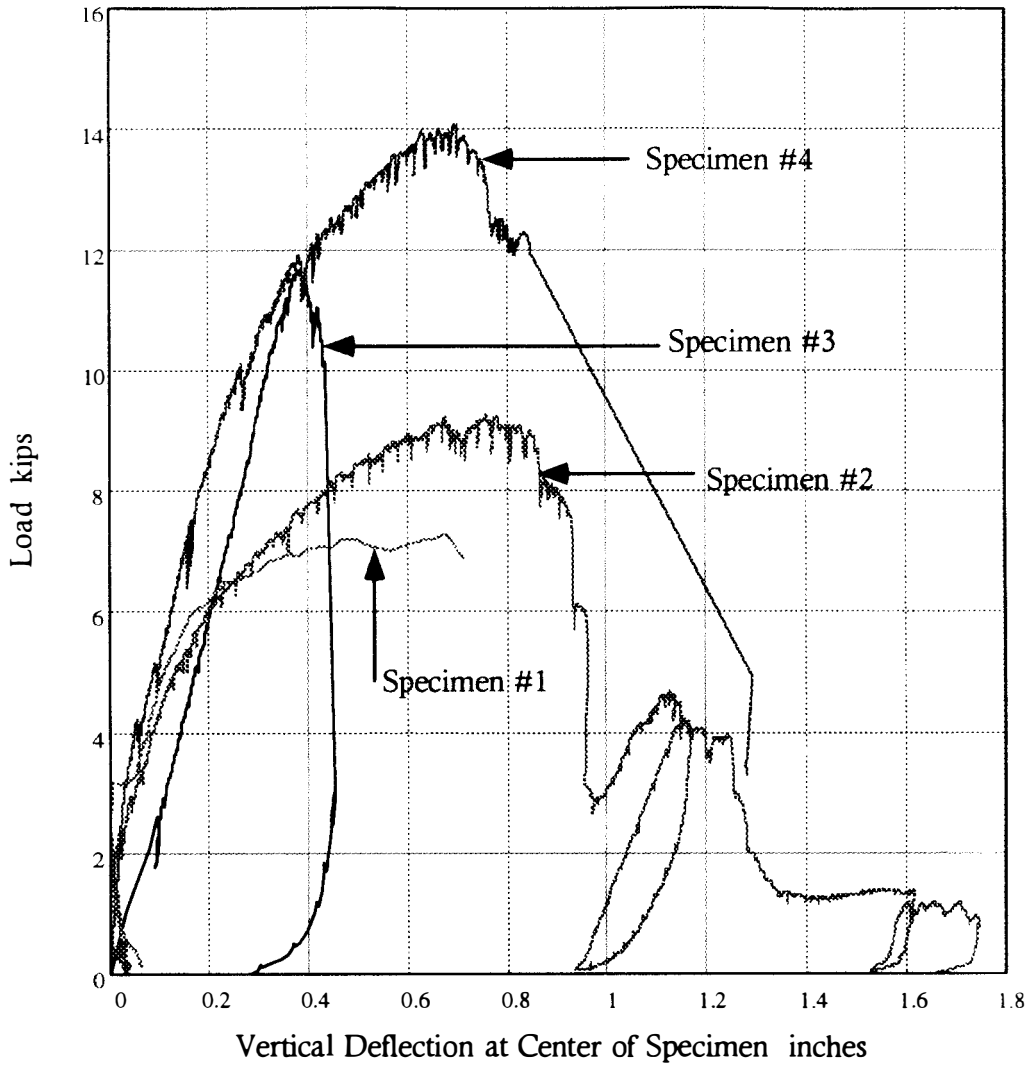


Figure 5.6

Small Scale Test Wall Specimens

Load Deflection Diagrams

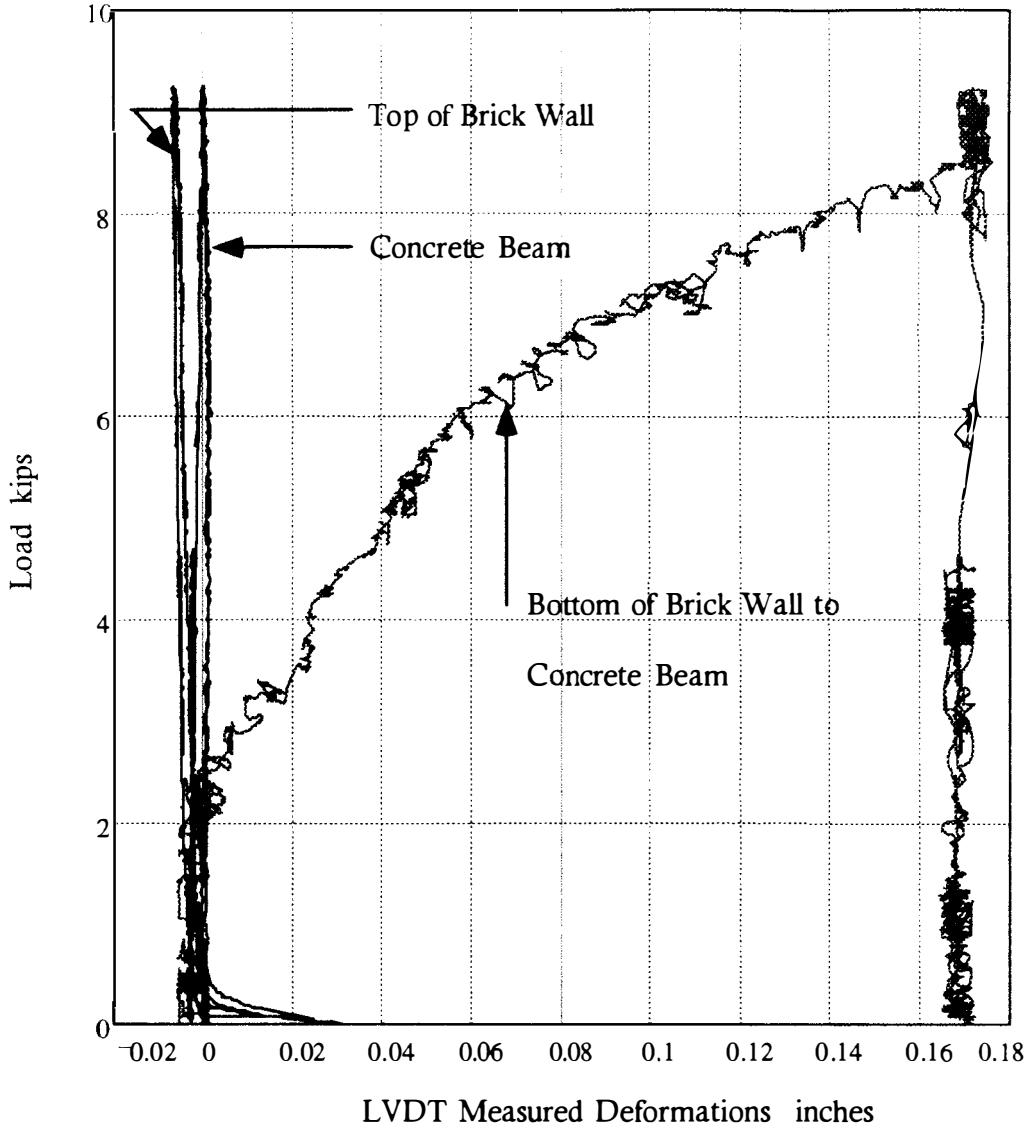


Figure 5.7

Load Deformation Curves For LVDTs At Center Of Specimen #2

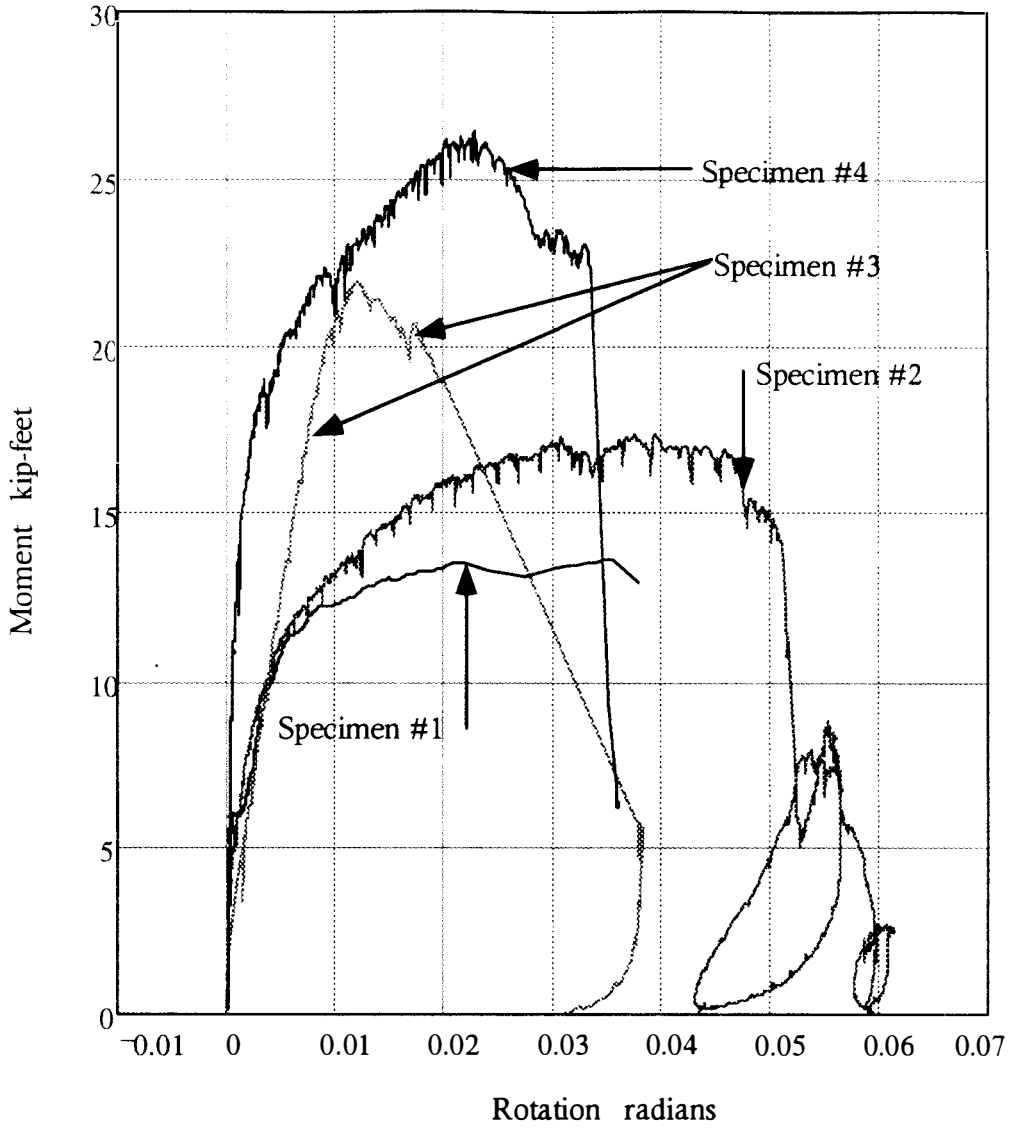


Figure 5.8

Small Scale Test Wall Specimens

Moment Versus Total Rotation Curves At Mid Span

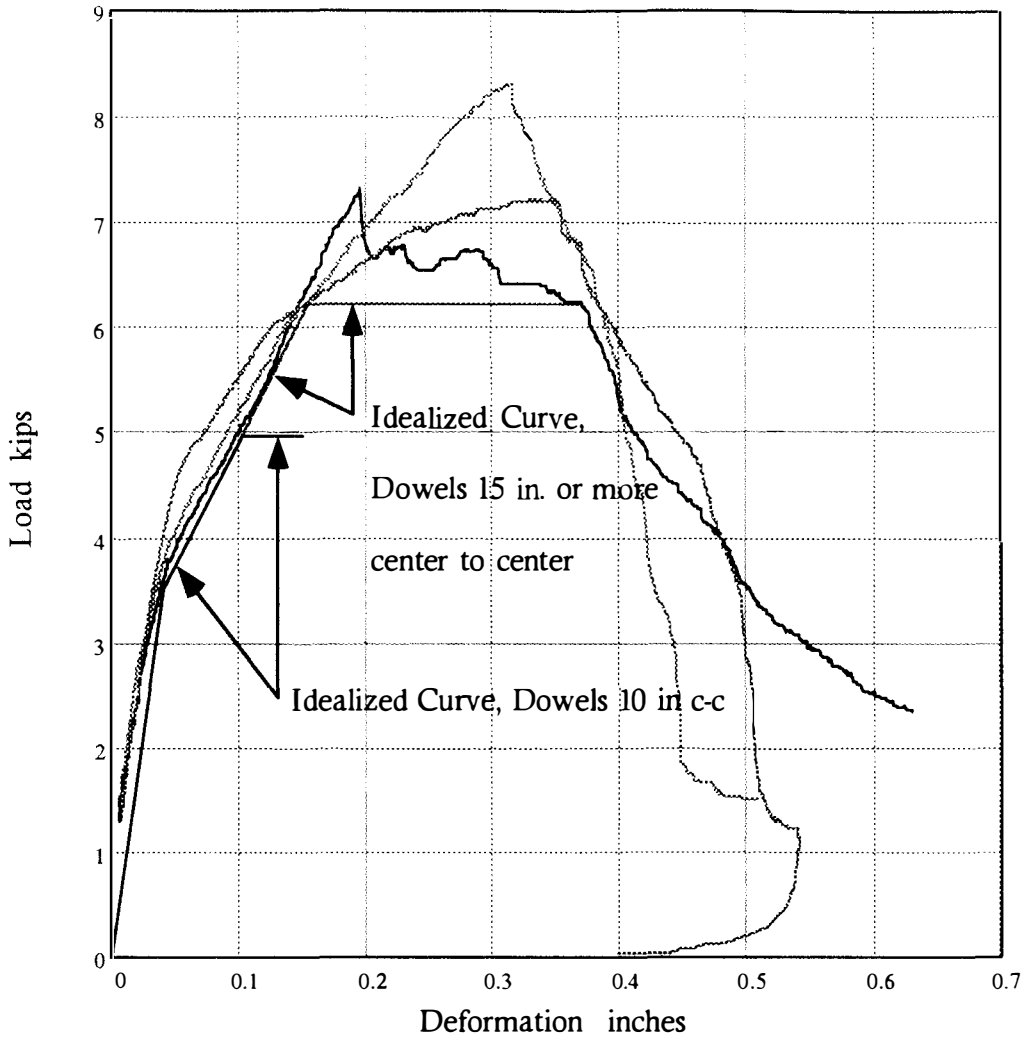


Figure 5.9

Comparison Of Idealized Joint Deformation Curve With Shear Test Results Divided By 2 For Joints With Vinyl Flashing, #4 Reinforcing Bar and 10K Grout In All Cells

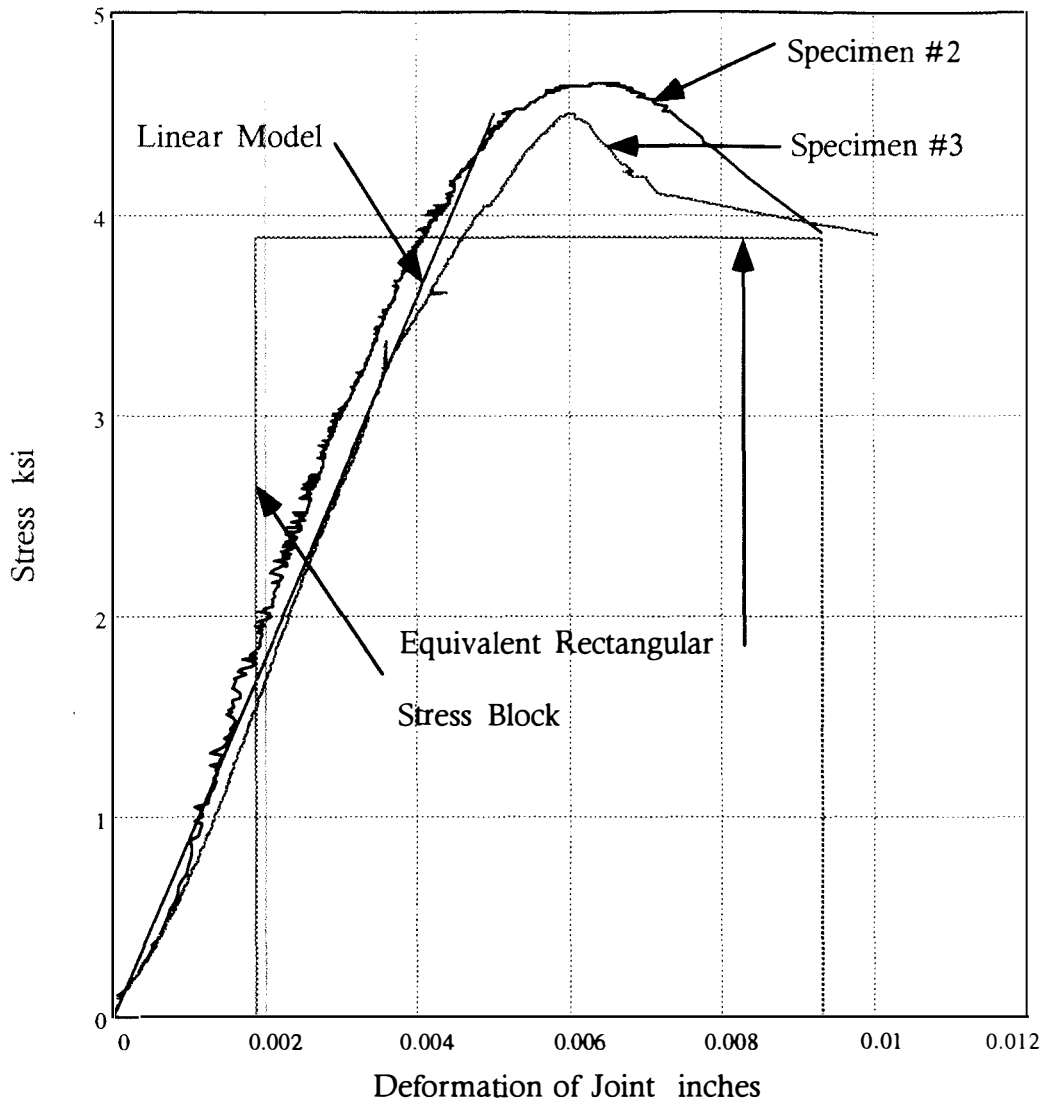


Figure 5.10

10K Grouted Prism Stress Deformation Curves - Specimens 2 & 3, Linear Load Deformation Curve For Brick Wall, And Equivalent Stress Block For Ultimate Bending Strength Compression Load

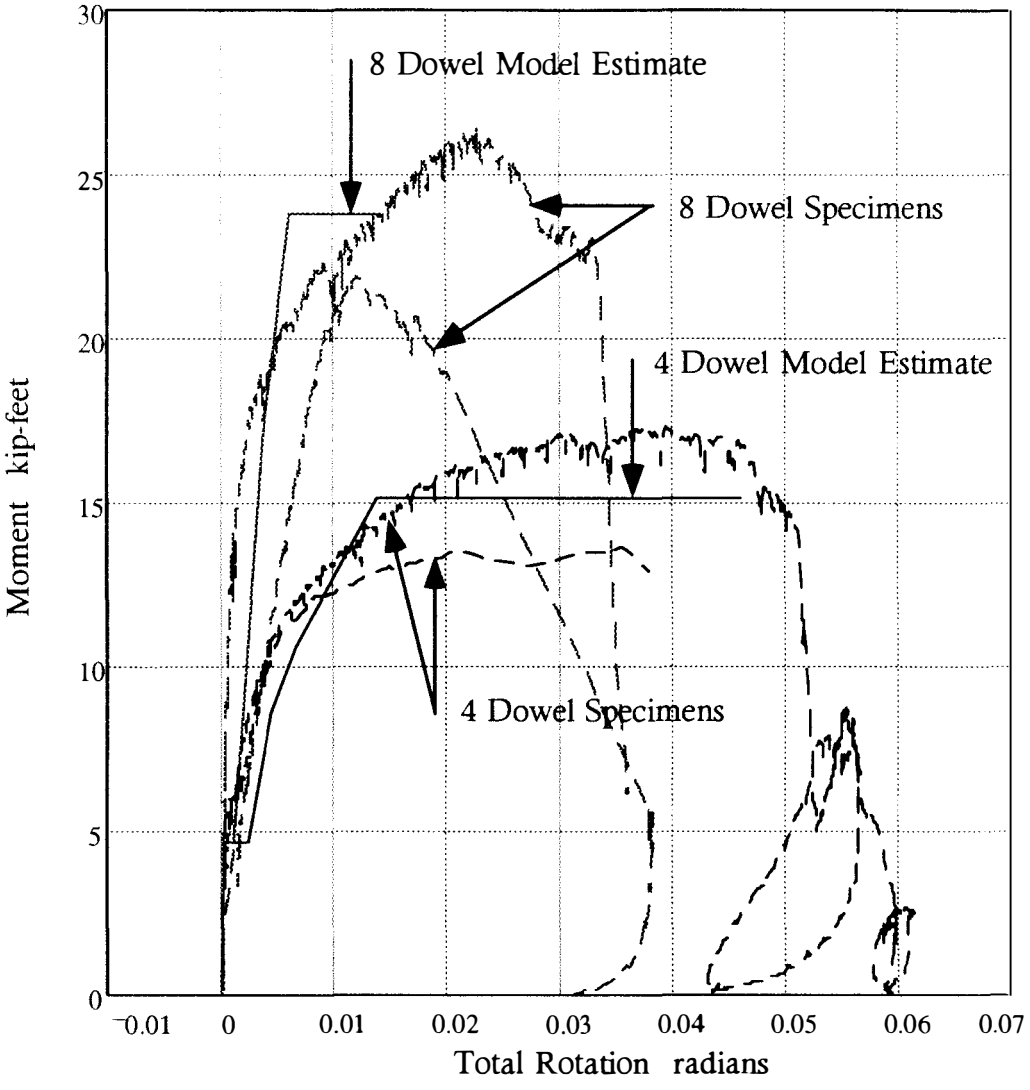


Figure 5.11

Comparison Of Measured And Predicted Moment Versus Total Rotation Diagrams At Mid Span Of Wall Specimens

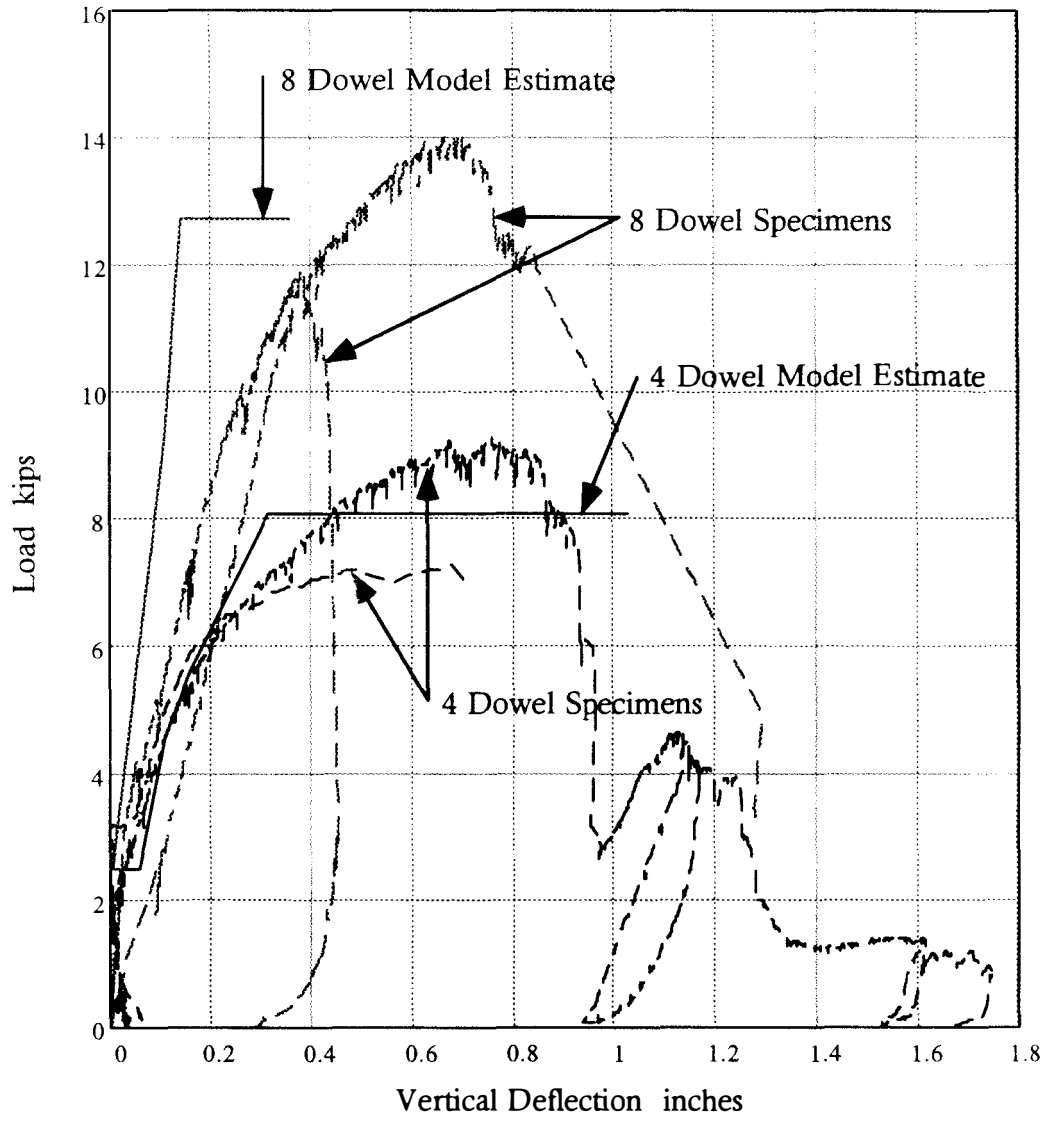
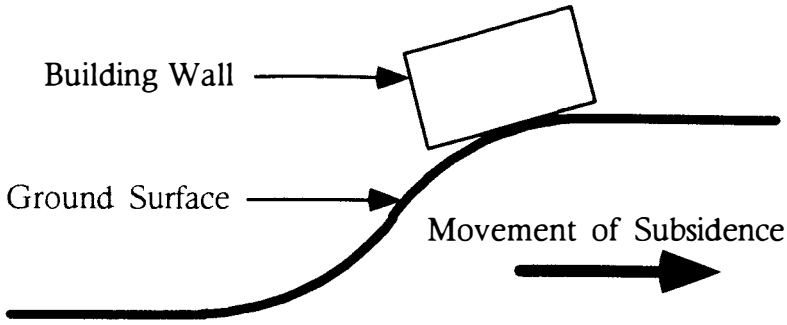
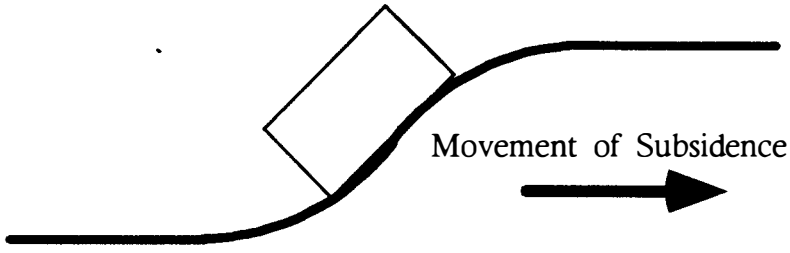


Figure 5.12

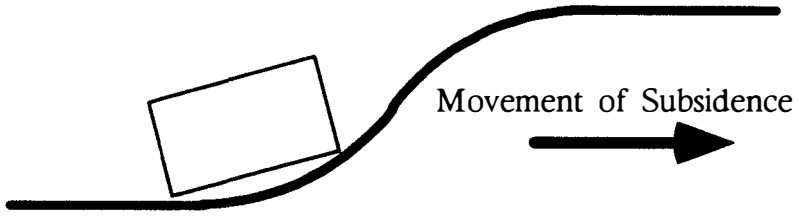
Comparison Of Measured And Predicted Load Versus Vertical Deflection Diagrams At Mid Span Of Wall Specimens



Stage 1 - Maximum Tensile Strain and Convex Curvature



Stage 2 - Maximum Tilt and Nil Curvature



Stage 3 - Maximum Compressive Strain and Concave Curvature

Figure 7.1

Movement And Deformation Of Wall

As

Subsidence Face Moves Under Wall

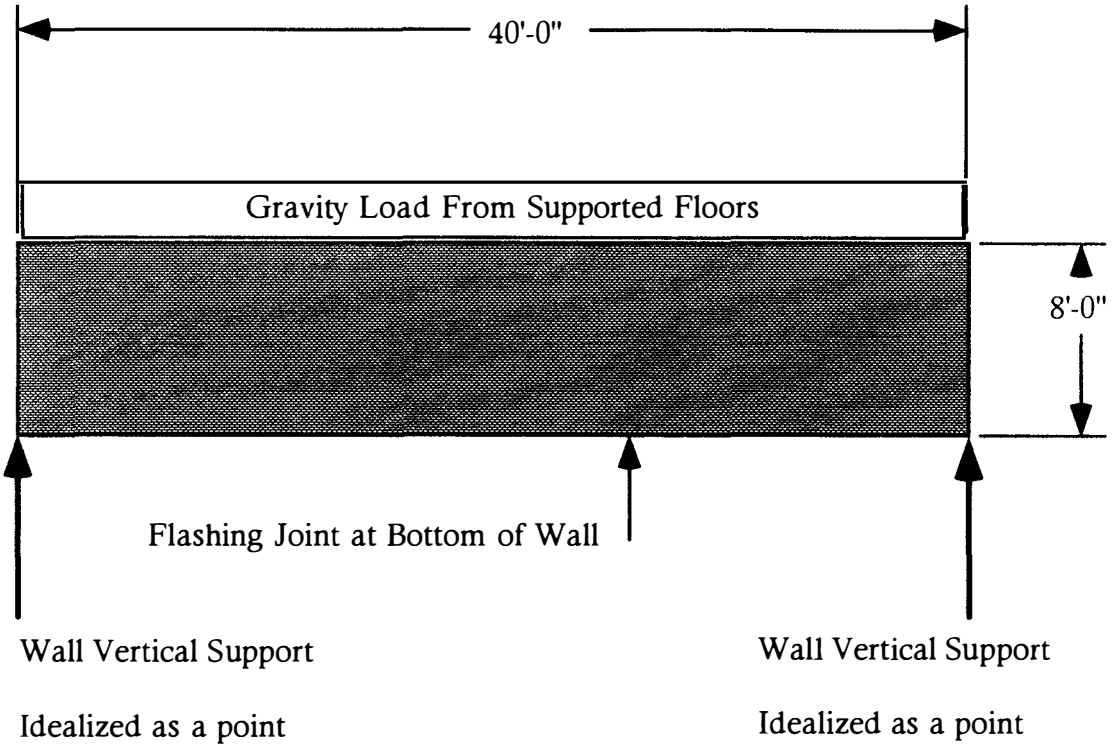


Figure 7.2

Sketch Of Example Brick Wall

Subject To Concave Curvature Due To Subsidence

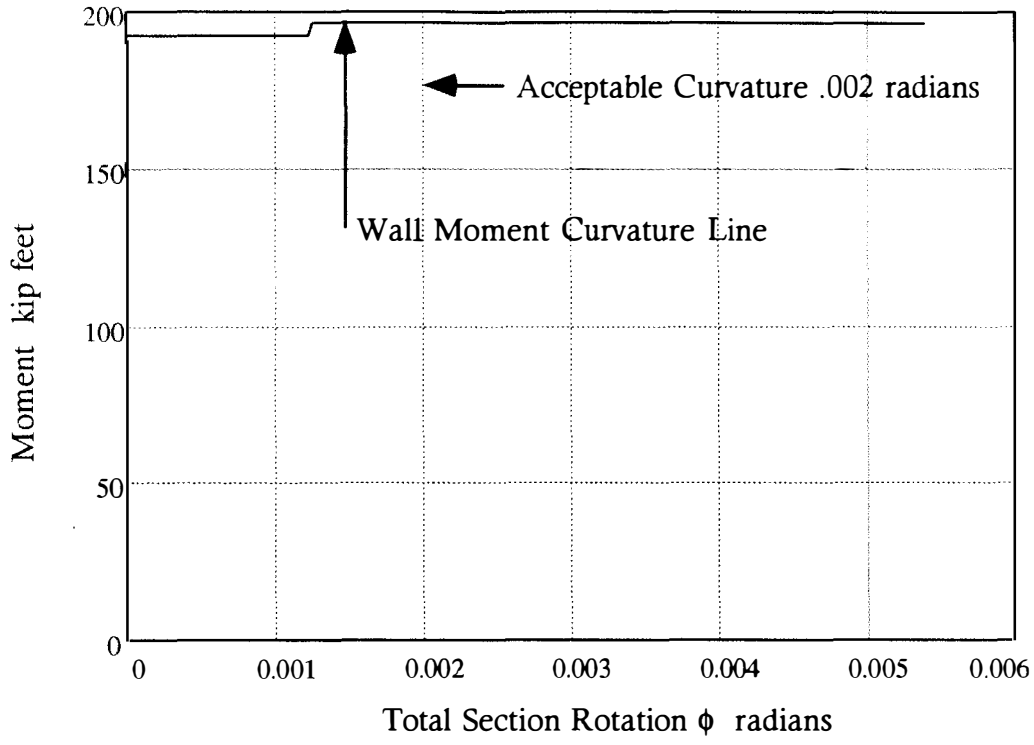


Figure 7.3

Diagram Of Moment Versus Curvature For Subsidence Example Wall

VITA

John Kennedy McCall was born on March 2, 1942 in Cleveland, Ohio. After moving several times during the Second World War, his family settled in Long Beach, California where he grew up. Mr. McCall's education after high school occurred in two phases. During the first phase from 1960 through 1968, he attended Claremont Men's College, Long Beach City College, and the University of California at Berkeley. He received both a BS and MS degree from the University of California at Berkeley. During the period at Berkeley, Mr. McCall was inducted into the Tau Beta Pi and the Chi Epsilon honorary fraternities. During the second phase of his education, Mr. McCall attended the University of Tennessee at Knoxville from 1993 to the present time.

Since 1968 Mr. McCall has worked as a civil engineer specializing in structural engineering. His assignments have involved engineering of multistory hospitals, regional mail handling facilities, Aluminum reduction plants, individual residences, apartment houses, resorts, and 21 Nuclear Power Plants. His level of responsibility has ranged from design engineer to Chief Civil Engineer. His major achievements during this period have included preparation of initial layout and criteria for a Nuclear Generating Station which remained unchanged during over ten years of construction and plant start-up, and developing scope and managing the civil engineering activities for start-up for several nuclear generating stations. Mr. McCall is a licensed Civil Engineer in California, Tennessee and Florida.